Heavy Ion Laboratory

ANNUAL REPORT 2019

UNIVERSITY OF WARSAW

HIL Heavy Ion Laboratory

Heavy Ion Laboratory
University of Warsaw

Annual Report

2019

Warszawa, May 2020

Various information concerning the Laboratory is distributed via the HIL mailing list.
In order to subscribe to the list please visit the page
`http://mail.slcj.uw.edu.pl/mailman`

Annual Report of the
Heavy Ion Laboratory, University of Warsaw
ul. Pasteura 5a, 02-093 Warszawa, Poland
phone (+48)22-8222123, (+48)22-5546000
fax (+48)22-6592714
`http://www.slcj.uw.edu.pl`

Editors:
Nicholas Keeley, Michalina Komorowska, Monika Paluch-Ferszt,
Justyna Samorajczyk-Pyśk, Marzena Wolińska-Cichocka
e-mail: raport@slcj.uw.edu.pl
ISSN 1895-6726

Cover design:
Ryszard Piwowar

Contents

Introduction

The year 2019 was marked by a number of meetings and conferences taking place at HIL. The year began with the conference on the "Future of Low-Energy Nuclear Physics in Poland and the Development of the National Research Infrastructure" that gathered 116 participants from Poland and abroad (January 14th–15th). One of the most important presentations was the project to replace the U-200P heavy-ion cyclotron currently operating at HIL with a new machine, with the aim of ensuring a higher intensity of ion beams with better energy parameters as well as an extended variety thereof. This project has been dubbed "HIL@ECOS", with reference to the European ECOS project, and has received support from NuPECC, JINR Dubna as well as numerous Polish institutions.

Among the most prestigious meetings was that of NuPECC, which took place at HIL at the beginning of March (March 1st–2nd). It was opened by the Rector of the University of Warsaw and the first day was devoted to presentations of the activities of Polish scientists in nuclear physics and its applications. This workshop was chaired by Professor Adam Maj from the Institute of Nuclear Physics, Polish Academy of Sciences, who serves as the representative of Polish physicists in NuPECC.

Another important meeting was devoted to scientific collaboration between three countries, Poland, France and Italy (March 5th–7th). The programme consisted of talks given by scientists from these countries presenting results of common projects as well as reporting on the status of national nuclear physics facilities.

During 2019 the scientific activity of HIL remained at a high level. It covered two main areas: fundamental research in nuclear physics and research related to applications in medicine and biology. It yielded sixty scientific papers, the largest number in the history of HIL, published in such prestigious journals as Nature Communications, Bioorganic Chemistry and Physical Review Letters. The personnel of HIL has constantly developed its skills. One of our young colleagues, Dr. Aleksandra Sentkowska. received a scholarship from the Minister of Science and Higher Education awarded for her high-quality research and impressive scientific achievements on an international scale. We are happy to note that Dr. Krzysztof Kilian obtained the Doctor of Science degree at the Department of Chemistry of the University of Warsaw. Another colleague, Dr. Grzegorz Kamiński, was appointed to the post of deputy director of the Flerov Laboratory of Nuclear Reactions at the Joint Institute of Nuclear Research in Dubna, Russia. Coming to technical achievements, the completion of the project to replace the old RF generators with the new ones must be mentioned. The tests, started in September, proved the correct operation of the power amplifier manufactured by Popek-Elektronik, the last stage of the new generators.

Prof. Krzysztof Rusek, Director of HIL

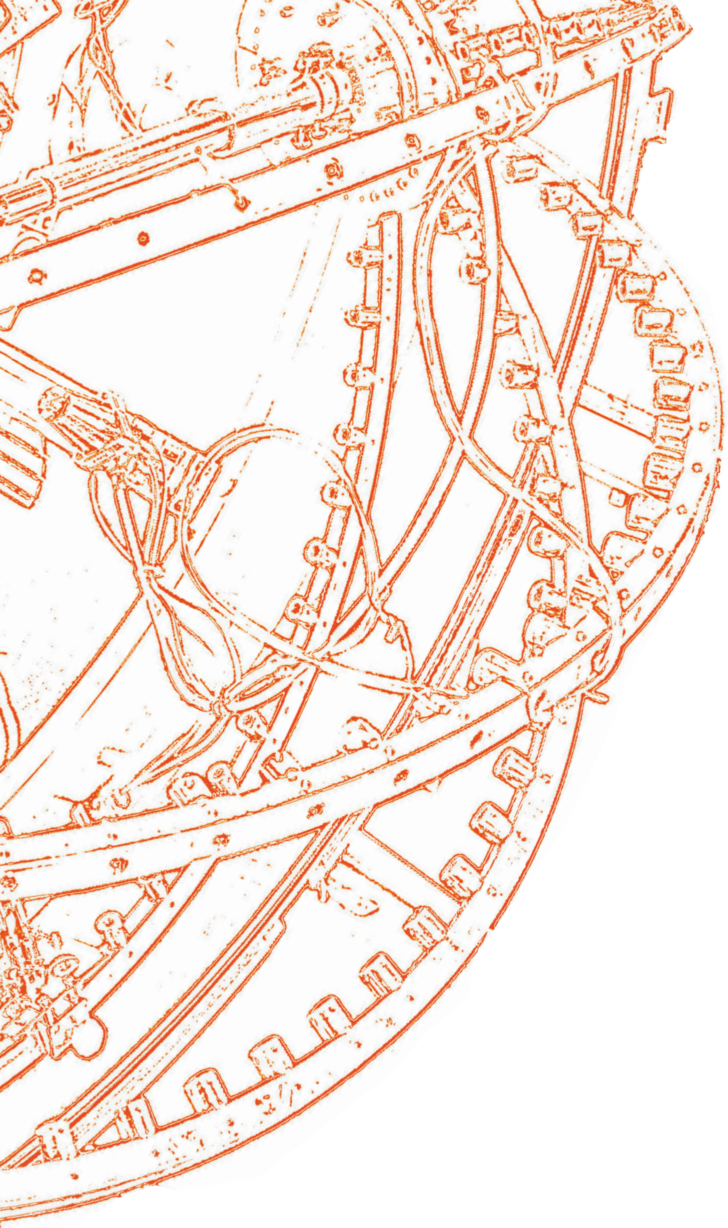

Part A
Laboratory Overview and technical developments

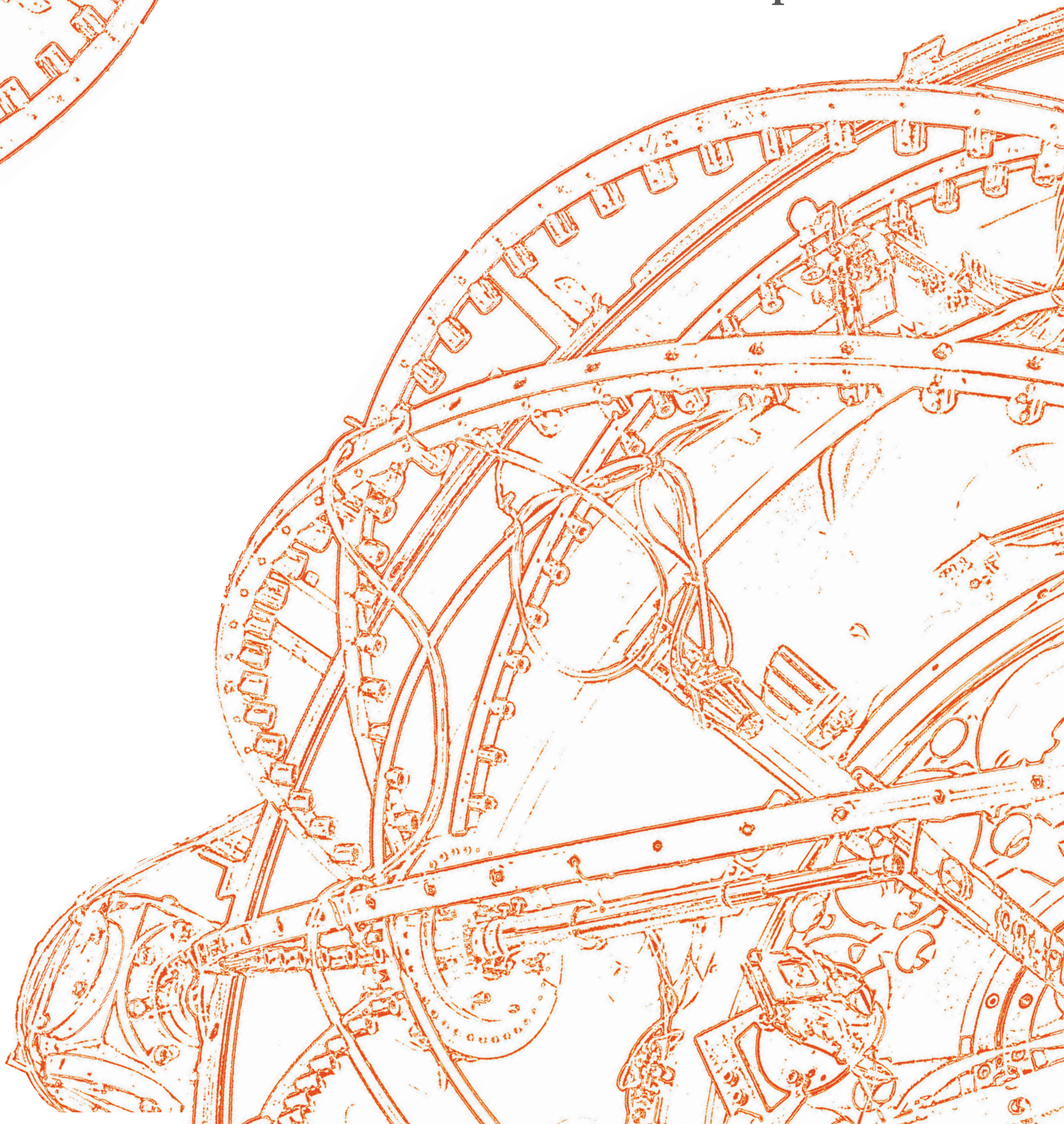

A.1 General information

J. Choiński, P.J. Napiorkowski, K. Rusek

Heavy Ion Laboratory, University of Warsaw, Warszawa, Poland

The Heavy Ion Laboratory (HIL) is a unit of the University of Warsaw, the largest university in Poland. HIL was founded jointly by the Ministry of Education, the Polish Academy of Sciences and the Polish Atomic Energy Agency. It is the largest experimental nuclear physics laboratory in the country, equipped with two cyclotrons – a K=160 U-200P heavy-ion cyclotron and a GE PETtrace K=16.5 commercial cyclotron delivering high intensity proton and deuteron beams.

The first heavy-ion beam was extracted from the U-200P in 1994 and since that time HIL has been an effective "user facility", serving up to the present time several hundred scientists from Poland and abroad and has become a recognised element of the European Research Community. From the 1st of March 2016 HIL has been among ten European laboratories with Transnational Access granted by the European Union by means of the ENSAR2 (European Nuclear Science and Application Research 2) project within the HORIZON 2020 framework. Beam time is allocated by the Director based on the recommendations of an international Programme Advisory Committee. The only criteria are the scientific merit of the project and its technical feasibility. The research programme is mostly focused on nuclear physics and medical applications including the production of radio-isotopes.

Experimental teams may take advantage of permanent set-ups installed on the beam lines or use their own dedicated equipment. Available arrays include IGISOL — a Scandinavian type on-line separator, CUDAC — a PIN-diode array particle detection system, JANOSIK — a multi-detector system consisting of a large NaI(Tl) crystal with passive and active shields and a 32-element multiplicity filter and ICARE, a charged particle detector system used for particle identification and energy measurements, moved to HIL from IReS Strasbourg. The most recent experimental tool, still being developed and improved, is the EAGLE array – a multi-detector γ-ray spectrometer, equipped with 16 HP germanium detectors with anti-Compton shields and up to 14 HP germanium detectors from the GAMMAPOOL consortium. It can be easily coupled to ancillary detectors such as the internal conversion electron spectrometer built by the University of Lodz, a charged particle 4 π multiplicity filter (Si-ball), a scattering chamber equipped with 100 PIN-diode detectors, a 60-element BaF_2 gamma-ray multiplicity filter, a sectored HPGe polarimeter and a plunger.

The Radiopharmaceuticals Production and Research Centre has formed an important part of HIL since 2012. Focused on the production of and research into Positron Emission Tomography radiopharmaceuticals, the production of longer-lived radioisotopes for life-sciences applications is also carried out.

Being a university unit, HIL is involved in teaching in a natural way. On average about 15 students/year (Bachelors, Masters, PhD, ERASMUS) from Poland and abroad work at HIL supervised by its staff members. As part of its broader educational mission HIL staff organize an annual one-week workshop on "Acceleration and applications of heavy ions" for about 20 students from various Polish universities.

A.2 Cyclotron operation in 2019 and tasks carried out in order to improve the cyclotron infrastructure and efficiency

J. Choiński, P. Gmaj, A. Bednarek, T. Bracha, A. Jakubowski, P. Jasiński, W. Kalisiewicz, M. Kopka, W. Kozaczka, P. Krysiak, K. Łabęda, K. Makowski, I. Mazur, J. Miszczak, B. Paprzycki, K. Pietrzak, B. Radomyski, K. Sosnowski, L. Standyło, K. Sudlitz

Heavy Ion Laboratory, University of Warsaw, Warszawa, Poland

Operation

It is characteristic that currently the physical experiments submitted for consideration by the PAC are becoming more and more demanding year by year in terms of the required dynamic parameters of the beam and types of accelerated ions. Increasing efficiency of reaction product detectors and increasingly smaller cross-sections for the expected effects, require delivery of more intense beams than previously. Geometrically complex apparatus containing reaction targets imposes additional conditions on the spatial properties of the beam. All this clearly shows the development direction of the cyclotron infrastructure which the design team and the laboratory's decision-making team must follow. Given the advanced age of the accelerator structure and the limited financial resources, the main effort of the technical group was directed in 2019 to increase the cyclotron's capacity capabilities without investing in major modernization projects. This includes the maintenance of functional and subsequent replacement of worn-out infrastructure components. The largest projects in this field implemented in 2019 included the replacement of high frequency amplifiers, which are currently being tuned to the resonant structure of the accelerator. However, projects approved for 2019 were carried out using the existing amplifiers. Due to their wear, this significantly limited the availability of the cyclotron for experiments in 2019. Another modernization project was the construction of a new system for target irradiation using internal beams. This design has a much more efficient cooling system, and therefore allows irradiation with a more intense beam, which is necessary for experiments related to the production of radiopharmaceuticals. Another project implemented in 2019 was a magnetic field measurement system. The implementation of this project is aimed at increasing the cyclotron transmission and therefore the intensity of the experimental beam. The project should be completed at the end of 2020 and in 2021 field measurements and development of a precise methodology for its adjustment are expected.

In 2019, the PAC approved 8 experimental projects for implementation using the U-200P cyclotron. Their implementation required a total of 1656 hours of cyclotron beam delivery. Three projects still needed completion from previous periods, requiring a total of 504 beam hours to be delivered. In total, we scheduled 11 projects for 2019 (2160 beam hours). From among 8 projects approved in 2019, we completed 7 and one project overdue from previous years. They accounted for a total of 65% of the plan. The remaining experiment constituting 35% of the plan is postponed to March '20.

Of the projects still awaiting implementation, it was not possible to obtain a sufficiently intense and stable beam of ^{58}Ni required for an experiment to measure the Coulomb excitation of ^{118}Sn, therefore we will continue work to obtain a sufficient Ni beam for this experiment in 2020.

The development of the ECR test bench was continued within the scope of the European ENSAR 2 project during 2019 (please see the specific report below). The bench allows the study of different physical phenomena occurring in plasma rather than mapping a specific production of beams using an ECRIS. Therefore, it can be used more to discover innovative solutions then to optimize specific ECR source parameters.

As in every year, the cyclotron division delivered beam for the students' workshop, which took place in the autumn.

A.3 Status of the EAGLE array

M. Palacz, T. Abraham, M. Kisieliński, M. Kowalczyk, J. Srebrny, for the EAGLE collaboration

Heavy Ion Laboratory, University of Warsaw, Warszawa, Poland

The central European Array for Gamma Levels Evaluations (EAGLE) is an array of High Purity Germanium (HPGe) detectors situated at HIL [1]. The flexible frame of the setup allows the installation of up to 30 HPGe detectors and various ancillary devices.

The frame has the form of a truncated icosahedron. Its hexagonal faces form 4 rings at ϑ angles with respect to the beam axis of 37°, 79°, 101° and 143°, and can accommodate up to 20 detectors (5 detectors in each ring). Additionally, 10 detectors can be mounted on the pentagonal faces (ϑ angles 63° and 117°), with again 5 detectors in each ring. The remaining 2 pentagonal faces are used for the beam inlet and outlet. The distance of the detectors to the target can be adjusted over a broad range. The minimum distance depends on the geometry of the particular detector and its anti-compton shield. It is typically about 4 cm larger in pentagons than in hexagons. The efficiency of the GAMMAPOOL detectors (see below) mounted in EAGLE at the minimum distance to the target is about 1‰ and 0.8‰ (per detector) at 1.3 MeV, for the hexagonal and pentagonal positions, respectively.

Since 2016 GAMMAPOOL [2] has loaned to the Heavy Ion Laboratory a number of HPGe detectors and anti-compton shields. An application to prolong this loan until December 2021 was submitted to the GAMMAPOOL Owners' Committee in July 2019 and was accepted in October. At present, altogether 19 GAMMAPOOL HPGe detectors are located at HIL. This number includes 3 detectors which are not operational and should be repaired at the cost of IPN Orsay. In 2019 HIL financed the repair of one detector and another one was repaired and shipped to HIL by IPN Orsay. One more detector is expected to be shipped from JYFL, Jyväskylä, Finland at the beginning of 2021. The detectors are routinely serviced at HIL. Procedures like annealing, FET replacements, repair of preamplifiers, pumping to restore vacuum, are performed in house, see also Ref. [3]. This effort is pursued with the aim of keeping the detectors in the best possible condition, and to ensure that at least 15 of them are available for experiments, which matches the number of the available GAMMAPOOL anti-compton shields. In addition, HIL owns 19 smaller detectors with anti-compton shields, which may also be installed in the EAGLE frame.

During 2019 a Memorandum of Understanding was negotiated between the GAMMAPOOL Owners' Committee and HIL, making HIL a home base of altogether 39 HPGe detectors and 30 anti-compton shields. The agreement became effective starting from 1 January 2020. The role of the home base laboratory is to follow the status of the detectors while they are used in various European laboratories, as well as to service and store the detectors when they are not in use. Presently, the detectors are located at HIL (as described above), JYFL Jyväskylä and IPN Orsay.

In 2019 four experiments were performed with EAGLE. Three of them are covered in separate contributions to this report [5–7]. The fourth one, by J. Perkowski et al., aimed at a search for E0 transitions in ^{160}Yb, was of a test character, and gave a negative result. In one of the experiments [6] the Cologne plunger was mounted in EAGLE for the first time.

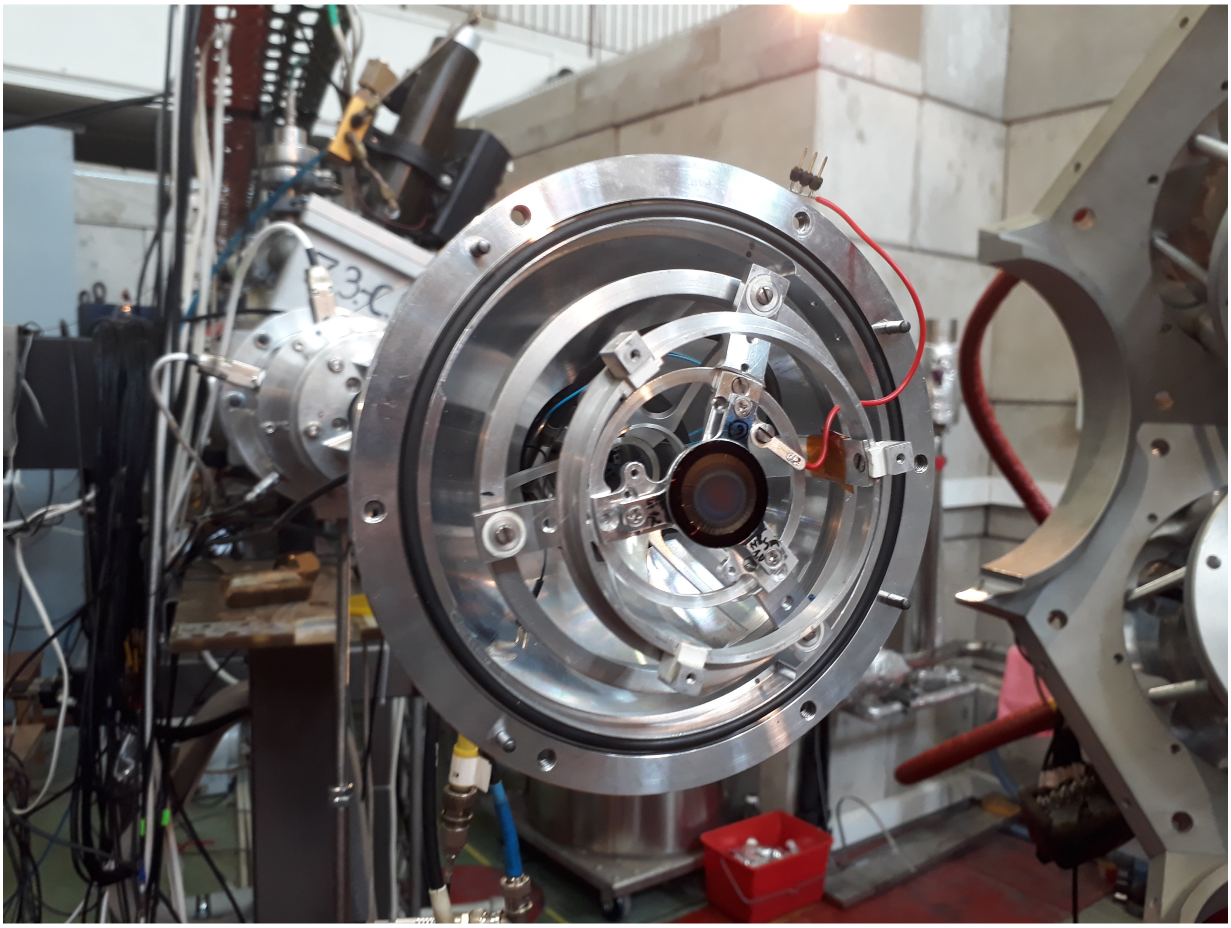

Figure 1: The Cologne plunger mounted in EAGLE.

The data acquisition system of EAGLE at present uses CAMAC based analogue units, which can serve up to 16 HPGe detectors. New digital electronics modules, developed at HIL [8, 9], should be used for the first time in experiments in 2020.

Bibliography

[1] J. Mierzejewski *et al.*, Nucl. Inst. and Meth. **A659** (2011) 84.
[2] T. Abraham *et al.*, HIL Annual Report 2016, page 17.
[3] T. Abraham *et al.*, HIL Annual Report 2017, page 14.
[4] E. Grodner *et al.*, HIL Annual Report 2018, page 53.
[5] A. Tucholski *et al.*, this Report, page 64.
[6] C. Fransen *et al.*, this Report, page 74.
[7] K. Hadyńska-Klęk *et al.*, this Report, page 53.
[8] M. Kowalczyk, HIL Annual Report 2017, page 16.
[9] T. Abraham *et al.*, HIL Annual Report 2018, page 51.

A.4 The project to replace the old RF generators with new ones

J. Choiński, A. Bednarek, T. Bracha, K. Sosnowski

Heavy Ion Laboratory, University of Warsaw, Warszawa, Poland

At the end of 2019 we completed the project to replace the old RF generators with new ones. The SAT test, started in September, proved the correct operation of the amplifiers. Currently our two RF generators consist of:

- low power stage – digital amplitude and phase stabilization system for high frequency voltage manufactured and delivered by COMtech – RDE Ltd., Poland (see Fig. 1)

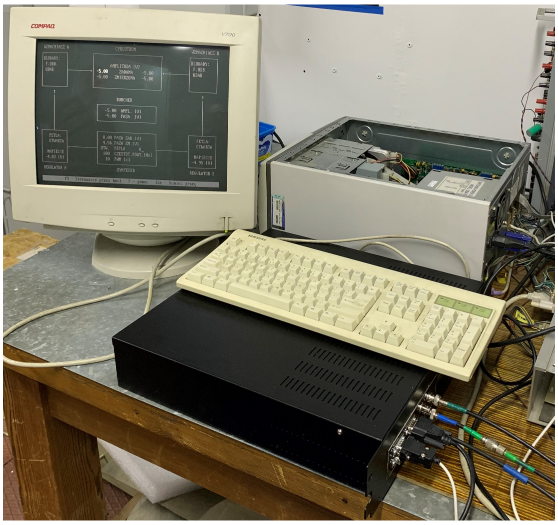

Figure 1: Digital amplitude and phase stabilization system (black box).

- medium power stage – a 4kW medium power semiconductor amplifier manufactured and delivered by Sy.E.S. System Engineering Solutlons S.r.l, Italy (see Fig. 2)

Figure 2: 4kW medium power semiconductor amplifier, part of "A" generator.

- high power stage – a 75kW high power amplifier manufactured and delivered by POPEK-ELEKTRONIK, Krzysztof Popek, Poland (see Fig. 3)

Part of generator "B" Part of generator "A"

Figure 3: The high power amplifiers.

First, the functionality of each generator was checked for a substitute load. Only after making sure that the power stages work together as expected did the cyclotron tests begin. A number of tests were carried out, which made it possible to remove noticed problems such as e.g. excitation of parasitic resonances in power tube resonance systems, see Fig. 4.

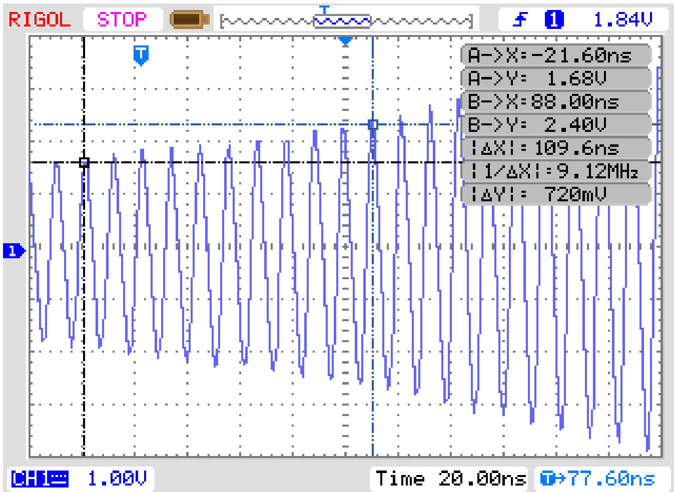

Figure 4: An example of parasitic resonance excitation in a power tube system.

Both RF generators are now operational with the cyclotron and will be further tested during scheduled experiments.

Acknowledgement

The replacement of the old RF generators with new ones was financed by the Ministry of Science and Higher Education, agreement no 589/FNiTP/540/2011.

A.5 A project for an internal, well cooled, target station for the U-200P cyclotron suitable for irradiation of different types of targets

J. Choiński, B. Radomyski, A. Pietrzak, A. Jakubowski, M. Antczak, T. Bracha, P. Jasiński, R. Kopik, K. Łabęda, Ł. Świątek

Heavy Ion Laboratory, University of Warsaw, Warszawa, Poland

For several years, the Heavy Ion Laboratory has been involved in medical radioisotope production, mostly Astatine-211 utilizing the alfa-particle beam from the U-200P cyclotron. During the last year we replaced the simple station which was designed for target irradiation utilizing internal beams of the cyclotron with a new one. This was done because the old station had several disadvantages, for example, a very weak water cooling system and all activities had to be done manually. This new station allows as to irradiate a target with the maximal available current of the internal beam. The range of available irradiation radii of the target can vary from 70 cm up to the maximum extraction radius, 85 cm. Currently, the system consists of a vacuum chamber, a target holder with tilted target, a drive system for the target holder, a drive system for the target station, valves, vacuum meters, water cooling system and main control system. A target can be clamped in the target holder with the help of the remotely controlled drive system of the target holder. The target holder can be positioned inside the cyclotron valley with the help of the remotely controlled drive system of the target station. The construction of the current version of the target holder with a metallic target should be strong enough to withstand about 500 W. Typically we use a beam of alpha particles with an energy about 33 MeV. During a target irradiation among others the beam current is monitored (on-line). Our remotely controlled system is an autonomous system based on a PLC controller. The station is attached to the cyclotron vacuum chamber, see Fig. 1.

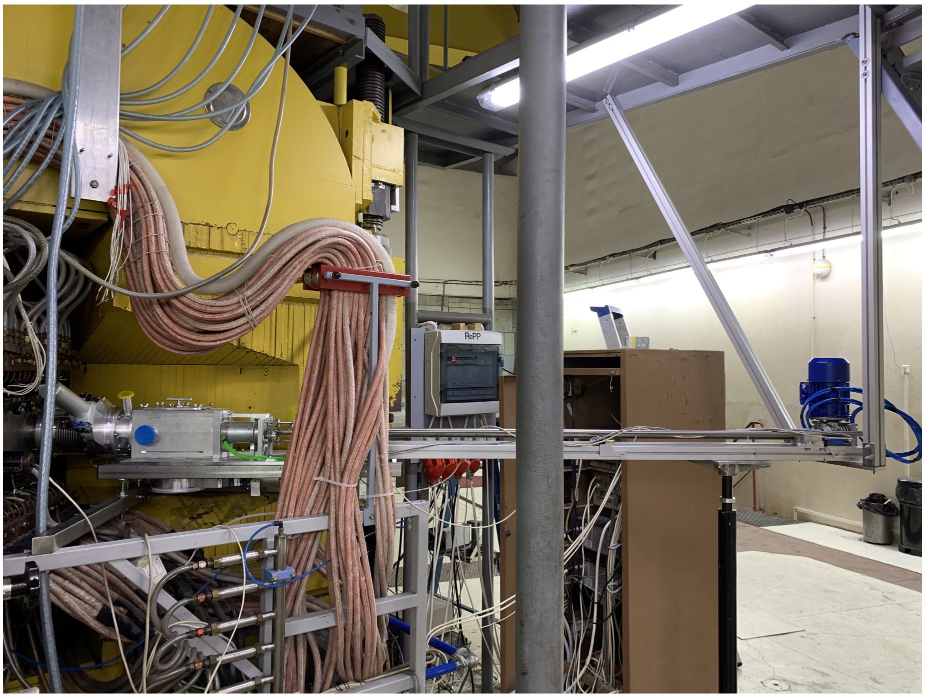

Figure 1: A view of the target station for the U-200P cyclotron.

In the coming year we will complete the GUI for communication between the operator of the station and the autonomous system based on the PLC controller. At the earliest opportunity, when the cyclotron is opened, we will mount a guide for the target head that will ensure the target head moves in the median plane of the cyclotron. The first experiment with the new station is expected in the first half of next year.

A.6 XXIII Warsaw Science Festival at HIL

M. Komorowska[1,2], P.J. Napiorkowski[1], A. Sentkowska[1], G. Jaworski[1], K. Hadyńska-Klęk[1], K. Wrzosek-Lipska[1]

1) Heavy Ion Laboratory, University of Warsaw, Warszawa, Poland
2) Institute of Experimental Physics, University of Warsaw, Warszawa, Poland

For many years the Heavy Ion Laboratory has participated in the Warsaw Science Festival [1]. This 10-day event is held annually during the penultimate week of September. It is the biggest science popularisation event in Poland. The Festival originated in 1996 with 72 meetings organised by 44 research institutions. Over the years the project has grown significantly and at present about 100 institutions are involved in over 700 meetings. In 2019 the XXIII edition of the Festival took place from 20–29 of September [2]. Four Festival Lectures for primary and secondary school students were organised:

- Physics for goalkeepers, given by P.J. Napiorkowski
- Is Mendeleev's table complete, given by P.J. Napiorkowski
- Accidents will happen – accidental discoveries in chemistry, given by A. Sentkowska
- Do you really know how to make tea? A few words about the antioxidant properties of tea, given by A. Sentkowska

During an open Weekend Festival Meeting Heavy Ion Laboratory staff gave tours of the Cyclotron and Experimental Hall preceded by a screening of a popular science movie "The Mysterious World of Atomic Nuclei" ("Tajemniczy Świat Jąder Atomowych" [3] written and directed by J. Grębosz from The H. Niewodniczański Institute of Nuclear Physics PAN, Kraków, Poland). The lectures and the weekend meetings were attended by 273 and 130 participants, respectively.

Bibliography

[1] Warsaw Science Festival https://festiwalnauki.edu.pl
[2] XIII Warsaw Science Festival at HIL http://slcj.uw.edu.pl/pl/xxiii-festiwal-nauki/
[3] "Tajemniczy Świat Jąder Atomowych" https://www.ifj.edu.pl/private/grebosz/film_jadra_pol.html

A.7 Polish Workshop on the Acceleration and Applications of Heavy Ions

J. Samorajczyk-Pyśk[1], T. Abraham[1], M. Filipek[1,2], P. Gmaj[1], K. Hadyńska-Klęk[1], G. Jaworski[1], K.W. Kemper[3], K. Kilian[1], M. Komorowska[1,2], K. Krutul[4], P.J. Napiorkowski[1], M. Palacz[1], M. Paluch-Ferszt[1], K. Rusek[1], A. Sentkowska[1], A. Stolarz[1], Z. Szefliński[1], R. Tańczyk[1], A. Trzcińska[1], D. Wójcik[1,2]

1) Heavy Ion Laboratory, University of Warsaw, Warszawa, Poland
2) Faculty of Physics, University of Warsaw, Warszawa, Poland
3) Physics Department, Florida State University, Tallahassee, USA
4) University of Białystok, Białystok, Poland

The 15th edition of the Polish Workshop on the Acceleration and Applications of Heavy Ions was organised at HIL in October, 2019. It was addressed to students of first cycle studies interested in nuclear physics, and offered a unique opportunity to gain experience in methods of data acquisition and analysis and charged particle and gamma-ray detection techniques. Medical applications of nuclear physics were also included in the programme of the Workshop.

This time 16 students attended the lectures and the practical training (see Fig. 1). There were 4 students from the University of Warsaw, 4 from the University of Zielona Góra, 3 from the Jagiellonian University in Kraków, 4 from the Maria Curie-Sklodowska University, and one student from the Poznan University of Technology.

In 2019, the programme of lectures was as follows:

- HIL in a nutshell (K. Rusek);
- Nuclear physics is an international science (K.W. Kemper);
- Radioprotection at the HIL (R. Tańczyk);
- Targets for research in nuclear physics (A. Stolarz);
- Detection of gamma radiation, charged particles and neutrons (M. Palacz);
- In-beam gamma spectroscopy (P. Napiorkowski);
- Radiopharmaceuticals for Positron Emission Tomography (K. Kilian);
- Nuclear reactions (K. Rusek);
- Bilogical response in vitro cell lines irradiated by heavy ions (Z. Szefliński);

Students took part in the following experimental tasks:

- Study of the Radiation Hardness Performance of PiN diodes in interaction with heavy ions;
- Gamma spectroscopy with the EAGLE multidetector setup;
- Targets: production and thickness measurements;
- Measurement of ^{137}Cs activity in environmental samples;

- Fast neutron detection;
- Gamma camera — a medical imaging tool.

As usual, the Workshop was completed by the student presentations session.

Figure 1: Participants in the 15th Polish Workshop on the Acceleration and Applications of Heavy Ions (photo. K. Łabęda).

A.8 Conference on the Future of Low-Energy Nuclear Physics in Poland and the Development of the National Research Infrastructure

U. Kaźmierczak and K. Rusek the chairman of the organizing committee

Heavy Ion Laboratory, University of Warsaw, Warszawa, Poland

The conference was held at the Heavy Ion Laboratory of the University of Warsaw on 14–15 January 2019. It was organized by the Nuclear Physics Section of the Polish Physical Society, the Heavy Ion Laboratory of the University of Warsaw and the Institute of Nuclear Physics of the Polish Academy of Sciences. The main aim of the conference was to integrate Polish nuclear scientists around research which in the immediate or near future could be conducted in Poland. As a follow-up to this meeting a " White Paper" could be prepared which will discuss future research in the area of nuclear physics, conducted by means of the national research infrastructure.

Figure 1: "The future of low-energy nuclear physics in Poland and the development of national research infrastructure" conference participants (photo by W. Trzaska).

The conference received a warm response from Polish nuclear scientists. 116 participants (see Fig. 1) attended this two-day event, among them a large number of young scientists (PhD students and postdoc fellows), representing 20 institutions conducting research in this area. 52 papers and 12 posters were presented.

One of the most important sessions was that devoted to the research infrastructure available in the country as well as its planned development. The following were presented: the Cyclotron Centre Bronowice (CCB) at the Institute of Nuclear Physics of the Polish Academy of Sciences in Krakow, the National Centre for Nuclear Research in Świerk, the eLBRUS laboratory of the University of Szczecin and the Heavy Ion Laboratory of the University of Warsaw (HIL). The most important presentation was the project to replace the operating U-200P cyclotron at HIL with a new machine. The aim is to ensure a higher intensity of ion beams with better energy parameters as well as an extended variety thereof. This project has been dubbed “HIL@ECOS”, with reference to the European ECOS project from the FP7 EURONS programme, recommended by The Nuclear Physics European Collaboration Committee (NuPECC). “HIL@ECOS” has received support from NuPECC, ZIBJ Dubna as well as numerous Polish institutions: the Polish Physical Society, the Jagiellonian University, the National Centre for Nuclear Research, the Institute of Nuclear Physics at the Polish Academy of Sciences, the University of Lodz, the University of Silesia and the University of Warsaw. The project has been submitted to the Ministry of Science and Higher Education with a motion to include it in the Polish Roadmap of Research Infrastructure. One of the last items on the agenda was a 90-minute discussion panel moderated by A. Maj and K. Rusek. Speakers that conducted the respective thematical sessions as well as many other conference participants took part in this discussion. Many challenges that face Polish nuclear physics were presented during the heated debate.

To conclude, prof. Marek Lewitowicz (GANIL, chair of NuPECC) summarized the most important items of the conference. An important request resulting directly from various discussions held at the conference was highlighted, the need to expand the available research infrastructure in the country. The new accelerator should enable experiments to be conducted in the following range of basic research: nuclear reaction mechanisms in simple and complex systems, gamma spectroscopy, and research into superheavy elements, among others. Among the potential plans to use the new accelerator one should mention interdisciplinary applications of nuclear physics, such as research into new radiopharmaceuticals, materials research or the post-radiation analysis of damage in biomaterials exposed to radiation. In response to a demand expressed by the scientists, the new device should provide a broad range of ions and energies as well as ensure appropriate high-intensity beams. The accelerator which fulfils those requirements best seems to be a state-of-the-art heavy-ion accelerator, for instance the DC-280 cyclotron undergoing current testing at the JINR in Dubna. The ambitious project of installing a new accelerator at the HIL will attract interest from a great number of scientists from Poland and abroad.

The conference contributed to the integration of Polish nuclear scientists and highlighted the necessity to organise such meetings on a regular basis. Details of the conference are available at the website: `http://slcj.uw.edu.pl/pl/konferencja-slcjecos/`.

A.9 ENSAR2-NUPIA Workshop "Nuclear Physics Research-Technology coaction 2"

T.J. Krawczyk, M. Paluch-Ferszt, P.J. Napiorkowski, J. Matuszczak, the organisers of the workshop

Heavy Ion Laboratory, University of Warsaw, Warszawa, Poland

The University of Warsaw organised the first "Nuclear Physics Research-Technology Coaction" workshop on 11–12 October 2018 in Warsaw, Poland at the Heavy Ion Laboratory of the University of Warsaw. The workshop "Nuclear Physics Research-technology coaction" was a space for a Laboratories-Industry meeting. The second "Nuclear Physics Research-Technology Coaction 2" workshop took place on 6–8 November 2019 at Seville in Spain. The workshop was organized by the Heavy Ion Laboratory of the University of Warsaw and the Centro Nacional de Aceleradores (CNA) laboratory as part of the Nuclear Physics Innovation ENSAR2 (NuPIA-ENSAR2) activity. As in Warsaw, the workshop supported a "Nuclear Physics Innovation-Seville" brokerage event for scientists and industry prepared by the Enterprise Europe Network. Brokerage meetings were organized by the DELab UW Enterprise Europe Network and Agencia Andaluza del Conocimiento - Junta de Andalucia Enterprise Europe Network.

Keynote speakers from nuclear-physics research centres and technology companies presented the current state-of-the-art in research techniques and proposed commercial solutions. Achievements in both fields were presented to attract prospective customers and collaborators. During the workshop directions for the improvement of methods of technology transfer between laboratories and industry were discussed.

Figure 1: Participants in the "Nuclear Physics Research-Technology coaction" ENSAR2-NUPIA Workshop.

During the workshop 25 presentations were presented focusing on aspects of cooperation between science and industry (see Fig. 1). Laboratory presentations were presented with particular emphasis on research infrastructure and services offered to industry, and scientific presentations on new discoveries that may lead to or require new industrial products; company presentations on new products that may be useful in current research, and presentations of successful cooperation between research institutions and industry. (Agenda: `https://www.ensar2-nupia.eu/workshop-sevilla`).

The workshop enabled recent achievements and challenges in the following areas to be presented:

- Medicine;
- Radiopharmaceutical production;
- Detectors and nuclear instrumentation;
- Computation and information technology (Big data application, data analysis);
- Energy and environmental technologies;
- Radiation;
- Lasers;
- Numeric machine tools and 3D printing – services;
- Metallurgy;
- Collaborative research, innovation networks, technology transfer.

The brokerage event at Nuclear Physics Innovation brings together scientists and companies (buyers as well as suppliers) from a large number of European countries. This is a unique opportunity to generate new cooperation contacts and contracts. Meetings took place in a dedicated area and were arranged in advance by means of this website `https://nupinno-sevilla.b2match.io/`

The nuclear physics laboratories had the chance to establish links with international industry and SMEs. The goal of a brokerage event is to create a strong network of laboratories and industrial partners in close relation with each other (better knowledge of existing facilities for industrial users, wider market for technology transfer possibilities).

During the workshop, 31 bilateral meetings (brokerage meetings) were organized between researchers and companies in which 23 participants took part (`https://nupinno-sevilla.b2match.io/`). The purpose of the bilateral meetings was to establish initial contacts that may lead to further research cooperation and to intensify the transfer of innovative technologies.

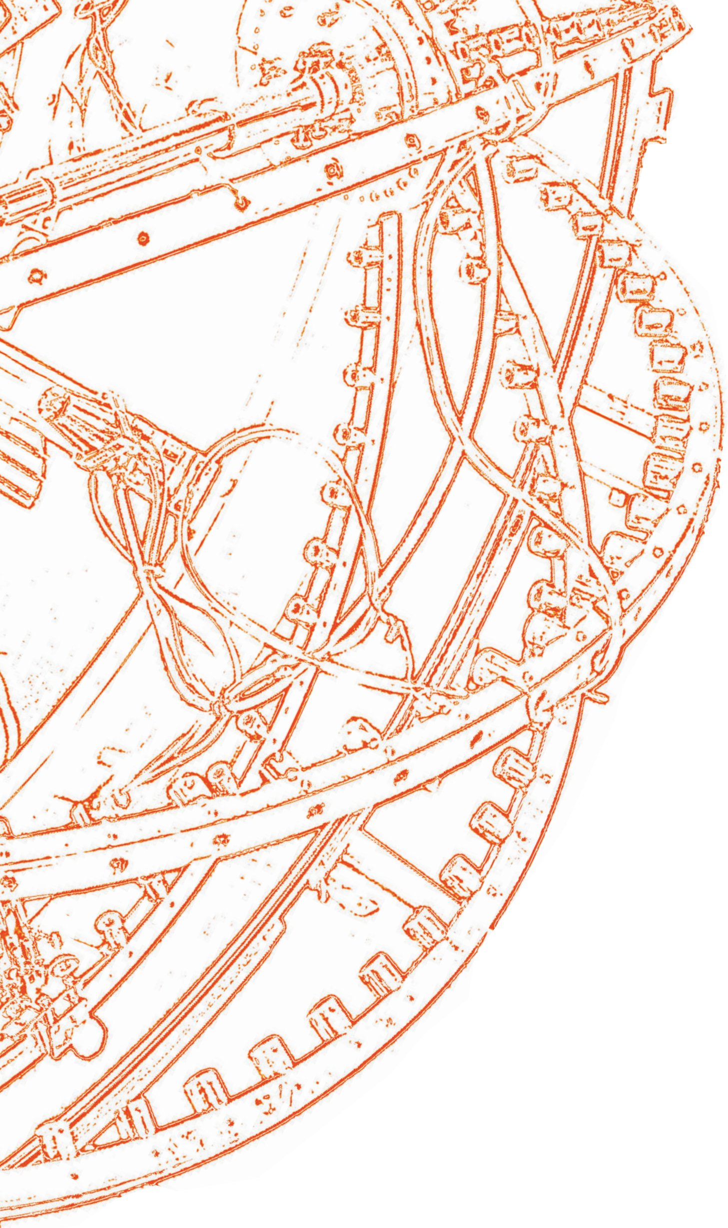

Part B
Research for medical and biological applications

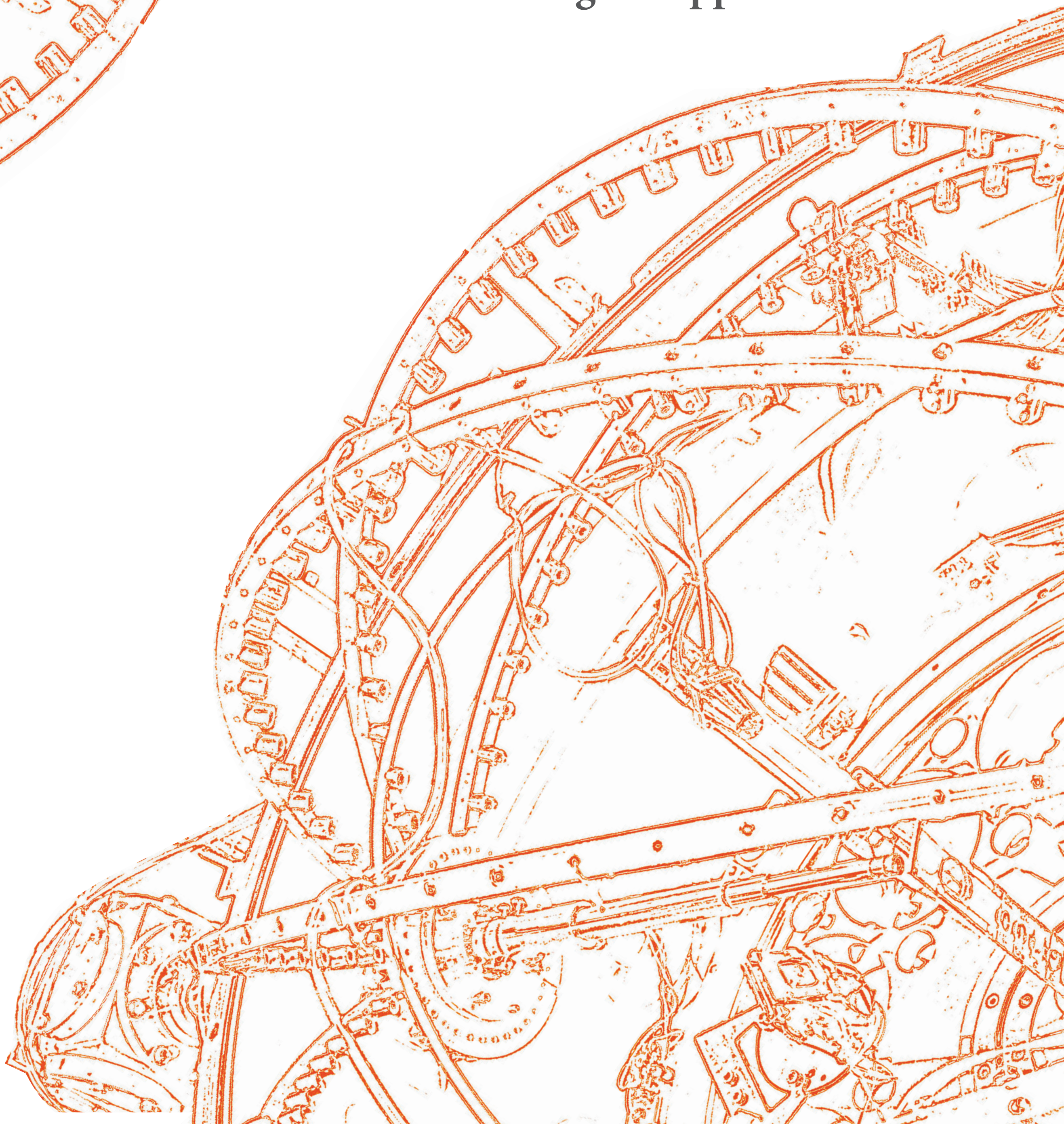

B.1 An external, well cooled, target holder for the PETtrace cyclotron suitable for irradiation of powder targets

J. Choiński, T. Bracha, B. Radomyski, Ł. Świątek, A. Stolarz, R. Tańczyk

Heavy Ion Laboratory, University of Warsaw, Warszawa, Poland

In addition to the standard targets (^{18}F, ^{11}C and ^{15}O) the PETtrace cyclotron is equipped with a standalone external target system designed for irradiation of both metal and powder targets. This target system is protected by RP patent no 227402. The dual beam proton/deuteron cyclotron is mainly used for commercial production of fluorine, ^{18}F. The Heavy Ion Laboratory team performs production of other radioisotopes in the intervals between regular production of ^{18}F. The external target system is connected to the cyclotron via a beam line consisting of: a drift tube of length a total of 3.4 m, two sets of steering magnets made of permanent magnets, one quadrupole doublet and a four-sector collimator, with shielding provided by a concrete wall of thickness 0.25 m (its specific weight is 3300 kg/m^3). This protective wall improves substantially the safety conditions for the centre staff, see Fig. 1. The beam line with the target station has its own autonomous vacuum system which allows a static vacuum of 4 x 10^{-7} mbar to be reached.

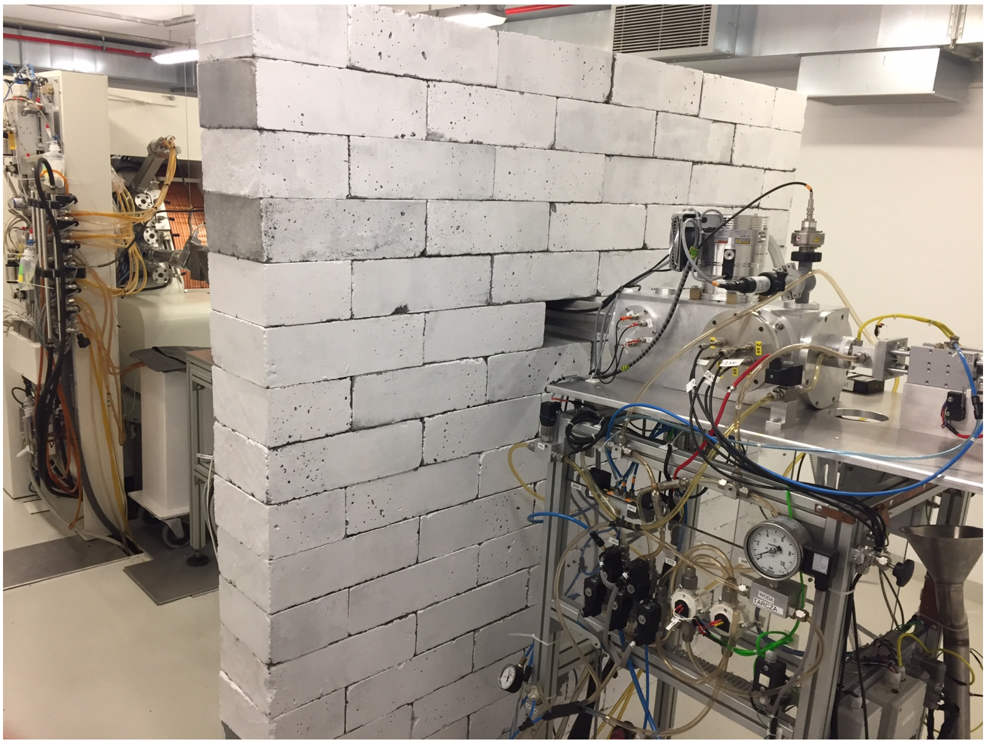

Figure 1: A view of the standalone external target system.

The beam transport efficiency to the 12 mm target is greater than 96%.

A fully remotely controlled robot loading the target into its position is an integral part of the target system. It is able to deliver the chosen target from an eight position carousel to the head of the target system. From the screen of the control panel one can choose the control panel of the robot ("Podajnik") where the arm of the robot and the carousel are depicted (see Fig. 2).

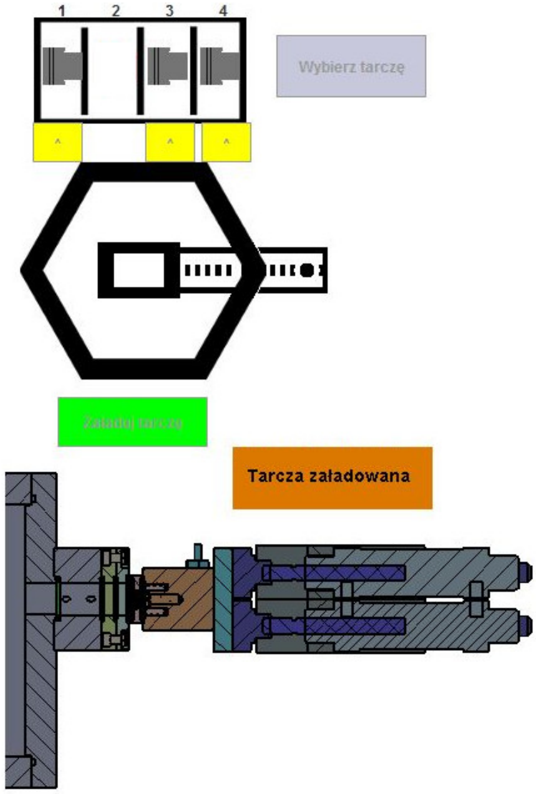

Figure 2: The control panel of the robot.

After irradiation the target drops into a lead container and is evacuated from the cyclotron vault on a remotely controlled trolley.

Last year we performed a few irradiations of targets for research groups cooperating with us, producing ^{135}La, ^{43}Sc and ^{44}Sc isotopes. This limitation of our activity was caused by the change of the company responsible for the daily commercial production of FDG. Based on experience gained, the GUI of the control system was upgraded making it more transparent and user-friendly, see Fig. 3.

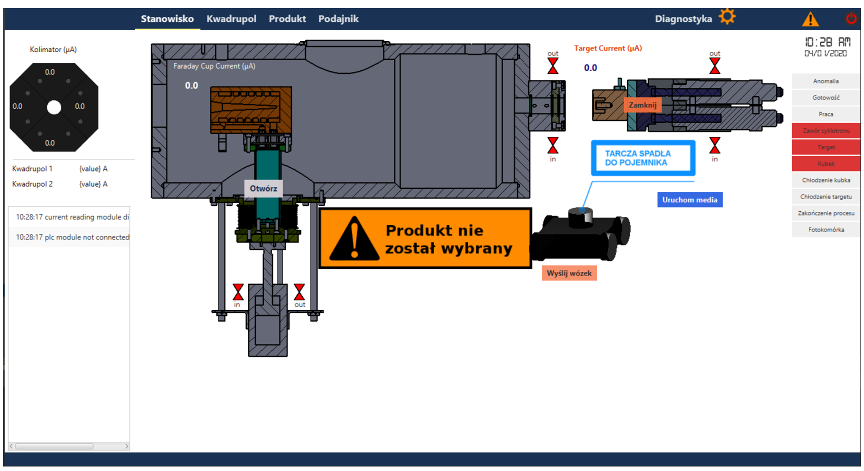

Figure 3: The upgraded GUI of the control system.

B.2 Scandium complexes with flavonoids for medical diagnostics

M. Adamowicz[1], A. Sentkowska[2], K. Kilian[2], K. Pyrzyńska[1]

1) Faculty of Chemistry, University of Warsaw, Warszawa, Poland
2) Heavy Ion Laboratory, University of Warsaw, Warszawa, Poland

Positron Emission Tomography (PET) belongs to the group of the most modern, non-invasive medical diagnostic techniques in which radiopharmaceuticals based on various radioisotopes are used. The widely used ^{68}Ga has too short a half-life (68 min). Hence the proposal to use radiopharmaceuticals based on ^{43}Sc and ^{44}Sc radionuclides, which have a much longer half-lives of 3.89 h and 3.93 h, respectively.

The complexation reaction of scandium (III) ions with a representative of the flavonoid group – morin (3, 5, 7, 2', 4'-pentahydroxyflavone) in various solutions was investigated. As a result of this research, it was possible to determine the optimal reaction conditions for complexing scand ions with morine, based on a series of absorption spectra. These conditions are borate buffer at pH = 6 with 75% ethanol content (Fig. 1A) and ammonium formate at pH = 5 with 75% ethanol content (Fig. 1B).

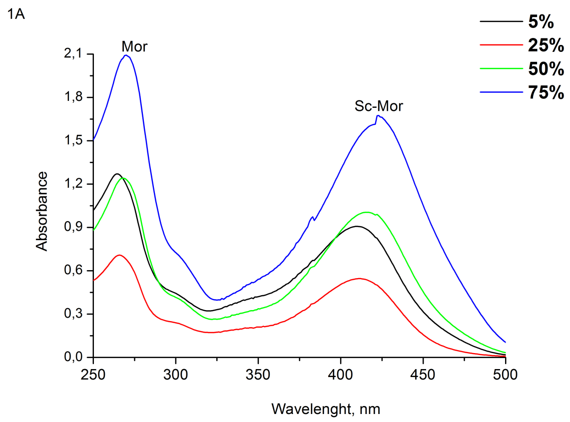

Fig. 1A

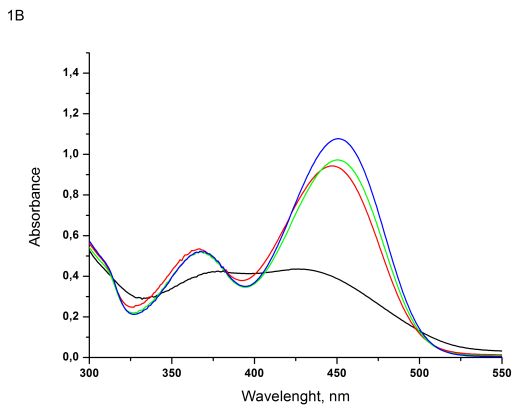

Fig. 1B

Figure 1: UV spectra of Sc-Morin complexes for different content of ethanol in borate buffer pH 6 (Fig. 1A) and ammonium formate pH 5 (Fig. 1B).

By using the Job and Jones method, the molar ratio of the complexes was determined. The complex, which was formed in a borate buffer (pH = 6 with 75% ethanol) was characterized by a metal to ligand ratio of 1:1. However, under conditions of ammonium formate (pH = 5 with 75% ethanol content) the complex is formed in the ratio of 1:2 according to the Job method, and in a ratio of 4:5, based on the Jones method. To determine the exact composition of the resulting complexes, mass spectra should be performed.

The results obtained give hope for the use of the complexes obtained under specific conditions in medical diagnostics. Further research undertaken in this direction should focus mainly on determining the optimal conditions for the complex synthesis process and the possibility of its separation from excess ligand.

B.3 Changes in the properties of superconducting 2G HTS tapes under the influence of ^{12}C ions - further research

M. Paluch-Ferszt[1], M. Kowalik[2], Z. Szefliński[1], U. Kaźmierczak[1], M. Filipek[1,3], W. Tokarz[2], J.M. Michalik[2], R. Zalecki[2], M. Giebułtowski[2], J. Niewolski[2], W.M. Woch[2]

1) Heavy Ion Laboratory, University of Warsaw, Warszawa, Poland
2) AGH University of Science and Technology, Kraków, Poland
3) Faculty of Physics, University of Warsaw, Warszawa, Poland

Superconductors and superconducting materials are metals, ceramics, organic materials, or heavily doped semiconductors that conduct electricity without resistance. Superconducting materials can transport electrons with no resistance, and hence release no heat, sound, or other energy forms. Superconductivity occurs at a specific critical temperature T_c for a given superconducting material. As the temperature decreases, a superconducting material's resistance gradually decreases until it reaches the critical temperature. At the present time, most materials must achieve an extremely low energy state via low temperatures and/or high pressures in order to achieve superconductivity.

Superconductors are classified into first generation (1G) and second generation (2G) materials. 1G metals achieve superconductivity through slowing down molecular activity via low temperatures. According to BCS theory [1], this creates an environment conducive to Cooper pairing so that electron pairs are able to overcome molecular obstacles, leading to free electron flow without an applied voltage. Copper, silver, and gold are three of the best metallic conductors but are not superconductive. This is due to their face-centered cubic (FCC) [2] unit cell lattice structures, which are so tightly packed that the low-temperature lattice vibrations essential to superconductivity fail to coerce free electrons into Cooper pairs. While some FCC metals such as lead are capable of superconductivity, this is due to outside factors such as lead's low modulus of elasticity.

2G materials are metallic compounds or alloys, although elemental vanadium, technetium, and niobium also fall within this group. They are capable of superconductivity at much higher critical temperatures. More common Type II materials have critical temperatures within the 10–130 K range. As of 2015 there is no scientific consensus as to the reason for these higher critical temperatures. 2G materials also take on a mixed state, which contrasts with plunging resistance at T_c for 1G materials, when approaching their critical temperature. Mixed states are caused by the fact that 2G superconductors never completely expel magnetic fields, so that microscopic superconducting "stripes" can be seen on the material.

2G high temperature superconductor tapes (HTS) allow the generation of strong magnetic fields that do not require the use of a high-power direct current power supply, just like typical electromagnets. The tape is 12 mm wide and has the thickness of a sheet of paper. It can conduct up to 600 A current at a temperature of 77 K before the superconducting state is destroyed [3].

The $REBa_2Cu_3O_{7-x}$ superconductor tape, also called "(RE)BCO", is produced by the ion beam-assisted deposition (IBAD) and metal-organic chemical vapour deposition (MOCVD) processes [4]. The tape structure is shown in Fig. 1.

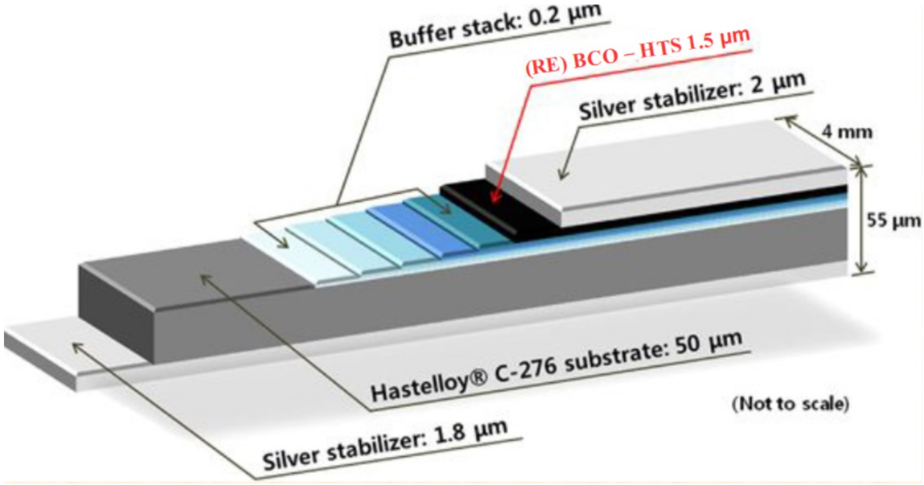

Figure 1: Schematic drawing of the (RE)BCO tape structure [7].

The small dimensions and weight of the tape are very promising features for use in the construction of magnetic shields protecting crews of spacecraft against cosmic radiation [5]. These (RE)BCO tape studies are a continuation of the experiment from last year [6].

Rectangular shaped samples of 2G HTS tapes were 10 mm long and had a width of 6 mm. Seven samples were inserted into the irradiation chamber in one experimental run. The samples were mounted in a Carousel and inserted in the vacuum chamber. The Carousel with tapes is shown in Fig. 2. Irradiation was carried out at the maximum kinetic energy of ^{12}C ions and also maximum fluence (number of particles per square cm per second) Tab. 1. The time of irradiation (dose rate) was about 18 hours to irradiate a sample with 10^{13} ions/cm^2. The tape was oriented in such a way that the superconducting layer was oriented towards the source of ions.

Table 1: All superconducting tape samples ((RE)BCO) irradiated with ^{12}C.

Sample no.	Average beam current	Number of ions/cm^2
1	0.6 nA	$5.3 \cdot 10^{13}$
2	0.6 nA	$5.0 \cdot 10^{13}$
3	0.4 nA	$1.7 \cdot 10^{13}$
4	1.0 nA	$1.6 \cdot 10^{13}$
5	0.92 nA	$2.7 \cdot 10^{13}$
6	0.87 nA	$1.8 \cdot 10^{13}$
7	0.2 nA	$2.6 \cdot 10^{12}$
8	Control sample	

In cooperation with the AGH University of Science and Technology in Cracow the superconducting properties of the irradiated samples will be studied by AC and DC magnetic susceptibility and magneto-transport measurements. Superconducting parameters such as the critical temperature T_c, T_{c0}, and critical current density J_c will be evaluated. The microstructure of the tapes and structural damage resulting from irradiation will be examined by scanning electron microscopy.

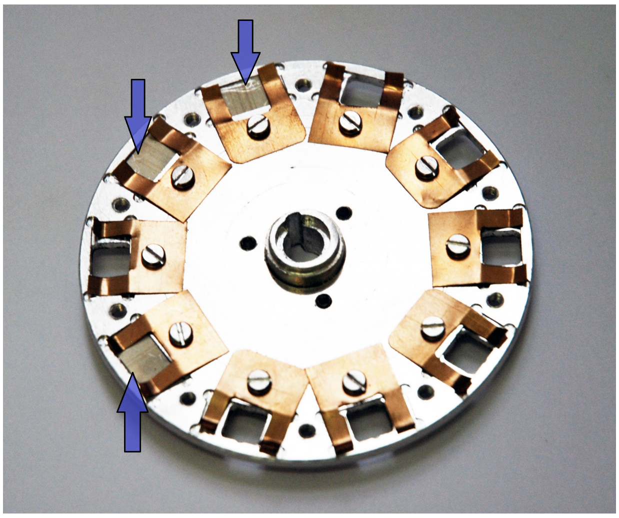

Figure 2: 3 samples of 2G HTS monuted on the Carousel.

Bibliography

[1] J. Bardeen, L.N. Cooper and J.R. Schrieffer, Phys. Rev. **108** (1957) 1175.
[2] P.M. de Wolff *et al.*, Acta Crystallographica **A 41** (1985) 278.
[3] D.W. Hazelton, http://www.superpower-inc.com/system/files/WAMHTS1.pdf
[4] http://www.superpower-inc.com/system/files/2010+DOE+Peer+Rev_2G+FINAL.pdf
[5] R. Battiston *et al.*, https://arxiv.org/abs/1209.1907.
[6] M. Paluch-Ferszt *et al.*, HIL Annual Report 2018, page 36.
[7] http://www.superpower-inc.com/system/files/2011_0913+MT22+2CO-3+Hazelton.pdf.

B.4 Study of the biological response of glioblastoma cells irradiated with alpha particles from ^{241}Am and a ^{12}C ion beam - preliminary research

M. Paluch-Ferszt[1], Z. Szefliński[1], U. Kaźmierczak[1], M. Filipek[1,2], J. Braziewicz[3] A. Lankoff[4]

1) Heavy Ion Laboratory, University of Warsaw, Warszawa, Poland
2) Faculty of Physics, University of Warsaw, Warszawa, Poland
3) Institute of Physics, Jan Kochanowski University, Kielce, Poland
4) Institute of Nuclear Chemistry and Technology, Warszawa, Poland

Glioblastoma multiforme (GBM; World Health Organization grade IV glioma) is the most common, highly invasive and malignant entity, making it the most aggressive primary brain tumour with very poor prognosis. Even for selected patients receiving optimal surgery followed by temozolomide-based chemoradiotherapy according to the EORTC trial 26981/22981-NCIC, survival remains poor, with a median survival that does not exceed 15 months [1]. Several in vitro studies have investigated the biological response of GBM cells to photon irradiation. Most of these studies focused on a limited aspect of the biological response and on only 2 or 3 cell lines [2, 3]. These limitation are even more highlighted for hadrontherapy because of its novelty and the difficulty of access to platforms [4]. Due to a better dose distribution in the tumour volume and a high relative biological effect (RBE) for cell killing, hadrontherapy with carbon ions seems to be particularly promising [5]. Because very few hadrontherapy centres exist, the number of biological and clinical studies is limited.

Therefore, molecular and cellular investigations of GBM are required in order to improve the prediction and treatment of brain tumours [6]. According to the cancer stem cell (CSC) hypothesis, the high recurrence rate and the failure of conventional treatments are expected to be related to the presence of radio-resistant CSCs inside the tumour mass. Cancer stem cells have the ability to self-renew and maintain tumour growth. Therefore, cancer treatment should be aimed not only at eliminating the bulk of cycling and differentiated cancer cells but also especially to the eradication of the stem cell population. Their resistance to chemical and radiation treatments makes CSCs the main target of more effective therapies, among them hadrontherapy [7].

The aim of our study was to increase knowledge of the radiobiological response of human CSCs from GBM to charged particles, investigating the mechanisms involved in the cellular and molecular long-term responses of glioblastomas to hadrontherapy in order to understand better the biological effects of carbon beams in cancer treatment and later to individualize appropriate radiotherapy treatment for patients who are good candidates.

GBM stem cells (GSCs) were isolated from surgical samples of patients with similar tumour location, gender and age but different clinical outcomes (cooperation with the Neurosurgery Unit of the 10th Military Research Hospital and Polyclinic in Bydgoszcz).

Prior to the essential research described above, it is necessary to perform preliminary studies, based on commercial cell lines. To investigate the mechanisms involved in the molecular and cellular responses of GBM to ionising radiation, in the proposed preliminary research two GBM cell lines (radiosensitive and radiation resistant) were irradiated with:

- alpha particles from an ^{241}Am surface radiation source with a diameter of 5 cm (diagram of the experimental system in Fig. 1);
- a carbon ion beam (^{12}C) from the U-200P cyclotron (diagram of the experimental system in Fig. 2).

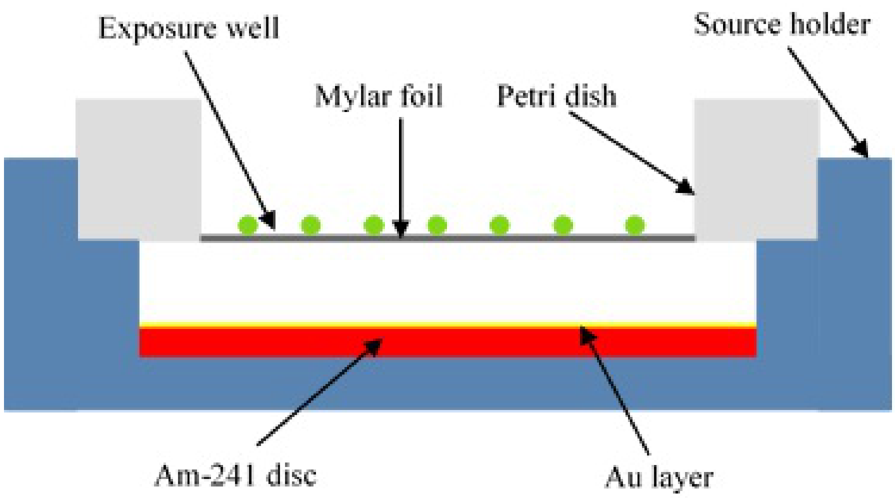

Figure 1: Schematic view of the irradiation with an ^{241}Am source for radiobiological studies at HIL [8].

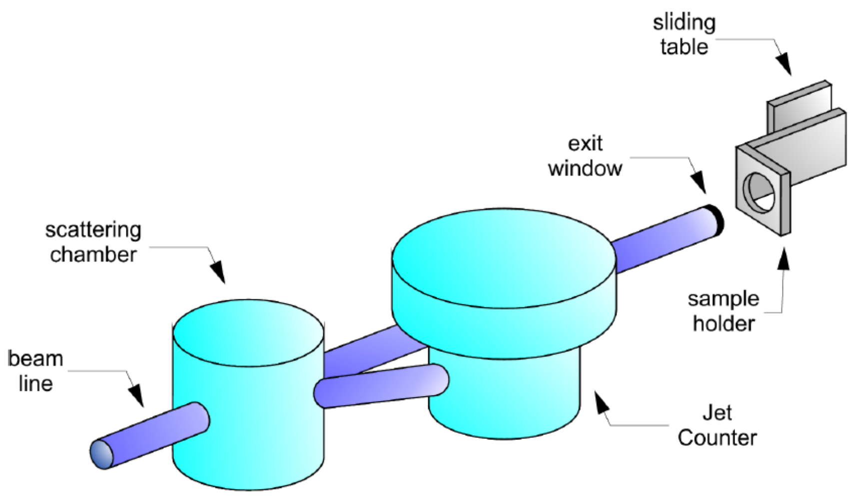

Figure 2: Schematic view of the setup with the horizontal beam line from the U-200P cyclotron for radiobiological studies at HIL [9].

The following biological effects will be analysed: cell death and DNA damage induction and repair.

The preliminary research presented above is necessary for further experiments. The subsequent stages of research are planned and they will be implemented with the cooperation of several national research centres with the expected acquisition of funding within the NCN, NCBiR and the Polish Science Foundation.

Bibliography

[1] R. Stupp, *et al.*, Lancet Oncol. **10** (2009) 459–466.
[2] S. Palumbo *et al.*, J. Cell. Biochem. **113** (2012) 2308–2318.
[3] O. Lanvin *et al.*, Eur. J. Cancer **49** (2013) 2884–2891.
[4] T. Oishi *et al.*, Cancer Res. **71** (2011) 3676–3687.
[5] X. Cui *et al.*, Cancer Res. **71** (2011) 3676–3687.
[6] S. Ferrandon *et al.*, Cellular and molecular Cancer Letters **360** (2015) 10–16.
[7] T. Pecchia *et al.*, Rad. Prot. Dos. **166 (1–4)** (2015) 374-378.
[8] Z. Szefliński *et al.*, RAP Conference Proceedings, **4** (2019) 7–9.
[9] U. Kaźmierczak *et al.*, Acta Phys. Pol. **A 127** (2015) 1516–1519.

B.5 Comparative Study of Ionic Liquid Extraction of Chlorogenic Acid from Different Plant Materials

A. Sentkowska[1], *K. Pyrzyńska*[2]

1) Heavy Ion Laboratory, University of Warsaw, Warszawa, Poland
2) Faculty of Chemistry, University of Warsaw, Warszawa, Poland

Over the past few years, ionic liquid solvents (ILs), a class of chemicals composed entirely of an asymmetric large-size organic cation with an anion of weak coordination properties, have received explosive interest as alternatives to traditional organic solvents [1]. ILs are defined as substances with melting points below 100°C and often show a broad temperature range over which they are liquid. Their unique physicochemical properties include very low to negligible vapour pressure, high thermal stability and conductivity as well as those which are tunable by proper cation-anion combinations, such as density, viscosity, hydrophobicity, polarity and acid-base properties. Among all ILs, alkylimidazolium cations combined with Cl^-, Br^-, BF_4^- or PF_6^- counter ions are the most used as extractants, also for separation of phenolic acids from different plant samples [2, 5].

The objective of this study was to evaluate the efficiency of extraction of chlorogenic acid from different plant materials such as heather (*Calluna vulgaris*) flowers, green tea (*Camellia sinensis*) leaves and blueberry (*Vaccinium myrtillus*) fruits using ILs. Organic solvents (ethanol-water mixture and ethyl acetate) and two imidazolium-based ionic liquids were used for comparison. The extracts from each plant were also evaluated for the determination of total phenolic content by DPPH radical-scavenging activity.

As the anion of an ionic liquid may significantly influence the extraction yields, 1-butyl-3-methylimidazolium ($[Bmim]^+$) ionic liquids with two types of anions (Cl^- and BF_4^-) were studied. These IL anions are strong and weak hydrogen-bond acceptors, respectively. IL water solutions at a concentration of 0.5 mol/L were used as several studies have shown that the extraction efficiency increased with increasing concentration up to 0.4–0.6 mol/L where a plateau was reached [6, 7]. Plant matrices (heather flowers, tea leaves and blueberries) were chosen as they contained different CGA concentrations and different polyphenol patterns. The preliminary study was performed by a simple infusion process (which is also called maceration or soaking) conducted for 60 min at room temperature. The content of CGA in the obtained extracts of three plant materials is presented in Table 1.

Results are expressed as mean ± SD (n = 3) in mg per 100 g. Values for the same sample bearing different superscript letters represent significant differences ($p < 0.05$).

The yield of chlorogenic acid extraction from each plant material varies with the solvent used, the highest content being obtained in heather flowers for a 60% EtOH aqueous solution. The higher transfer of CGA observed for the heather sample and ILs containing the tetrafluoroborate anion compared to chloride can be explained by better rupture of that plant's cell walls, allowing improved access to the active ingredients. From the other side, [Bmim]Cl ionic liquid proved to be the optimum solvent for green tea and blueberry matrices because it extracted the highest amounts of CGA. The lowest extraction yield was obtained using ethyl acetate. The extractability of the solvent mainly depends on the solubility of the compounds in the solvent system, the mass transfer kinetics of the product and the strength of the solute/matrix interaction. The simple solid-liquid extraction process may require a long extraction time and usually higher yields and faster extraction

Table 1: Content of CGA in the studied plant materials using different extractants.

Sample	Extractant	Content
Heather flowers	60% EtOH	520 ± 2.8^a
	EtOAc	10.9 ± 0.04^b
	[Bmim]Cl	24.2 ± 1.13^c
	[Bmim]BF_4	92.5 ± 0.75^d
Green tea leaves	60% EtOH	9.10 ± 0.09^a
	EtOAc	0.21 ± 0.005^b
	[Bmim]Cl	12.8 ± 0.94^c
	[Bmim]BF_4	5.75 ± 0.14^d
Blueberry fruits	60% EtOH	3.77 ± 0.16^a
	EtOAc	1.72 ± 0.009^b
	[Bmim]Cl	34.4 ± 1.53^a
	[Bmim]BF_4	14.2 ± 0.68^c

of bioactive compounds can be achieved through ultrasound-assisted extraction (UAE). Ultrasonic time is generally regarded as a predominant factor influencing the efficiency of extraction, however, the use of UAE may have a significant impact on the stability of the extract. Chlorogenic acid was degraded under these conditions resulting in reduced yield. The peak area for CGA decreased in the order: EtOAc $<$ 60% EtOH $<$ [Bmim]Cl $\approx$ [Bmim]BF_4. Caffeic acid is formed as the product of the CGA degradation process and its content increased with prolonged time of ultrasound treatment. The effect of ultrasonic time on the chlorogenic acid signal intensity in the ethanol is presented in Fig. 1. Similar behaviour was observed for heather and green tea matrices using both ILs. Yang et al. [8] also reported reduced yield of CGA from ramie (Boehmeria nivea L.), a Chinese medicinal plant, with increasing ultrasonic treatment and acidic ionic liquids.

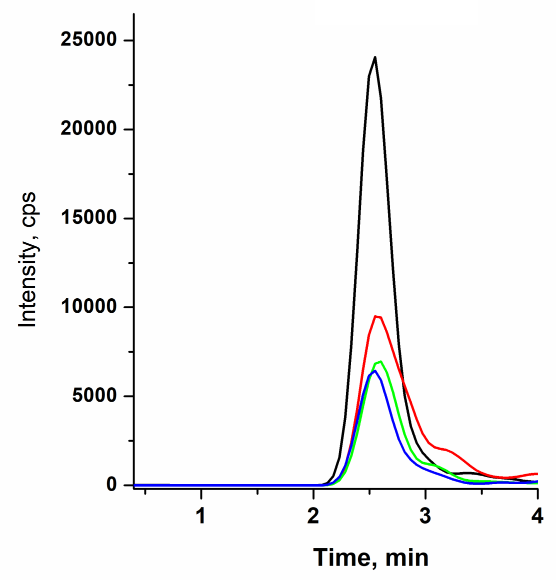

Figure 1: Peak for chlorogenic acid solution (30 mg/L) in the ethanol solution sonicated for different times.

The antioxidant activity of the extracts was also evaluated by the scavenging effect on the DPPH radicals. The highest values were recorded for green tea matrix and both ionic liquids as well as 60% ethanol. Green tea contains a significant amount of catechins, which mainly contributed to the antioxidant activity of its extracts [9]. Moreover, the high amount of chlorogenic acid and total phenolics may be explained by their high antioxidant properties. For heather flowers the scavenging effect on the DPPH increased in the order: ethyl acetate $<$ 60% EtOH $<$ [Bmim]BF_4 $<$ [Bmim]Cl and generally increases with prolonged ultrasonic extraction. On the contrary, the antioxidant activity for blueberry fruit extracts with both ionic liquids used was reduced, probably by degradation of monomeric anthocyanins. Sun et al. [10] reported that ultrasound extraction significantly degraded pelargonidin-3-glucoside, one of the major anthocyanins present in fruits, which leads to decreased antioxidant capacity. Martins and de Rosso [11] also observed a decrease of the antioxidant activity of tomato carotenoids IL extract relative to acetone extract. It should be noted that the antioxidant activity in DPPH assay for [Bmim]Cl and [Bmim]BF4 solutions alone were 50.4 and 34.0 μmol TRE/L, which was not always noted in previous work.

These studies demonstrate the usefulness of imidazolium-based ionic liquids for the extraction of chlorogenic acid from green tea and blueberry matrices in comparison to the widely used aqueous-ethanol solution or ethyl acetate. However, the CGA extraction efficiency from heather flowers was higher for 60% EtOH than for the ILs studied. Thus, the overall opinion repeated in the published papers that ILs are promising and green solvents, and may even be better than classical ones begins to become doubtful. Their performance in the sample preparation step depends on several factors such as the kind of plant material, the solute to be extracted as well as the kind of ionic liquid used. Moreover, the extracts from plant materials containing natural antioxidants can be used for nutraceutical and pharmaceutical applications or even in the food industry. Thus, a quite easy step for further isolation of these compounds from IL solutions should be considered. Thus far little is known about the toxicity of ionic liquids and their harm to humans and the environment.

It is worth mentioning that the experiments described above were aimed at testing the instrumentation and sample preparation methodologies that can be used to control the quality of radiopharmaceuticals synthezised in HIL.

Bibliography

[1] S.P.M. Ventura *et al.*, Chem. Rev. **117** (2017) 698.
[2] S.K. Shukla *et al.*, J. Chromatogr. **A 1559** (2018) 44.
[3] S.E. Arnell *et al.*, Anal. Chim. Acta **903** (2016) 90.
[4] Y. Fan *et al.*, Sep. Purif. Technol. **179** (2017) 126.
[5] T.V. Ding *et al.*, Sep. Purif. Technol. **196** (2018) 287.
[6] X.H. Wang *et al.*, Int. J. Chem. Eng. (2016) Article ID 5217802.
[7] Y. Fan *et al.*, Ind. Crops Prod. **126** (2018) 59.
[8] Z. Yang *et al.*, Ind. Crops Prod. **89** (2016) 78–86.
[9] E. Mancini *et al.*, Phytomedicine **34** (2017) 26.
[10] J. Sun *et al.*, Molecules **21** (2016) 1109.
[11] P.L.G. Martins *et al.*, Food Res. Intern. **82** (2016) 156.

B.6 The investigation of antioxidant interaction between green tea polyphenols and pharmaceuticals using isobolographic analysis and interaction indexes

A. Sentkowska[1], *K. Pyrzyńska*[2]

1) Heavy Ion Laboratory, University of Warsaw, Warszawa, Poland
2) Faculty of Chemistry, University of Warsaw, Warszawa, Poland

Commonly used painkillers known as non-steroidal anti-inflammatory drugs (NSAIDs) – a class which includes ibuprofen, naproxen, paracetamol and diclophenac – are used in both human and veterinary medicine to reduce pain and inflammation in different arthritic and postoperative conditions. Ibuprofen, introduced in 1969, was the first propionic acid derivative introduced as an alternative to aspirin [1]. Since then an increase in the development of new drugs has been observed. All analgesic and anti-inflammatory drugs produce their therapeutic effects by inhibiting various prostaglandins substances involved in the development of pain and inflammation as well as the regulation of body temperature [2]. Prolonged use of these drugs can lead to damage to certain internal organs such as the liver and kidneys [2]. It has also been found that side effects may also include gastric damage, which can be silent [3].

In this study the interactions between the commonly used NSAIDs such as ibuprofen, naproxen, diclofenac and paracetamol and green tea polyphenols were investigated using isobolographic analysis and interaction indexes. The addition of non-steroidal anti-inflammatory drugs can influence the antioxidant activity of green tea polyphenols and this depedence was the main object of this research. For this purpose two assays were used: the DPPH method and CUPRAC assay. The results of this study could be very useful in designing new drugs with the addition of polyphenolic compounds, which can prevent or minimize the negative impact of drugs on the human body.

In the case of diclofenac the observed interaction strictly depends on the ratio in which the compounds are mixed with each other when the CUPRAC method is applied. For the higher concentrations of green tea polyphenols a synergistic effect is observed. These observations were confirmed by the values of the interaction indexes (Table 1). For GT to drug ratios equal to 10:1 and 5:1 the related values of the interaction indexes are lower than 1 which suggests that a synergistic effect is observed. A concentration ratio of 2:1 showed an additive effect (interaction index equal to 1), however mixtures where the concentration of green tea was relatively low in comparison to the concentration of diclofenac showed an antagonistic effect. This was confirmed by higher than 1 values of the interaction indexes. When the results obtained for diclofenac and green tea using the DPPH assay were studied, the conclusions were totally different. In this case all the analyzed concentration ratios showed an antagonistic effect, with the exception of 1:10 (GT:D), where a synergistic effect was observed. This differences in the results obtained using both assays may be due to differences in the mechanisms of both tests. When the results obtained for ibuprofen were analyzed it turned out that depending on the test used, the results are opposite. The effect between green tea polyphenols and ibuprofen is synergistic according to the CUPRAC method and antagonistic based on the DPPH assay. In both cases the exception from the rule is the ratio 1:10 (GT:I) which showed antagonism in the CUPRAC

Table 1: Interaction indexes of studied pharmaceuticals and green tea polyphenols mixtures in different concentration ratios.

Ratio[1]	Diclofenac		Ibuprofen		Naproxen		Paracetamol	
	DPPH	CUPRAC	DPPH	CUPRAC	DPPH	CUPRAC	DPPH	CUPRAC
10:1	1.94	0.95	1.07	0.96	1.25	0.87	1.04	0.95
5:1	0.85	0.82	1.07	0.93	1.05	0.87	1.31	0.71
2:1	1.21	1.00	1.14	0.99	1.31	0.91	1.24	0.87
1:1	1.87	1.05	1.03	0.88	1.04	0.91	1.10	0.81
1:2	1.69	1.28	1.14	0.99	1.67	1.35	1.65	0.83
1:5	4.92	1.46	2.17	0.97	2.93	1.05	1.03	0.88
1:10	0.34	1.30	2.31	1.22	4.03	0.93	1.07	0.83

[1] GT: Drug ratio.

method and synergism in the DPPH assay. More diversified results were obtained for naproxen. For this pharmaceutical the data obtained using the DPPH assay suggest that the observed effect between naproxen and green tea is antagonistic for all concentration ratios studied. The situation is more complicated when the isobolograph obtained from the CUPRAC assay is analyzed. For most relationships the observed effect is synergistic, however in the middle of the studied concentration range there are some points located under the isobola related to an antagonistic effect. These points are related to concentration ratios 1:2 and 1:5 (GT:N). The same conclusions can be reached based on the interaction indexes. The data obtained for paracetamol showed some kind of similarity to the results obtained for ibuprofen. In this case the conclusions made based on the two methods used are opposite. Synergism was observed in the CUPRAC method and antagonism when the DPPH assay was used. This was confirmed by the values of the interaction indexes.

The results obtained from the DPPH results showed that the effect between the pharmaceutical and polyphenols is antagonistic. In the CUPRAC methods it was strictly dependent on the concentration ratio between the drug and green tea. However, future studies are needed to explain the interaction mechanisms of drug-green tea interactions.

It is worth mentioning that the experiments described above were aimed at testing the instrumentation and sample preparation methodologies that can be used to control the quality of radiopharmaceuticals synthezised in HIL.

Bibliography

[1] R. Bushra, N. Aslam, Oman Med. J. **25** (2010) 155.
[2] C.M. Modi *et al.*, J. Applied Pharm. Sci. **2** (2012) 149.
[3] H.P. Rang *et al.*, Pharmacology. 5th ed., 1999, page 248.

B.7 Synthesis of modified magnetic nanoparticles for separation and preconcentration of scandium

M. Pęgier[1,2], *K. Kilian*[1], *K. Pyrzyńska*[2]

1) Heavy Ion Laboratory, University of Warsaw, Warszawa, Poland
2) Faculty of Chemistry, University of Warsaw, Warszawa, Poland

In recent years there has been growing interest in the utilization of nanoparticles with magnetic properties (MNPs magnetic nanoparticles) in solid phase extraction [1]. These materials are obtained by surface modification of a magnetic core (mainly Fe_3O_4) with a sorptive material with high affinity towards analyte. These mobile sorbents can be quickly and effectively separated from solution with preconcentrated analyte using an external magnetic field. The group of compounds that can be used for modification of MNPs are flavonoids, compounds of plant origin, that have the ability to form complexes with metal ions, including scandium. Scandium is an emerging element that can be utilized not only in high-tech industry but also in nuclear medicine as a positron emitter (e.g. ^{44}Sc) for positron emission tomography (PET) diagnostics [2].

The aim of this study was the synthesis of magnetic sorbents for separation and preconcentration of scandium that contain morin, a member of the flavonoid group. Two synthetic approaches were used.

The first sorbents were Fe_3O_4 MNPs that were synthesized by mixing Fe(II) and Fe(III) ions and adding NH_3 solution under a nitrogen atmosphere. The raw MNPs were then coated with silica using TEOS resulting in Fe_3O_4@SiO_2 nanoparticles. They were functionalized with amine groups using APTES (Fe_3O_4@NH_2). The last step was covalent modification with morin in absolute ethanol in 110 which led to Fe_3O_4@SiO_2-N-morin nanoparticles.

In the second sorbent carbon encapsulated magnetic nanoparticles (CEMN) with a ferromagnetic iron core were utilized. The CEMN were further oxidized using HNO_3 to produce surface acidic groups [3]. The oxidized material (CEMN-COOH) was treated with $SOCl_2$ to obtain CEMN-COCl that was reacted with morin, resulting in the desired product CEMN-COO-morin.

Sorption of scandium(III) was studied on both sorbents. To check the influence of morin unmodified Fe_3O_4@SiO_2 and and CEMN-COOH were also used. Static experiments were performed in which a certain amount of synthesized sorbent was shaken with a scandium(III) ion solution for 4 h. Different pH conditions were checked.

Sorption curves (see Fig. 1) show that sorption of scandium increases with increasing pH. Also above pH 5 precipitiation of $Sc(OH)_3$ can occur, which gives a contribution to total retention on the sorbent. Fe_3O_4@SiO_2-N-morin shows poor results. Sorption is generally low and does not exceed 20%. Sorption of Sc(III) on unmodified Fe_3O_4@SiO_2 is much higher. The probable cause of this is unsuccessful modification of the sorbent surface, which is confirmed by the IR spectrum in which there are no peaks of morin and surface degradation which leads to lower affinity towards scandium. Much better results were obtained using CEMN-COO-morin sorbent. The presence of morin improves the properties of the material. In the case of CEMN-COOH maximum sorption was reached at pH 5.7 (68%) whereas CEMN-COO-morin shows quantitative sorption (>95%). However, due to precipitation of $Sc(OH)_3$ optimal conditions for sorption of Sc(III) were set at pH 5, where

94% of Sc was retained. An additional advantage of a CEMN based sorbent in relation to Fe_3O_4 is the lack of aggregation without an external magnetic field.

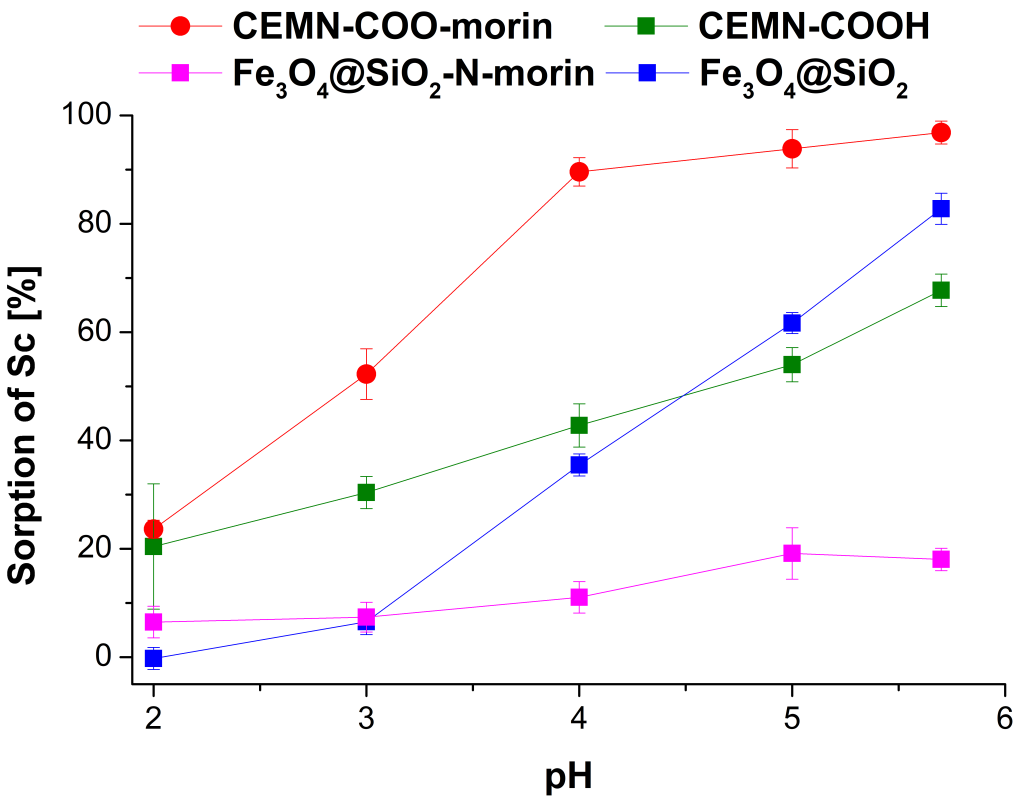

Figure 1: Sorption of scandium(III) on magnetic sorbents at different pH values.

Bibliography

[1] M. Hemmati, M. Rajabi, A. Asghari, Microchim. Acta. **185** (2018) 160.
[2] K. Pyrzyńska, K. Kilian, M. Pęgier, Sep. Purif. Rev. **40** (2019) 65.
[3] K. Kilian, K. Pyrzyńska, M. Pęgier, Solvent Extr. Ion Exch. **35** (2017) 450.

B.8 Theoretical results for production cross sections of theranostic ^{117m}Sn and its contaminants

L. De Dominicis[1], *F. Barbaro*[2], *L. Canton*[2], *M. P. Carante*[3], *A. Colombi*[3,4], *A. Fontana*[3], *L. Mou*[5], *G. Pupillo*[5] *A. Stolarz*[1]

1) *Heavy Ion Laboratory, University of Warsaw, Warszawa, Poland*
2) *INFN Sezione di Padova, Padova, Italy*
3) *INFN Sezione di Pavia, Pavia, Italy*
4) *Dipartimento di Fisica, Università di Pavia, Pavia, Italy*
5) *INFN Laboratori Nazionali di Legnaro, Padova, Italy*

The nucleus ^{117m}Sn has an important physical characteristic, the emission of conversion electrons of discrete energies ($E_{c.e.}$=126.82 keV (65.7%), 129.360 keV (11.65%), 151.56 keV (26.5%) [3]) that makes it a promising radionuclide employable in the palliation of bone metastases pain. The low energy of these conversion electrons allows the delivery of a high dose of radiation to sites of bony metastatic disease with a relative sparing of the bone marrow. In conjunction with conversion electrons, ^{117m}Sn also emits γ-rays (E_γ = 156.02 keV (2.113%), 158.56 (86.4%) [3]) suitable for SPECT imaging. It follows that ^{117m}Sn can be used as a theranostic radionuclide, i.e. it can be used both for therapy and diagnosis.

Although this radioisotope is not used in medical routine, several ligands are already tested, and the most promising are involved in clinical and pre-clinical trials. The critical aspect is that ^{117m}Sn production is carried out only at nuclear reactors and with a low specific activity. A valid alternative is to find a convenient way to produce the radioisotope using, as projectiles, charged particles accelerated at cyclotrons.

In this work we investigated the feasibility of producing ^{117m}Sn with a 30 MeV α-particle beam, generated by the HIL U-200P cyclotron, on ^{nat}Cd and ^{nat}In targets. We evaluated cross section trends of the ^{nat}Cd(α,x)^{117m}Sn and ^{nat}In(α,x)^{117m}Sn reactions with both the Talys and FLUKA codes. The nuclear reaction code Talys (v.1.9) [1] has several preequilibrium (PE) and level-density (LD) models to choose from. Specifically, we considered PE from 1 to 3 and LD from 1 to 6, leading to 18 different combinations of models. The PE range 1–3 corresponds to the analytical exciton model, the numerical exciton model, exciton and optical model respectively; while the LD range 1–6 splits into three phenomenological models (i.e. a Fermi gas with constant temperature, a back shifted Fermi gas, and generalized superfluid model) and three microscopic models (specifically, Goriely's tabulated Harthree-Fock level densities, Hilaire's tabulation based on the combinatorial model, and others from the Hartree-Fock-Bogoliubov temperature-dependent framework). A statistical analysis of the 18 models has been carried out, considering the variability of Talys models. An interquartile range, which measures the statistical dispersion between the lower (Q1) and upper (Q3) quartile, and includes 50% of the models, is identified by the grey band in the figures. The upper and lower dashed lines describe the min/max limits spanned by all 18 models, while the best theoretical evaluation (BTE), defined as the centre of the interquartile range, is given as a solid magenta line. Finally, as is customary, we take as Talys default (solid black line in the Figure) the model with PE 2 and LD 1.

We also used a second nuclear reaction code, FLUKA (v. 2018.2.dev) [2], which is based on the PEANUT (PreEquilibrium Approach to Nuclear Thermalisation) model, with results given by the solid green line.

As can be seen from the figures, in this study we focused on the ^{117m}Sn ($T_{1/2}$=14.00 d [3]) cross section as much as on excitation functions of all its contaminants. In particular,

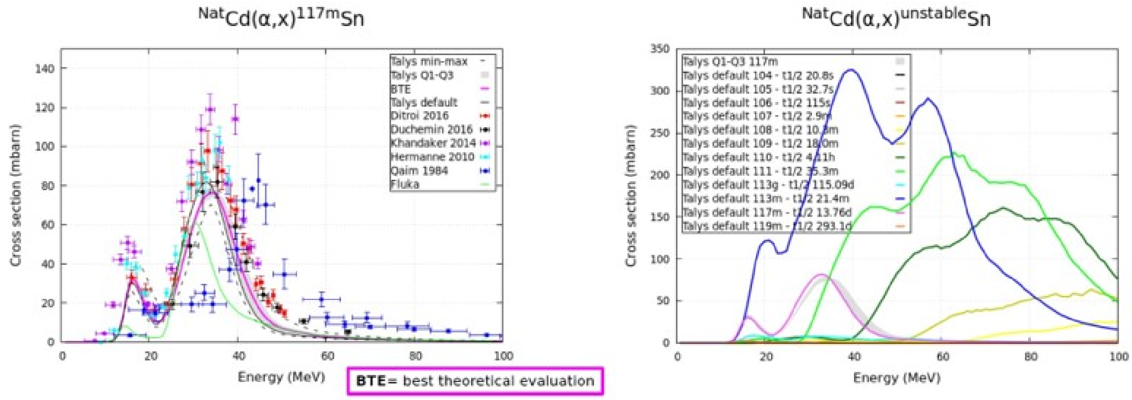

Figure 1: Left: theoretical estimations compared to data available in the literature [4]. Right: theoretical calculations for all radioactive Sn-isotopes co-produced using ^{nat}Cd targets.

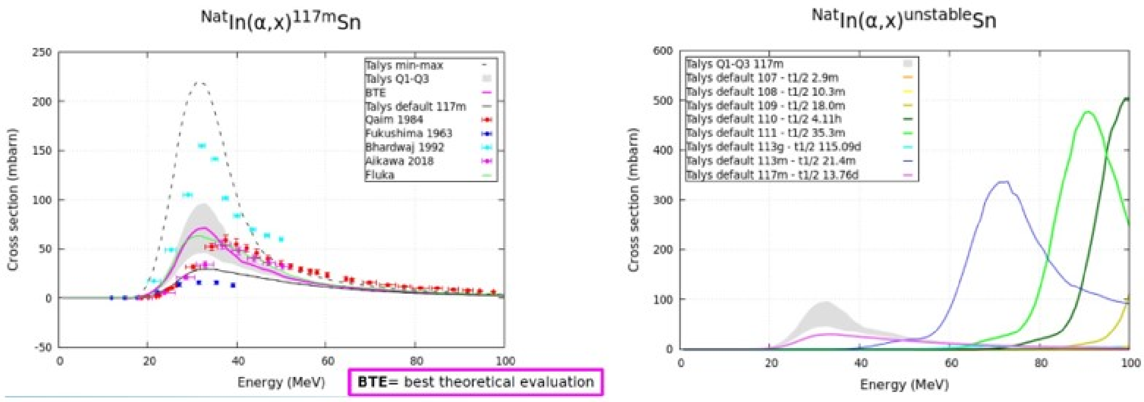

Figure 2: Left: theoretical estimations compared to data available in the literature [4]. Rright: theoretical calculations for all radioactive Sn-isotopes co-produced using ^{nat}In targets.

the radioisotope ^{113g}Sn ($T_{1/2}$=115.09 d [3]) turns out to be the only co-produced contaminant that cannot be chemically separated from ^{117m}Sn, with a half-life longer than the desired radionucide. ^{113g}Sn is produced directly during the bombardment, but also by the decay of ^{113m}Sn ($T_{1/2}$=21.4 m, IT decay mode 91.1% [3]). In the case of ^{nat}Cd targets, the production of a contaminant with a long half-life, ^{119m}Sn ($T_{1/2}$=293.1 d [3]), also takes place. This radioisotope cannot be detected experimentally because of its low-energy γ-emission (E_γ=23.875 keV (16.50%) [3]) so the theoretical calculation is of relevant importance. Anyway, from the results reported in Fig. 1, on the right, we observe that the ^{119m}Sn cross section values should be low.

It is interesting to evaluate the activity produced per unit of current at the End-Of-Bombardment (EOB), considering a current I = 1 µA, t_{irrad} = 24 h and t_{cool} = 0 s. Using the Talys code we predict the activity of a target of a given thickness, here characterized by the beam energy loss in the target, E_{in} - E_{out}. The range of the energy loss for ^{nat}Cd corresponds to 32–20 MeV and for ^{nat}In to 32–25 MeV. This reflects a target thickness of 110 and 85 µm, respectively, for the two materials. Table 1 shows the final results related to ^{117m}Sn and its main contaminants, for both investigated targets, for an energy range suitable for the HIL cyclotron. The analysis is based on a multi-model theoretical study for the production of ^{117m}Sn, using a statistical treatment of the model dependence, that defines a theoretical uncertainty band.

Table 1: Talys evaluation of integral yields of ^{117m}Sn, ^{113g}Sn and ^{119m}Sn in ^{nat}Cd and ^{nat}In targets for an irradiation of 24 h with a current of 1 μA.

	^{nat}Cd (E_{in}=32 MeV-E_{out}=20 MeV)	^{nat}In (E_{in}=32 MeV-E_{out}=25 MeV)
	Integral Yield (MBq/μA)	Integral Yield (MBq/μA)
^{117m}Sn-24 h	2.75±0.21	2.56±1.09
^{113g}Sn-24 h	1.16±0.07	$1 \cdot E^{-5} \pm 8 \cdot E^{-7}$
^{119m}Sn-24 h	0.0022±0.0005	—

From these results it is clear that more measurements of cross sections in the low energy region are needed since here the production of ^{113g}Sn seems to be less predominant. It also seems that ^{nat}In targets are more promising but they are more difficult to produce in thin foils, so both target materials are taken into consideration.

The theoretical results will be complemented by an experimental investigation that will be performed in the context of the ENSAR2 project, a proposal of the European Commission Horizon 2020 programme. The experimental idea is to irradiate different targets realized with the stacked-foils technique. Each target will be constituted of a set of thin ^{nat}Cd (or ^{nat}In) foils alternated with ^{nat}Cu monitor foils, to evaluate beam-energy exploiting IAEA monitor reactions [5], and ^{nat}Al as a beam energy degrader. This configuration allows different cross section values at different energies to be measured with one irradiation run. After irradiation, the activated foils will be measured with a HPGe detector. Several γ-spectra will be acquired for ^{nat}Cd (or ^{nat}In) foils at different times after EOB (End Of Bombardment). This strategy will be useful to give smaller uncertainties from the data analysis and to take into consideration eventual interference by two or more radionuclides in the γ-peaks of the spectra.

Bibliography

[1] The TALYS code www.talys.eu
[2] The Fluka code www.fluka.org
[3] NuDat database 2.8 https://www.nndc.bnl.gov/
[4] EXFOR database https://www-nds.iaea.org/exfor/exfor.htm
[5] IAEA Monitor Reactions 2017 https://www-nds.iaea.org/medical/monitor_reactions.html

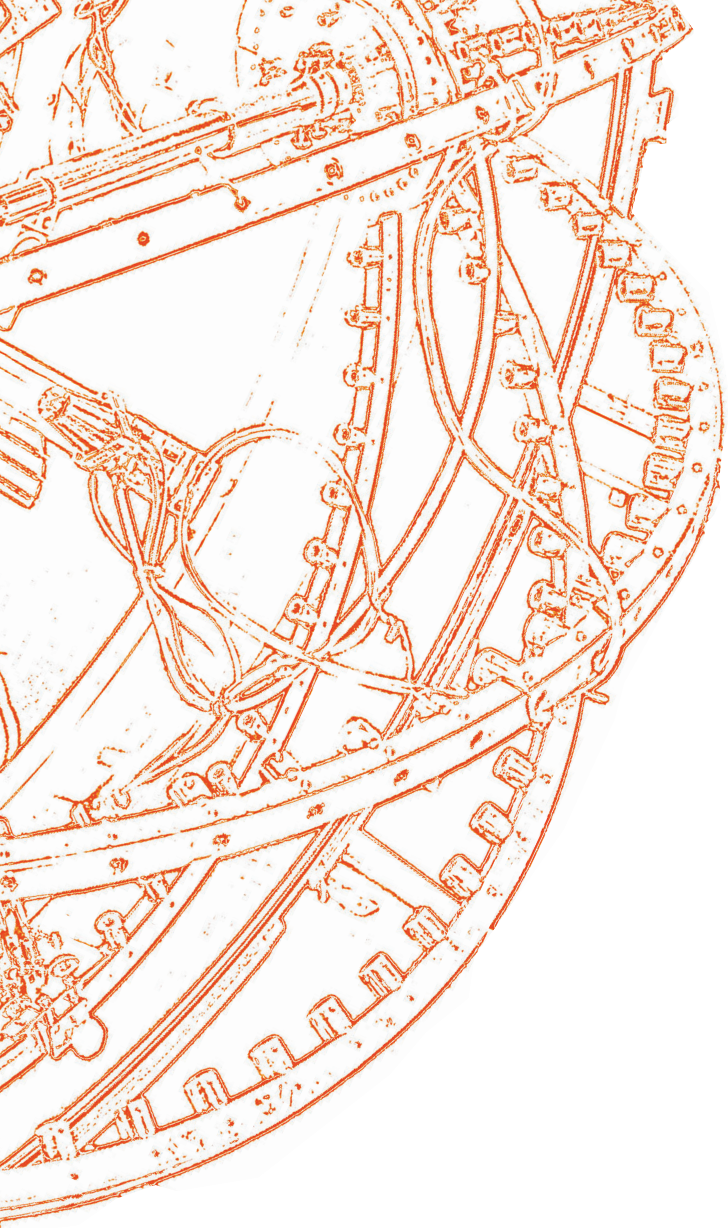

Part C
Nuclear physics

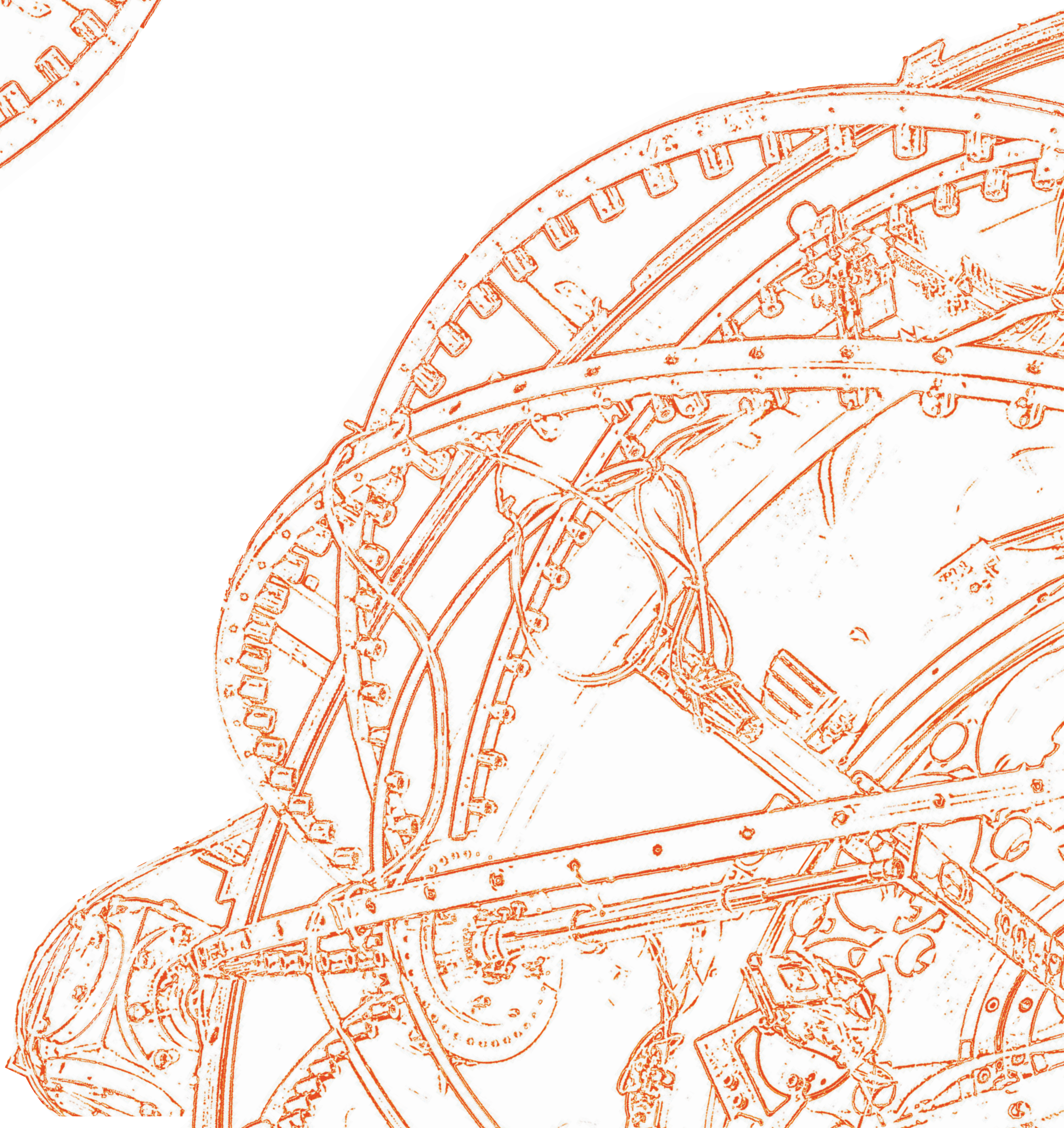

C.1 Coulomb excitation of ^{107}Ag – preliminary results for $7/2^-_1$ and $9/2^-_1$ states

K. Wrzosek-Lipska[1]*, T. Lehmann*[2]*, P.J. Napiorkowski*[1]
on behalf of the "Quadrupole moments of excited states in ^{107}Ag" experiment collaboration

1) Heavy Ion Laboratory, University of Warsaw, Warszawa, Poland
2) Faculty of Physics, Warsaw University of Technology, Warszawa, Poland

A Coulomb excitation experiment to study the electromagnetic properties of low-lying states of ^{107}Ag was performed at the Heavy Ion Laboratory of the University of Warsaw. The states of interest were populated using on 84 MeV ^{32}S beam delivered by the Warsaw cyclotron. Details of the experiment and analysis were described in Refs. [1, 2]. In the current report chosen, recently obtained results are presented.

The low-energy part of the level scheme of ^{107}Ag with the γ-rays observed in the experiment is presented in Fig. 1. The $7/2^-_1$ and $9/2^-_1$ states, populated in the double-step Coulomb excitation process, were clearly observed via de-excitated γ-ray transitions: pure $E2$ 724 keV and 649 keV transitions, and a mixed $E2/M1$ of energy of 550 keV. The $7/2^-_1$ and $9/2^-_1$ states were previously populated via Coulomb excitation in only one such experiment performed with a 45.5 MeV ^{16}O ion-beam [3]. As a result, however, only relative intensities of the relevant γ-rays deexciting the $7/2^-_1$ and $9/2^-_1$ states were given and no matrix elements were extracted.

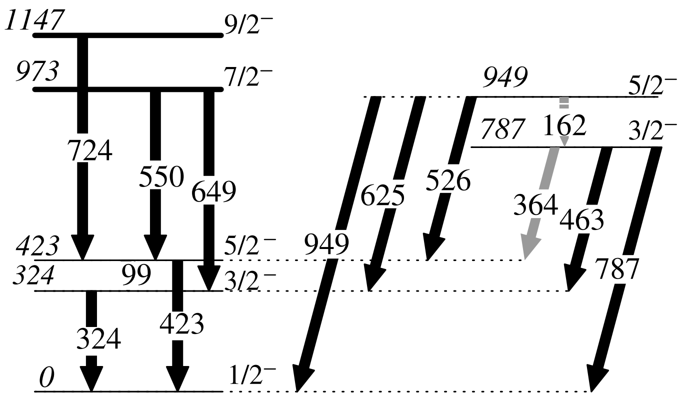

Figure 1: Low-energy part of the level scheme of ^{107}Ag populated in the Coulomb excitation experiment performed at HIL. The energies of all levels and γ-ray transitions are given in keV. The 162 keV and 364 keV γ-ray transitions marked in grey were not observed in the current experiment, however they were included in the analysis.

The set of $E2$ and $M1$ matrix elements coupling low-energy states populated in ^{107}Ag was determined using the Coulomb-excitation least-squares fitting code GOSIA [4–6]. The code fits a set of reduced matrix elements to the γ-ray yields measured in the Coulomb-excitation experiment, including known spectroscopic data: lifetimes of excited states, γ-ray branching ratios, $E2/M1$ mixing coeffcients [3, 7].

For most of the mixed γ-ray transitions observed in the current experiment in ^{107}Ag the mixing coeffcients, $\delta(\frac{E2}{M1})$, are known [7]. The only exception is the value of the $\delta(\frac{E2}{M1},\ 7/2^-_1 \rightarrow 5/2^-_1)$. The influence of the unknown $E2/M1$ mixing ratio on the extracted set of matrix elements was investigated. The $E2/M1$ ratio was varied over several values between -3.0 and 2. For each value of the mixing ratio a full minimization with the GOSIA code was performed. The lowest χ^2 values were obtained for negative values of $\delta(\frac{E2}{M1})$. The solutions obtained with $-1.8 < \delta(\frac{E2}{M1},\ 7/2^-_1 \rightarrow 5/2^-_1) < -0.4$ correspond to similar χ^2 values and no considerable change in the other matrix elements was observed.

The performed analysis reported here allowed us to evaluate for the first time the lifetime values, τ, of the $9/2^-_1$ and $7/2^-_1$ excited states. The preliminary result for the $9/2^-_1$ state indicates a value of τ=3.4(5) ps. The lifetime of the $7/2^-_1$ state was estimated to be $2.1 < \tau < 3.9$ ps depending on the value of the unknown mixing coefficient, $\delta(\frac{E2}{M1},\ 7/2^-_1 \rightarrow 5/2^-_1)$.

This work was the subject of the MSc thesis of T. Lehmann defended in September 2019 at the Faculty of Physics, Warsaw University of Technology.

Bibliography

[1] K. Wrzosek-Lipska *et al.*, HIL Annual Report 2012, page 51.
[2] K. Wrzosek-Lipska *et al.*, HIL Annual Report 2017, page 43.
[3] R.L. Robinson *et al.*, Nucl. Phys. **A150** (1970) 225.
[4] T. Czosnyka, D. Cline, C.Y. Wu, Bull. Amer. Phys. Soc. **28** (1983) 745.
[5] `www.slcj.uw.edu.pl/pl/gosia/`.
[6] M. Zielińska *et al.*, Eur. Phys. J. **A 52** (2016) 99.
[7] J. Blachot, Nucl. Data Sheets **109** (2008) 1383.

C.2 Quadrupole deformation of ^{110}Cd: A Coulomb excitation study

K. Wrzosek-Lipska[1], L. Próchniak[1], P.E. Garrett[2], M. Zielińska[3], P.J. Napiorkowski[1] on behalf of the "Electromagnetic structure of low-lying states in ^{110}Cd studied with multiple-step Coulomb excitation" experiment collaboration

1) Heavy Ion Laboratory, University of Warsaw, Warszawa, Poland
2) University of Guelph, Ontario, Canada
3) IRFU/SPhN, CEA, Université Paris-Saclay, Gif-sur-Yvette, France

The low-energy electromagnetic structure of ^{110}Cd was studied using the Coulomb excitation method. Details of the experiment and chosen aspects of the analysis concerning the target composition were described in Refs. [1, 2]. This report presents selected, preliminary results concerning the quadrupole deformation of the low-lying 0^+ states in ^{110}Cd and their comparison with the most recent theoretical mean-field based models (for more details see Ref. [3]).

The low-energy part of the level scheme of ^{110}Cd indicating the γ rays observed in the experiment is presented in Fig. 1.

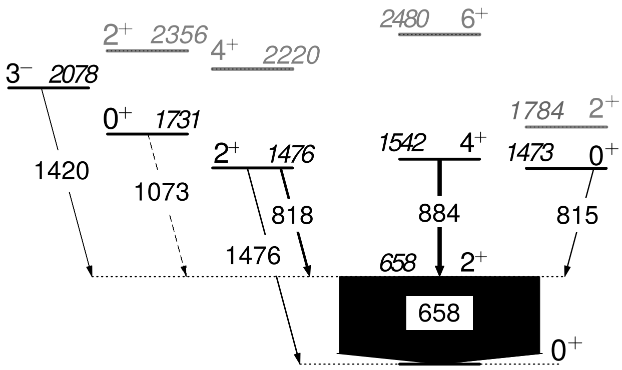

Figure 1: Low-energy portion of the ^{110}Cd level scheme. Widths of the arrows are proportional to the γ-ray intensities observed in the present experiment. The weak $0_3^+ \rightarrow 2_1^+$ γ-ray transition is shown with a dashed arrow. The states marked in grey were not observed in the present experiment, but were included in the Coulomb-excitation data analysis.

The on-going analysis, with the aim of extracting a complete set of reduced electromagnetic matrix elements between all low-lying states populated in this experiment, uses the GOSIA code. The preliminary results yield a set of transitional and diagonal $E2$ matrix elements, including signs. This permits some conclusions to be reached on the quadrupole deformation of ^{110}Cd in its ground and first excited 0^+ states. A similar overall deformation is found for the 0_1^+ and 0_2^+ states of ^{110}Cd, as indicated by the $\langle Q^2 \rangle$ values of 0.44(1) e^2b^2 ($\langle \beta^2 \rangle^{1/2} \approx 0.17$) and 0.51(8) e^2b^2 ($\langle \beta^2 \rangle^{1/2} \approx 0.19$), respectively. The $\langle \cos(3\delta) \rangle$ value for the 0_1^+ ground state was estimated to be 0.35(5), which corresponds to a non-axiality parameter $\langle \delta \rangle \approx \langle \gamma \rangle \approx 23°$. The lack of experimental information on key matrix elements, particularly $\langle 2_3^+ || E2 || 2_3^+ \rangle$, prevents us from drawing firm conclusions on the nature of the deformation of the 0_2^+ state.

The structure of the stable even-even Cd nuclei was recently investigated using various theoretical models. In particular, the results of recent beyond-mean-field (BMF) calculations [4, 5] suggest that the Cd isotopes exhibit multiple shape coexistence, i.e., different and unique quadrupole shapes were predicted for the first four 0^+ states in ^{110}Cd and ^{112}Cd. These theoretical findings are consistent with those of self-consistent calculations performed with the General Bohr Hamiltonian (GBH) model [3, 6, 7].

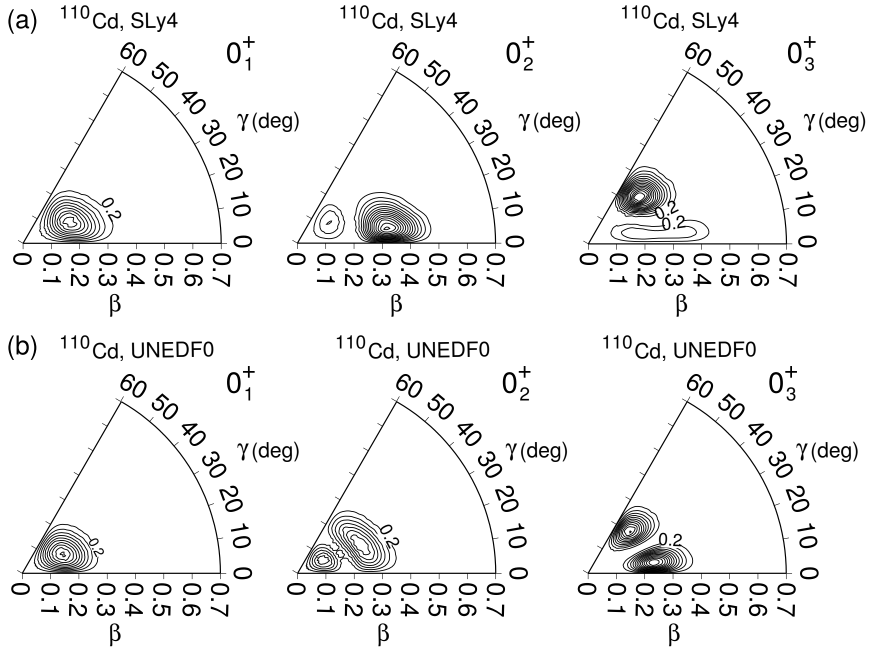

Figure 2: Probability density distributions for the 0_1^+, 0_2^+ and 0_3^+ states in ^{110}Cd calculated within the GBH approach using Skyrme SLy4 (a) and UNEDF0 (b) interactions.

The probability density distributions in the $\beta - \gamma$ plane determined by the eigenfunctions of the Bohr Hamiltonian are presented in Fig. 1 for the three lowest-lying 0^+ states in ^{110}Cd. The results obtained for the excited 0_2^+ and 0_3^+ states clearly differ depending on the interaction (SLy4 or UNEDF0) used in the calculations (see Fig. 2). The GBH(UNEDF0) calculations suggest a similar magnitude of the overall deformation for all considered 0^+ states with their probability density distributions being widely spread in the γ parameter and resembling those obtained for a harmonic oscillator potential. The results obtained with the SLy4 interaction are considerably different, indicating that the first three 0^+ states are characterized by various types of deformation. This scenario closely resembles that predicted by the BMF calculations of Refs. [4, 5].

The GBH model predictions for the deformation of the 0^+ ground state of ^{110}Cd, including its non-axiality, reproduce well the preliminary experimental findings. However, the overall deformation of the 0_2^+ state is overestimated by GBH(SLy4) by a factor of $\sim$1.5. The use of the UNEDF0 parametrization in GBH calculations yields a slightly lower deformation for the 0_2^+ state, which is more consistent with the presented experimental result.

Bibliography

[1] K. Wrzosek-Lipska *et al.*, HIL Annual Report 2015, page 68.
[2] K. Wrzosek-Lipska *et al.*, HIL Annual Report 2018, page 49.
[3] K. Wrzosek-Lipska *et al.*, Acta Phys. Pol. **B51** (2020) 789.
[4] P.E. Garrett *et al.*, Phys. Rev. Lett. **123** (2019) 142502.
[5] P.E. Garrett *et al.*, Phys. Rev. C **101** (2020) 044302.
[6] L. Próchniak, P. Quentin, M. Imadalou, Int. J. Mod. Phys. **E21** (2012) 1250036.
[7] L. Próchniak *et al.*, HIL Annual Report 2018, page 57.

C.3 Coulomb excitation of the strongly deformed band in ^{40}Ar (HIL–085 and HIL–045)

K. Hadyńska-Klęk[1], M. Rocchini[2,3], P.J. Napiorkowski[1], N. Marchini[2,4] T. Abraham[1], P. Bednarczyk[5], K. Belvedere[6], F. Bello Garrote[7], M. Ciemała[5], D. T. Doherty[6], S. Dutt[1], A. Giaz[8], J. Iwanicki[1], G. Jaworski[1], M. Kicińska-Habior[9], M. Komorowska[1], M. Kowalczyk[1], M. Kmiecik[5], M. Matejska-Minda[5], T. Marchlewski[1], V. Modamio[7], L. Morrison[6], A. Nannini[2], D.R. Napoli[10], M. Palacz[1], W. Piątek[1], A.M. Quynh[11], B. Reed[6], J. Samorajczyk-Pyśk[1], E. Sahin[7], J. Srebrny[1], A. Tucholski[1], B. Wasilewska[5], M. Wiedeking[12], K. Wrzosek-Lipska[1] M. Zielińska[13]

1) Heavy Ion Laboratory, University of Warsaw, Warszawa, Poland
2) University of Florence, INFN Sezione di Firenze, Italy
3) University of Guelph, Ontario, Canada
4) Università di Camerino, Camerino, Italy
5) The H. Niewodniczański Institute of Nuclear Physics PAN, Kraków, Poland
6) Department of Physics, University of Surrey, Guildford, UK
7) Department of Physics, University of Oslo, Oslo, Norway
8) I.N.F.N. Sezione di Milano, Milano, Italy
9) Inst. of Exp. Physics, Univ. of Warsaw, Warszawa, Poland
10) Padova University, Padova, Italy
11) Joint Institute for Nuclear Research, Dubna, Russia
12) iThemba Lab. for Accelerator Based Sciences, Faure, South Africa
13) IRFU/SPhN, CEA, Université Paris-Saclay, Gif-sur-Yvette, France

The idea of employing the Coulomb excitation technique to investigate the deformation of the states in superdeformed (SD) bands in the A∼40 mass region was triggered by the recent research on the high spin states in the rotational SD structures in ^{40}Ca [1], ^{36,38}Ar [2–4], ^{44}Ti [5] and also in ^{42}Ca [6]. Since the SD bands in the A∼40 mass region are linked to the yrast structure via discrete gamma transitions, the last state in the side band observed in the gamma cascade coming from the high spins is usually 2^+_2, decaying via E2 transitions to 2^+_1 and 0^+_1 states. The B(E2; $2^+_2 \rightarrow 0^+_2$) value has not been reported in any of the listed isotopes because this transition is hindered due to the competition with higher energy decay transitions ($2^+_2 \rightarrow 2^+_1$ and $2^+_2 \rightarrow 0^+_1$). In consequence, the decay to the bandhead of the SD band had never been investigated before 2010 when the first dedicated Coulomb excitation experiment aimed at exploring a SD band was performed at the INFN Laboratori Nazionali di Legnaro in Italy, focused on the electromagnetic structure of the ^{42}Ca isotope [7–10].

The level structure of ^{40}Ar is very similar to that of the neighbouring superdeformed ^{42}Ca. Because ^{40}Ar is a stable nucleus, it has been the subject of many experimental studies over the years. Surprisingly though, the electromagnetic properties of the low-spin region in this isotope remain poorly known and the precision of the previously measured transition probability values needs verification and improvement.

Our first attempt to Coulomb excite ^{40}Ar was made at the Heavy Ion Laboratory in Warsaw in June 2015 with the EAGLE array coupled to the PiN-diode scattering chamber. The main goal of the project was to determine the deformation parameters of the 0^+ and 2^+ states and the non-axiality parameters of 0^+ states in this isotope. However, due to technical issues and the low-efficiency of the γ-ray detectors used (4 of the total available 14 HIL-owned HPGe detectors and 7 out of 48 PiN diodes could not be used in the data analysis), apart from the dominant $2^+_1 \rightarrow 0^+_1$ the only other transition clearly observed in the spectrum was the $0^+_2 \rightarrow 2^+_1$. The γ-ray spectrum Doppler-corrected for the ^{40}Ar velocity collected with a 1 mg/cm^2 thick ^{208}Pb target and measured in coincidence with the back-scattered ^{40}Ar beam particles is shown in Fig. 1.

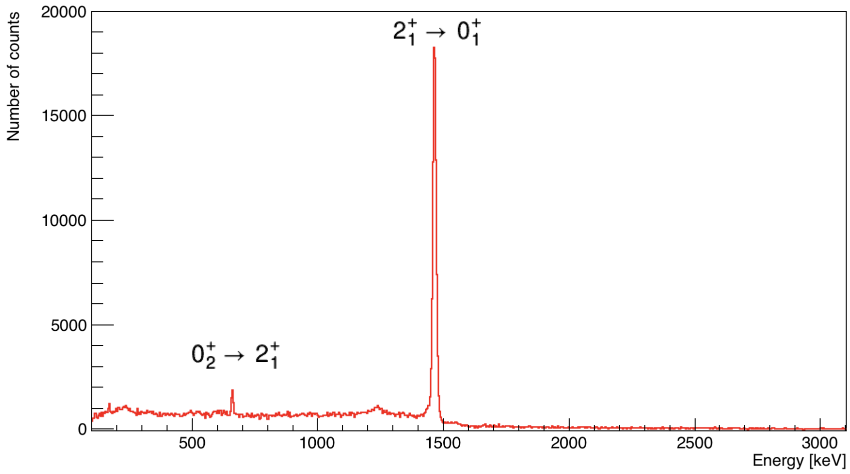

Figure 1: The experimental particle-γ coincidence spectrum Doppler-corrected for the ^{40}Ar velocity (July 2015). The $2_1^+ \rightarrow 0_1^+$ (1460 keV) and $0_2^+ \rightarrow 2_1^+$ (660 keV) lines are visible.

In November 2019 a second attempt to Coulomb excite the SD band in ^{40}Ar was made at HIL Warsaw with a 2 mg/cm^2 thick ^{197}Au target. In this experiment the EAGLE array in a configuration with 16 Compton–shielded HPGe detectors (14 Phase-1 EUROBALL detectors lent by the GAMMAPOOL consortium and 2 additional detectors, of about half the efficiency, provided by HIL) was coupled to the scattering chamber, equipped with 46 0.5x0.5 cm^2 PIN-diodes, which were used for detection of the backscattered beam particles. The PIN-diodes were placed at angles covering the range from 120 to 168 degrees. Due to a number of technical difficulties with the ion transmission and a major power cut, the experiment collected only around 1/16 of the expected statistics. This allowed us to observe only the 1460 keV $2_1^+ \rightarrow 0_1^+$ and the 660 keV $0_2^+ \rightarrow 2_1^+$ transitions (no progress since the 2015 experiment). The γ-ray spectrum Doppler-corrected for the ^{40}Ar velocity and measured in coincidence with the back-scattered ^{40}Ar beam particles is shown in Fig. 2. The data analysis is ongoing.

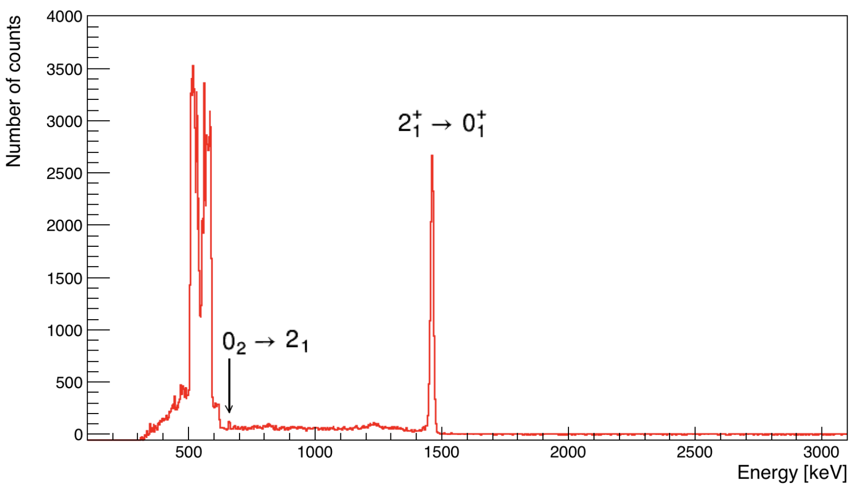

Figure 2: The experimental particle-γ coincidence spectrum Doppler-corrected for the ^{40}Ar velocity (November 2019). The $2_1^+ \rightarrow 0_1^+$ (1460 keV) and $0_2^+ \rightarrow 2_1^+$ (660 keV) lines are visible.

This project has received funding from the European Union's Horizon 2020 research and innovation programme under grant agreement n°654002.

Bibliography

[1] E. Ideguchi *et al.,* Phys. Rev. Lett. **87** (2001) 222501.
[2] C.E. Svensson *et al.,* Phys. Rev. Lett. **85** (2000) 2693.
[3] C.E. Svensson *et al.,* Phys. Rev. **C 63** (2001) 061301.
[4] D. Rudolph *et al.,* Phys. Rev. **C 65** (2002) 034305.
[5] D.C. O'Leary *et al.,* Phys. Rev. **C 61** (2000) 064314.
[6] M. Lach *et al.,* Eur. Phys. J. **a 16** (2003) 309.
[7] K. Hadyńska-Klęk *et al.,* Acta Phys. Pol. **B 42** (2011) 817.
[8] K. Hadyńska-Klęk *et al.,* Acta Phys. Pol. **B 44** (2013) 617.
[9] K. Hadyńska-Klęk *et al.*, Phys. Rev. Lett. **117** (2016) 062501.
[10] K. Hadyńska-Klęk *et al.*, Phys. Rev. **C97** (2018) 024326.

C.4 New setup design for Coulomb excitation studies

M. Komorowska[1,2], P.J. Napiorkowski[1], A. Iwanicki[3], J. Iwanicki[1], A. Bezbakh[4]

1) Heavy Ion Laboratory, University of Warsaw, Warszawa, Poland
2) Institute of Experimental Physics, University of Warsaw, Warszawa, Poland
3) University of Nottingham, Nottingham, United Kingdom
4) Joint Institute for Nuclear Research, Dubna, Russia

To reach a higher efficiency in the detection of back scattered particles in Coulomb excitation experiments performed at HIL, the COULEX group has initiated a project to build a new detection setup that exploits the particle-gamma-ray coincidence technique. For this purpose a new scattering chamber has been in development in collaboration with the Joint Institute for Nuclear Research, Dubna, Russia. As always in such cases, the design must overcome many obstacles and meet several constraints to be most useful as an experimental tool. The chosen system of detectors should address the requirements of the physics studied. The chamber design should have the minimum influence on the gamma spectrometer performance. There are several purely mechanical restrictions placed on the physical size and symmetry of the chamber by the dimensions of the cavity in the middle of the spectrometer in which it must be placed. In this case the diameter of the target chamber was chosen to be 20 cm. This makes the device quite small and compact but provides room to place many particle detectors inside to cover 20° – 120° scattering angles.

The mechanical part consists of several independent pieces connected together in a vacuum-tight whole. The core piece is the target chamber (see Fig.1) made of two hemispherical parts joined along the 90° plane with an annular ring with the target ladder holder. At the current stage of the project, target and source positions are changed manually. In the future there will be a piezoelectric engine for changing position. The chamber is connected to the ion beam via two pipes of length depending on the spectrometer in which it is be mounted. The pipes are capped with lids with vacuum feedthroughs for signal cables. The whole structure is symmetrical, thus signal readout is possible from both sides of the ion beam connectors.

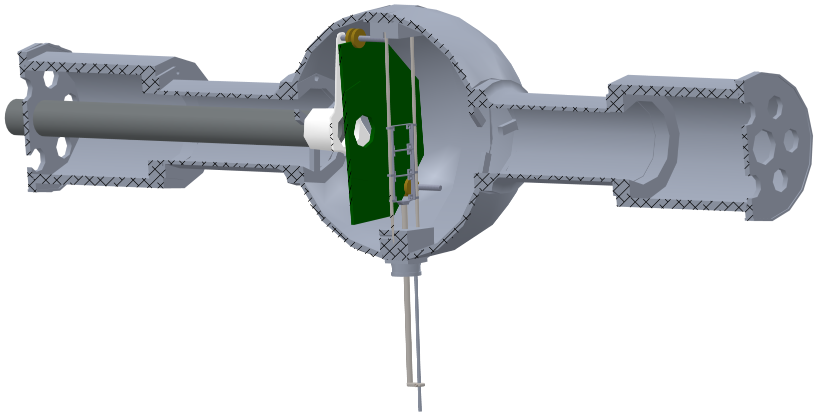

Figure 1: The final design of the new Coulomb excitation chamber with one DSSSD detector mounted.

The main goal of the design is to mount a CD-like Double Sided Silicon Strip Detector delivered by the Joint Institute for Nuclear Research, Dubna, Russia at backward angles. It is foreseen to accommodate additional heavy ion detectors in the forward hemisphere. The annular ring could be modified for mounting additional pad-like detectors placed at 90°. The chamber production will utilise technologies such as 3d printing and CNC machining.

C.5 Octupole collective space. Construction of basis functions in the intrinsic coordinate frame

L. Próchniak

Heavy Ion Laboratory, University of Warsaw, Warszawa, Poland

The concept of an intrinsic (of principal axes) frame of reference has appeared to be very fruitful in the case of quadrupole variables. However, extension of this concept to the octupole case is not straightforward. To define an intrinsic system for the octupole space we exploit the properties of the octupole variables with respect to the octahedral group $O_h \subset O(3)$, for more details see [1, 2]. The octupole space can be decomposed as $\mathrm{A}_2^- \oplus \mathrm{F}_1^- \oplus \mathrm{F}_2^-$ of irreducible representations of O_h, with dimensions $1, 3, 3$, respectively. Coordinates compatible with this decomposition are denoted as $(b, \boldsymbol{f}, \boldsymbol{g}) = (b, f_x, f_y, f_z, g_x, g_y, g_z)$, where b, f_k, g_k, $k = x, y, z$ span representations A_2^-, F_1^-, F_2^-, respectively. In [1, 2] we introduced two variants of the intrinsic system: the F_1^--type and the F_2^--type. In the case of the F_1^- variant instead of the LAB system $(b, \boldsymbol{f}, \boldsymbol{g})$ variables one uses the $(b', \boldsymbol{f'}, \boldsymbol{\omega})$ variables where the $\boldsymbol{\omega}$ are the Euler angles of the rotation such that the result of this rotation has the form $(b', \boldsymbol{f'}, 0)$. The F_2^- case is defined analogously, with $\boldsymbol{f}$ and $\boldsymbol{g}$ interchanged.

In order to apply this formalism in nuclear theory, one requires one more important component, namely an appropriate basis in the Hilbert space of functions defined on the octupole space. Again, the construction of such a basis is more difficult than in the quadrupole case, see e.g. [3]. Here I follow the general idea of the method applied in [5] for the quadrupole case and which can be summarized as follows. From a properly chosen set of functions of the intrinsic octupole variables one constructs a subspace of functions which fulfill two conditions. First (A), they are invariant with respect to the action of the octahedral group. Second (B), they belong to the domain of the Laplace-Beltrami operator which is compatible with the scalar product induced in the intrinsic system by the standard Cartesian scalar product in the laboratory system. From the physical point of view this operator is (up to a constant factor) the simplest form of the kinetic energy operator. Standard orthonormalization methods may then be applied.

In the deformation part of the octupole space we take all polynomials of the $(b, \boldsymbol{f})$ variables times the Gaussian factor $\exp(-(b^2+\boldsymbol{f}^2)/2)$. By using the spherical coordinates for $\boldsymbol{f}$ this can be put into the form

$$
\begin{aligned}
&b^{n_b} t^{n_t} Y_{lm}(\xi_1, \xi_2) e^{-(b^2+t^2)/2}\, \mathcal{D}^J_{MK}(\boldsymbol{\omega}) \;, \\
&N = n_b + n_t,\;\; N = 0, 1, 2, ...,\quad l = n_t, n_t - 2, ..., 0(1) \;,
\end{aligned}
\tag{1}
$$

where $\mathcal{D}^J_{MK}$ are the rotation matrices

Condition A. Symmetrization. To obtain O_h-invariant functions from (1) one can apply the projection operator

$$
P_3 P_2 P_1 = (I + R_3 + R_3^2)(I + R_2 + R_2^2 + R_2^3)(I + R_1) \;, \tag{2}
$$

where $R_k, k = 1, 2, 3$ are well known generators of O_h. After the projection one should choose linearly independent functions, which is rather easy in the case considered. In particular, one can obtain a simple analytical formula for a number of such functions for given (n_b, n_t, l, J).

Condition B. Domain of the Laplace-Beltrami operator. This operator can be written as

$$\Delta = \frac{1}{d}\frac{\partial}{\partial b}d\frac{\partial}{\partial b} + \sum_{s=x,y,z}\frac{1}{d}\frac{\partial}{\partial f_s}d\frac{\partial}{\partial f_s} + \frac{1}{d}\sum_{k,j=1,2,3} W_k d M_{kj} W_j \ , \tag{3}$$

where

$$d = 8\left(b^3 - (15/16)b(f_x^2+f_y^2+f_z^2) + 2(15/16)^{3/2} f_x f_y f_z\right) \tag{4}$$

is the deformation part of the Jacobian of the change of variables (from the laboratory system to the intrinsic system), M is a 3×3 matrix and the W_k are differential operators dependent on $(b, \boldsymbol{f})$, see [4].

It can be verified that the functions obtained through symmetrization in the previous stage, denoted as

$$G(b, \boldsymbol{f}, \boldsymbol{\omega}) e^{-(t^2+b^2)/2} \ ,$$

belong to the domain of Δ provided that

$$d^2 \sum_{\beta=b,\boldsymbol{f}} \partial_\beta(d\partial_\beta G) + d\sum_{kj} W_k(d^2 M_{kj} W_j G) - \sum_{kj}(W_k d) d^2 M_{kj} W_j G \tag{5}$$

can be expressed as $d^3 p(b,\boldsymbol{f})$ where p is a polynomial (0 non excluded). This condition is far from trivial; even for low values of N (the order of G in the $(b,\boldsymbol{f})$ variables), say $N=4$, we have to deal with polynomials of order greater than 10. Hence, to find a linear combination of the symmetrized functions that fulfill condition (B) I have used the Maxima system for symbolic computations. The developed procedures can be applied for $N \le 10$, $J \le 12$ but at present a more detailed analysis has been done for N up to 4 and J up to 6.

A few remarks and examples.

1. J=0. For even N the conditions (A) and (B) are fulfilled by polynomials $\eta_2^{N/2} = (b^2+\boldsymbol{f}^2)^{N/2}$ from which one can easily build Laguerre polynomials $L_{N/2}^{(5/2)}$, which enter the eigenfunctions of the octupole harmonic oscillator with seniority number $\lambda = 0$, see [3].

2. N=4, J=0, in this case we have 5 functions after stage (A) from which 2 linear combinations fulfilling condition (B) can be built. One is, as expected, proportional to η_2^2 while the second one is proportional to η_4, where η_2, η_4 are the 2nd and 4th order scalar invaraints, respectively. This is again a nontrivial fact, because this result is obtained in a way that is completely independent from the theory of invariants.

Bibliography

[1] S.G. Rohoziński and L. Próchniak, Acta Phys. Pol. B, Suppl. Proc. **10** (2017) 191.

[2] S. G. Rohoziński and L. Próchniak, in: Greiner Memorial Volume, eds. P. O. Hess and H. Stöcker, World Scientific, Singapore (2018) pp. 309–326, `arXiv:1802.01703 [nucl-th]`.

[3] S. G. Rohoziński, J. Phys. G: Nucl. Phys. **4**, 1075 (1978).

[4] L. Próchniak, to be published, `arXiv:2003.01990 [nucl-th]`.

[5] L. Próchniak, K. Zajac, K. Pomorski, S. G. Rohoziński and J. Srebrny, Nucl. Phys. **A648**, 181 (1998).

C.6 Dissipation and tunnelling in heavy-ion reactions near the Coulomb barrier

E. Piasecki[1], M. Kowalczyk[1], S. Yusa[2], A. Trzcińska[1], K. Hagino[2,3]

1) Heavy Ion Laboratory, University of Warsaw, Warszawa, Poland
2) Department of Physics, Tohoku University, Sendai 980-8578, Japan
3) Research Center for Electron Photon Science, Tohoku University, 1-2-1 Mikamine, Sendai 982-0826, Japan

The influence of couplings to collective excitations on the fusion process has been well established experimentally and theoretically, see Ref. [1] and references therein. Much less is known about the influence of dissipation caused by transfer reactions, even less due to noncollective excitations. In Ref. [1] we report the results of a comparison of experimental barrier distributions with CC + RMT model calculations taking into account noncollective excitations, in which the stationary coupled channels (CC) method is merged with a statistical approach based on random matrix theory (RMT). Despite many assumptions and approximations, we find that the model works well for medium mass systems without fitting parameters, describing the influence of dissipation on tunneling. Examples are shown in Fig. 1.

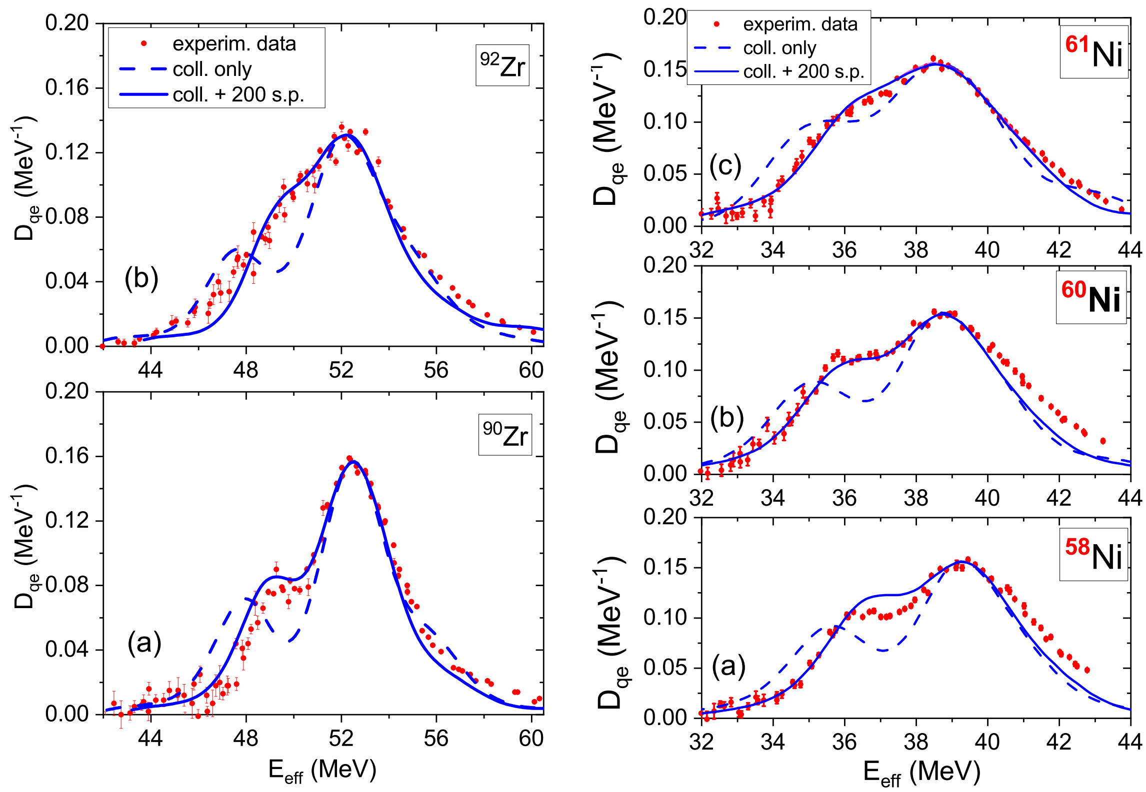

Figure 1: Experimental (points) and theoretical barrier distributions for the ^{20}Ne + ^{90,92}Zr and ^{20}Ne + ^{58,60,61}Ni systems. The dashed lines show the results of standard CC calculations taking into account couplings to collective excitations only, and the solid lines were obtained after taking into account partial kinetic energy dissipation, i.e. also including couplings to 200 noncollective levels.

The change in the fusion barrier penetrability for the ^{20}Ne + ^{92}Zr system calculated according to the same model including collective excitations only as well as single particle excitations is shown in Fig. 2.

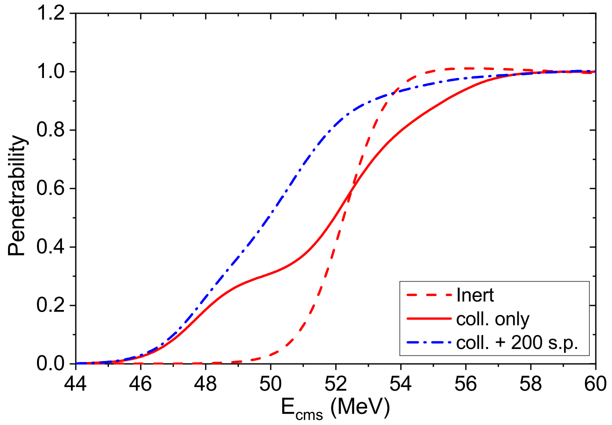

Figure 2: Calculated barrier penetrability for the ^{20}Ne + ^{92}Zr system as a function of the projectile energy in the centre-of-mass frame for three situations: (a) inert target and projectile, (b) taking into account only collective excitations, (c) taking into account collective and non collective excitations.

In Ref. [1] we have shown that for heavier systems the dissipation via the noncollective excitations mechanism does not appear to be sufficient to explain the experimental results. This points to the importance of other dissipation mechanisms for these systems, such as nucleon transfer processes.

Some results of the model calculations and comparisons with experimental results concerning the ^{24}Mg + ^{90,92}Zr systems are presented in Ref. [2].

The continuation of the project will be performed within the NCN SHENG1 grant 2018/30/Q/ST2/00163, Poland-JINR project 75/36/2020 and is supported in part by the PL-Grid Infrastructure. The calculations concerning the influence of dissipation on tunnelling for the ^{16}O, ^{20}Ne, ^{24}Mg, and ^{28}Si + ^{92,94}Mo systems are being performed and the relevant experiments are in preparation.

Bibliography

[1] E. Piasecki *et al.*, Phys. Rev. **C 100** (2019) 014616.
[2] A. Trzcińska *et al.*, this Report, page 83

C.7 Mechanism of the ^{144}Sm(^{7}Li,^{6}Li$_{3+}$)^{145}Sm reaction at 30 MeV

K. Rusek
Heavy Ion Laboratory, University of Warsaw, Warszawa, Poland

The production of α particles in reactions induced by the weakly bound lithium isotopes, ^{6,7}Li, at near barrier energies has attracted considerable attention. Many reactions may lead to the emission of α particles, one of the most obvious being breakup of the projectiles that are known to have a well developed cluster structure. Recently, an interesting set of data was published for the ^{144}Sm(^{7}Li,^{6}Li$_{3+} \rightarrow \alpha$+d)^{145}Sm process [1]. In the experiment, coincident α-d measurements were performed and the angular distribution of the differential cross section for this reaction was obtained (Fig. 1). The contribution of this reaction to the total α yield measured at a projectile energy of 30 MeV was found to be about 20%. The data were analysed by means of a classical dynamical model using the code PLATYPUS [2, 3].

In this contribution, this data set is analysed by quantum-mechanical coupled reaction channels calculations (CRC), similar to those performed previously for ^{7}Li+^{120}Sn [4]. In the ^{7}Li+^{144}Sm entrance channel, coupling to the low-lying first excited state of ^{7}Li was taken into account while the optical model (OM) potential was adopted from the elastic scattering studies of Figueira et al. [5]. It was assumed that the ground and the first excited states of ^{7}Li belong to a K=1/2 rotational band with quadrupole deformation parameters $M(E2)$, δ_2 taken from [6]. In the exit channel, the OM potential was determined by means of the single folding technique using empirical α-target and d-target optical potentials adopted from [7]. The ^{6}Li$_{g.s.}$=α+d wave function was taken from [8]. The real and imaginary parts of the single folding potential were renormalized by factors of 1.5 and 0.6, respectively, in order to reproduce the ^{6}Li+^{144}Sm elastic scattering data published in [5] (to the beat of our knowledge ^{6}Li+^{145}Sm elastic scattering has not been investigated). The continuum-discretized coupled-channel technique was used to generate the ^{6}Li$_{3+}$ resonance wave function as well as the g.s. $\rightarrow 3^+$ coupling potential [8]. Apart from direct transfer of one-neutron, ^{144}Sm(^{7}Li,^{6}Li$_{3+}$)^{145}Sm, the two-step process, ^{7}Li+^{144}Sm $\rightarrow$ ^{6}Li$_{g.s.}$+^{145}Sm$\rightarrow$ ^{6}Li$_{3+}$+^{145}Sm was included in the coupling scheme. The spectroscopic amplitudes S for ^{7}Li$_{g.s.}$=^{6}Li$_{g.s.}$+n, ^{7}Li$_{1exc.}$=^{6}Li$_{g.s.}$+n and ^{7}Li$_{g.s.}$=^{6}Li$_{3+}$+n were taken from the predictions of Cohen and Kurath [9] and are listed in Table 1. For the final nucleus, ^{145}Sm=^{144}Sm+n, the spectroscopic amplitude was set to unity (one neutron above the N=82 closed shell). Concerning the binding potentials, they were taken of WS form with standard geometry, r_0 = 1.25 fm, a_0 = 0.65 fm.

The results of the calculations are plotted in Fig. 1 as the solid and dashed curves (full coupling scheme and two-step contribution, respectively). The full calculation, without any free parameter, reproduces reasonably well the experimental data. The two step contribution is negligibly small, thus the mechanism of this "transfer induced breakup" reaction is mainly direct transfer of one-neutron. The results of the standard quantum-mechanical model are similar to those of the classical dynamical model presented in Ref. [1].

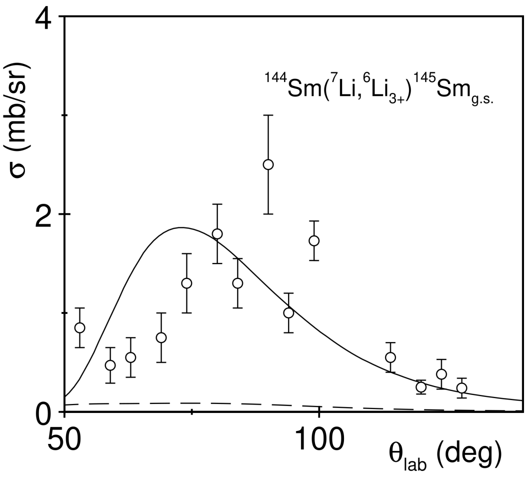

Figure 1: Angular distribution of ^{6}Li$_{3+}$ compared with the results of CRC calculations (solid curve – full coupling scheme, dashed curve – two-step contribution only).

Table 1: Spectroscopic amplitudes S for the different configurations listed in the first column [9].

	nlj	S
^{7}Li$_{g.s.}$=^{6}Li$_{g.s.}$+n	1p3/2	0.6567
^{7}Li$_{g.s.}$=^{6}Li$_{g.s.}$+n	1p1/2	-0.5378
^{7}Li$_{1exc.}$=^{6}Li$_{g.s.}$+n	1p3/2	0.9244
^{7}Li$_{1exc.}$=^{6}Li$_{g.s.}$+n	1p1/2	-0.1965
^{7}Li$_{g.s.}$=^{6}Li$_{3+}$+n	1p3/2	-0.7442

Bibliography

[1] P.F.F. Carnelli *et al.*, Nucl. Phys. **A 969**, (2018) 94.
[2] A. Diaz-Torres, Comput. Phys. Commun. **182**, (2011) 1100.
[3] R. Rafiei *et al.*, Phys. Rev. **C 81**,(2010) 024601.
[4] N.J. Davis *et al.*, Phys. Rev. **C 69**, (2004) 064605.
[5] J.M. Figueira *et al.*, Phys. Rev. **C 81**, (2010) 024613.
[6] K. Rusek *et al.*, Nucl. Phys. **A 575**, (1994) 412.
[7] B. Mukeru *et al.*, Nucl. Phys. **A 965**, (2017) 1.
[8] A. Pakou *et al.*, Phys. Lett. **B 633**, (2006) 691.
[9] S. Cohen, D. Kurath, Nucl. Phys. **A 101**, (1967) 1.

C.8 Spin deorientation measurements via the Coulomb excitation of ^{148}Nd with a plunger device

A. Tucholski[1], C. Fransen[2], A. Blazhev[2] J. Srebrny[1], Ch. Droste[3], T. Marchlewski[1], K. Hadyńska-Klęk[1], L. Próchniak[1], M. Palacz[1], P. Napiorkowski[1], T. Abraham[1], A. Stolarz[1], M. Kowalczyk[1], K. Wrzosek-Lipska[1], J. Samorajczyk-Pyśk[1]

1) Heavy Ion Laboratory, University of Warsaw, Warszawa, Poland
2) Institut für Kernphysik, Universität zu Köln, Köln, Germany
3) Faculty of Physics, University of Warsaw, Warszawa, Poland

In recent measurements of the lifetime of the 10^+ state (3279 keV) in ^{136}Nd [1] the question arose of the structural features of the state. Structural information can be obtained experimentally only by g-factor or quadruple moment measurements. The problem is that we can only measure the product $g < H >$ of the g-factor and the mean strength of the magnetic field of the surrounding electrons, $< H >$. This implies that we have to know the strength of the magnetic field to measure the g-factor, or to know the g-factor to measure the strength of the magnetic field of the 10^+ state (3279 keV).

To do so, we performed a second experiment with ^{148}Nd, complementary to the previous one [1] where the strength of the magnetic field could be measured. This is based on the work presented by H.D. Betz et al. [2] who studied heavy ions penetrating solid state materials. Betz showed experimentally that the charge state of the ions depends on the velocity when traversing a solid material and is the same for all isotopes. The charge state determines the electron-configuration and the strength of the hyperfine field.

We prepared the experiment with ^{148}Nd where the g-factor of the 2^+ state is already known ($g(2^+) = 0.36(6)$) [3] using exactly the same recoil velocity as in the ^{136}Nd experiment. This time for simplicity we used Coulomb excitation of ^{148}Nd by ^{10}B as a beam particle. The velocity of the beam was selected to obtain the same ^{148}Nd velocity as ^{136}Nd in the previous experiment [1]. The beam energy was 56.5 MeV, resulting in a ^{148}Nd velocity of 1.03(3)% c, the same as in the ^{136}Nd experiment. In Fig. 1 one can see the energy spectrum including gammas from the $2^+ \rightarrow 0^+$ transition in ^{148}Nd. The velocity was calculated from the energy distance between the stopped and the in-flight peaks.

Experimental Setup

We studied magnetic moments of short-lived states in Nd isotopes using the Recoil Doppler Shift Method (RDSM) by measuring a time dependent γ-ray angular distribution of the $2^+ \rightarrow 0^+$ transition in the Coulomb excitation of ^{148}Nd. The idea was to get the strength of the hyperfine field in the ^{148}Nd recoils to measure the g-factors in the other Nd isotopes, in particular ^{136}Nd. The experiment was realized with a plunger device centred in the EAGLE array.

The g-factor can be obtained from the angular distribution anisotropy measured along the time axis. The ^{10}B beam at an energy of 56.5 MeV was produced by the U-200P cyclotron at the Heavy Ion Laboratory in Warsaw. The ^{148}Nd target had a thickness of 0.3 mg/cm^2, evaporated onto a Nb supporting foil of thickness 4.5 mg/cm^2 and covered by a ^{197}Au layer of 0.1 mg/cm^2 thickness. The supporting foil was facing the beam. We used a thin layer of Au to preserv the neodymium from oxidation. The trick with

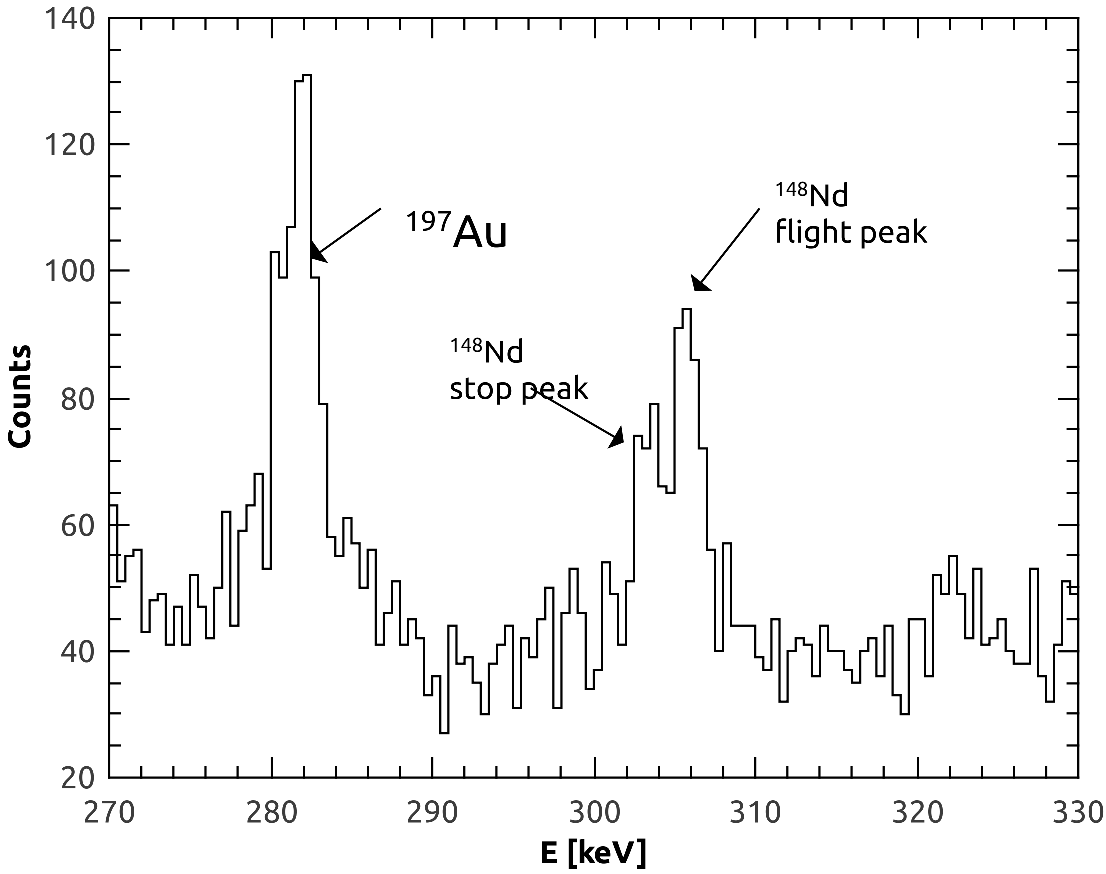

Figure 1: Energy spectrum of gamma rays showing the transition from the first excited state of ^{148} Nd, $2^+ \rightarrow 0^+$.

the gold foil can be done without consequences as the Coulomb excitation of gold can be easily distinguished in the off-line analysis of the energy spectra. To measure properly the angular distribution of a γ-ray we had to choose only events which ^{148}Nd ions recoiling along the beam axis (within 3° accuracy). For this the Si back scattering detector array was used, choosing only ^{10}B particles back scattered within 15° to 30° angles backward.

The plunger device was centred inside the EAGLE array [4] consisting of 15 HPGe detectors, each one surrounded by an anti-Compton shield and collimator. The Ge detectors were positioned in rings at each of four angles with respect to the beam axis: 37° (4 detectors), 63° (4 detectors), 79° (4 detectors), and 143° (3 detectors). Data were recorded at 7 instances in the plunger device ranging from 50 μm to 300 μm.

Bibliography

[1] A. Tucholski *et al.*, Phys. Rev. **C 100** (2019) 004300.
[2] H.D. Betz, Rev. Mod. Phys. **44** (1972) 3.
[3] J. Holden *et al.*, Phys. Rev. **C 63** (2001) 024315.
[4] J. Mierzejewski *et al.*, Nucl. Inst. and Meth. **659** (2011) 84–90.

C.9 An attempt at a theoretical interpretation of low lying $I = 0$ states in the ^{140}Sm nucleus

J. Samorajczyk-Pyśk[1], L. Próchniak[1] J. Srebrny[1], Ch. Droste[2], S.G. Rohoziński[2] and the EAGLE collaboration[a]

1) Heavy Ion Laboratory, University of Warsaw, Warszawa, Poland
2) Faculty of Physics, University of Warsaw, Warszawa, Poland

Proper interpretation of relatively low-lying 0^+ states in even-even nuclei is a challenge to nuclear theory. In particular, the question whether these states are of a deformation-driven collective nature is still open. In an attempt to answer this question in the case of the ^{140}Sm nucleus (Z=62, N=78) we applied two variants of the collective model.

1. A simple phenomenological model with a γ-independent potential energy and constant mass parameter [2]. The model can describe the smooth transition from the standard vibrational model to large β deformation (Wilets–Jean model [3]).

2. A five-dimensional General Bohr Hamiltonian (microscopic GBH) with the potential energy and six inertial functions (mass parameters) dependent on the β, γ variables calculated in the frame of a microscopic theory [4].

The first, phenomenological, approach happens to be quite successful and gives the possibility of a rather simple classification of the collective excitation in terms of the quantum numbers responsible for different modes of excitation: n_β, the number of β vibrational phonons and λ describing the coupled rotational and γ-vibrational excitations (for more details see [2]). It also gives several useful selection rules for the E2 transitions. The picture produced by the microscopic GBH model is more complicated but we found that some qualitative conclusions regarding the nature of the states in this model can be drawn from comparing probability distributions in the β, γ plane calculated in both models.

Some details of the models. The calculations with the phenomenological model were performed using a potential energy $V(\beta,\gamma) = V(\beta^2) = C\beta^2/2 + G[e^{-(\beta/a)^2} - 1]$ with $C = 73.5$ MeV, $a = 0.103$, $G = 4.11$ MeV, see Fig. 1 and with mass parameter $B = 135\ \hbar^2$/MeV (more precisely $B_{\beta\beta} = B_{\gamma\gamma} = B_x = B_y = Bz = B$ and $B_{\beta\gamma} = 0$). In the case of the GBH model we used the well known SLy4 variant of the Skyrme interaction and seniority-type pairing.

Theoretical results of both models compared to the experimental level scheme are shown in Fig. 2. Of particular interest are two 0^+ levels at very close energies 1599 keV and 1629 keV. Based on the experimental B(E2; $0 \to 2_1$)/ B(E2; $0 \to 2_2$) ratio the 1599 keV level was tentatively identified as a γ-vibrational state and the 1629 keV level as a β-vibrational one. It is a very rare case when the γ-vibrational 0^+ level lies very close to the β-vibrational and, moreover, even a bit lower in energy. Inspection of the probability distribution plots for the six lowest 0^+ states shown in Fig. 3 suggests that in the case of $0^+_{1,2,3,4}$ the qualitative classification provided by the phenomenological model is still useful for the more sophisticated, and hopefully more reliable, microscopic approach. However, to obtain a more conclusive answer to the question posed at the beginning of this contribution one needs more experimental data, in particular on $B(E2)$ transitions and transfer reactions.

[a] For a full list of authors see [1]

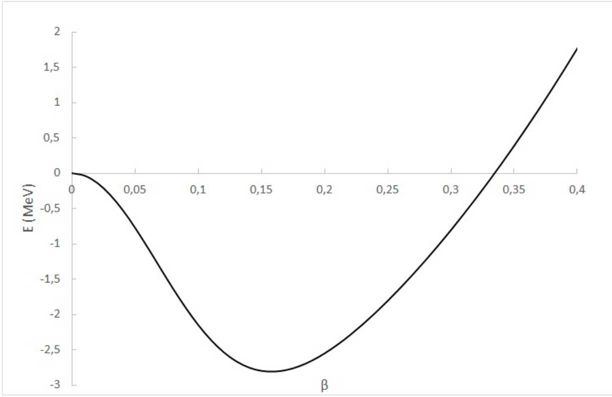

Figure 1: Plot of the potential energy function used in the phenomenological collective model.

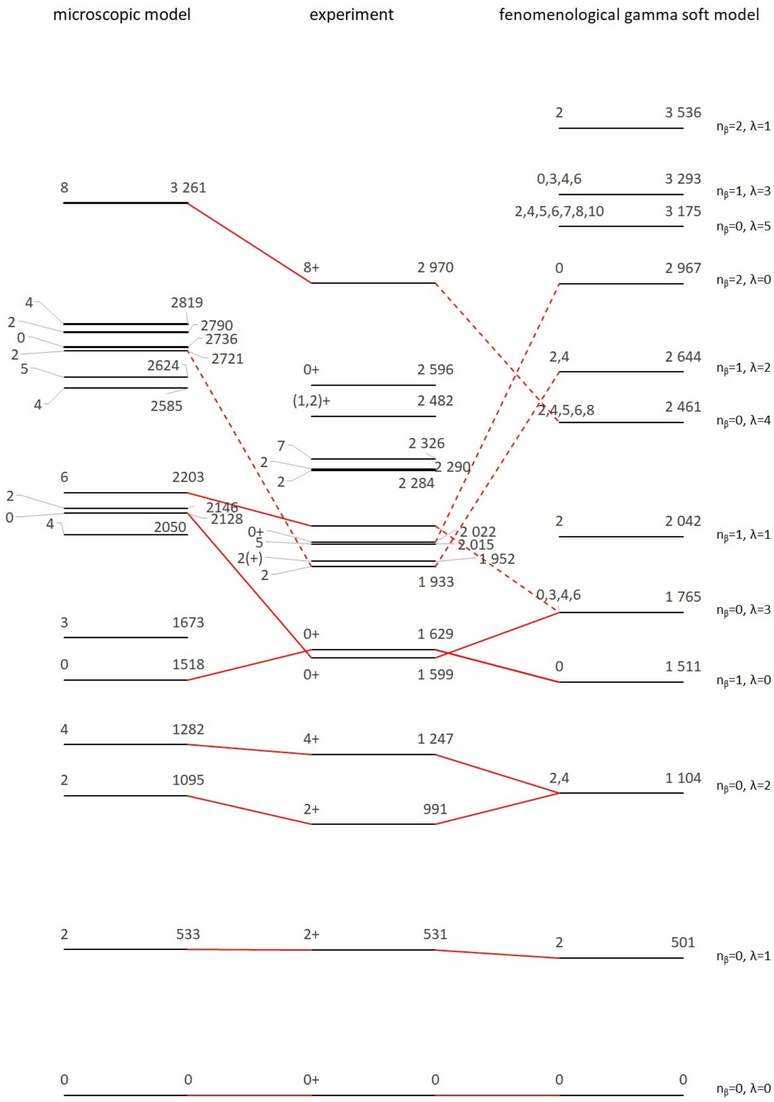

Figure 2: Comparison of experimental and theoretical energy levels in the ^{140}Sm nucleus.

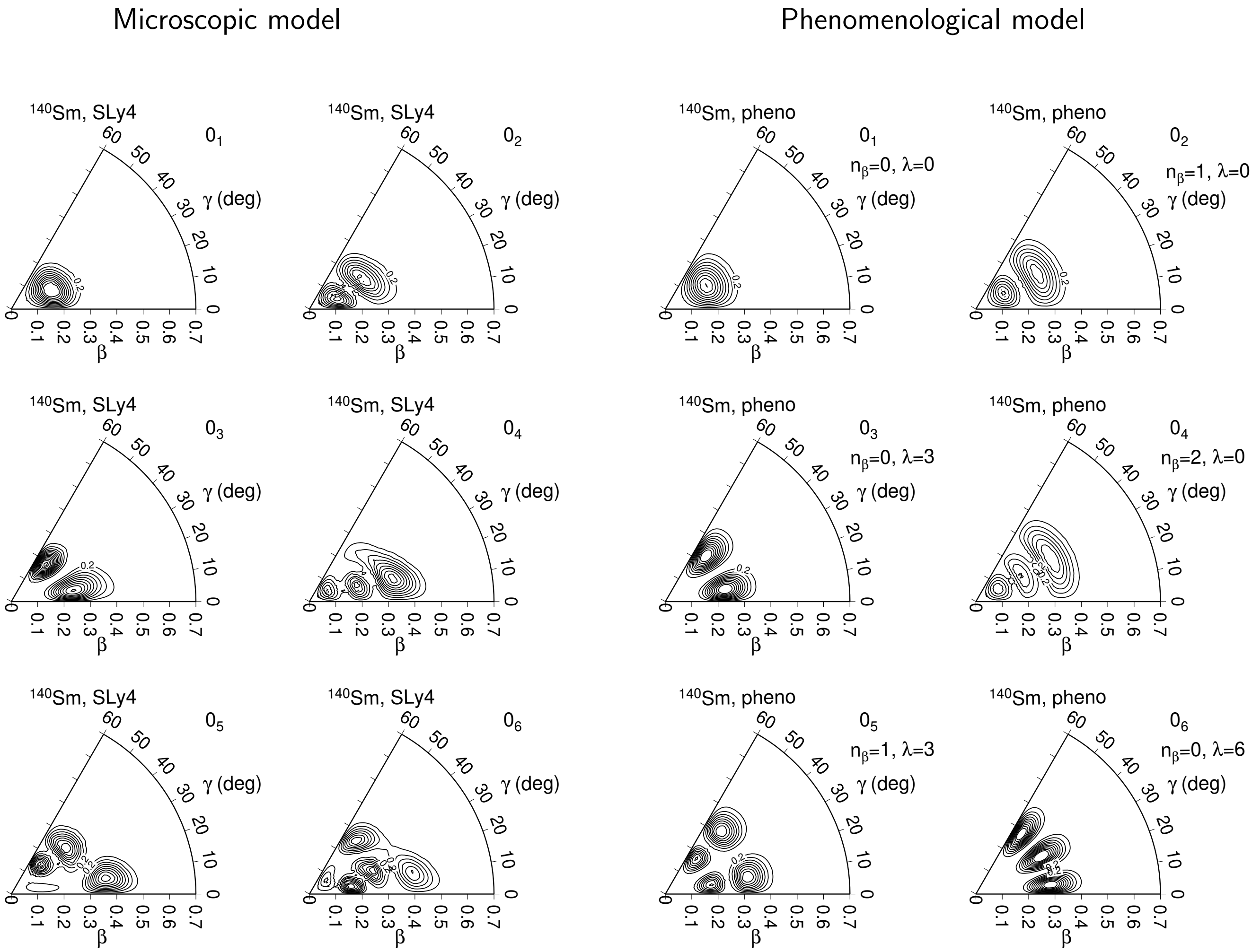

Figure 3: Probability distributions for the six lowest 0^+ levels calculated with both theoretical models.

Bibliography

[1] J. Samorajczyk *et al.*, HIL Annual Report 2018, page 63.
[2] S.G. Rohoziński *et al.*, Zeitschrift für Physik **268** (1974) 401.
[3] L. Wilets, M. Jean, Phys. Rev. **102** (1956) 788.
[4] L. Próchniak, S.G. Rohoziński, J. Phys. G: Nucl. Phys. **36** (2009) 123101.

C.10 Experimental measurements and theoretical investigation of the ^{12}C(^{10}B, ^{9}Be)^{13}N proton transfer reaction at 41.3 MeV

N. Burtebayev[1,2], *S.V. Artemov*[3], *R. Yarmukhamedov*[3], *S.B. Sakuta*[4], *K. Rusek*[5], *M. Nassurlla*[1,2], *N. Amangeldi*[6], *M. Nassurlla*[1,2], *F.Kh. Ergashev*[3], *A.A. Karakhodjaev*[3], *O.R. Tojiboev*[3], *A. Trzcińska*[5], *M. Wolińska-Cichocka*[5], *E. Piasecki*[5], *W. Trzaska*[7], *B. Mauyey*[1,8], *M. Kowalczyk*[5], *M. Kisieliński*[5]

1) Institute of Nuclear Physics of the National Nuclear Center, Almaty, Kazakhstan
2) Al-Farabi Kazakh National University, Almaty, Kazakhstan
3) Uzbekistan Academy of Sciences, Institute of Nuclear Physics, Tashkent, Uzbekistan
4) National Research Center "Kurchatov Institute", Moscow, Russia
5) Heavy Ion Laboratory, University of Warsaw, Warszawa, Poland
6) L.N. Gumilyov Eurasian National University, Astana, Kazakhstan
7) Department of Physics, University of Jyväskylä, Finland
8) Joint Institute for Nuclear Research, Dubna, Russia

A reliable estimate of the rates of nuclear-astrophysical processes is one of the most important problems of modern nuclear astrophysics [1] as it is the main link of the cold CNO cycle of hydrogen burning and plays an important role both in the generation of energy in massive stars and as a source of low-energy solar neutrinos (GALLEX experiment) [2]. The ANC (asymptotic normalization coefficient) values were successfully used [2, 3] for the evaluation of the ratio of the direct mechanism yield to the proton radiative capture cross section (or astrophysical S-factor). The ANC values can be obtained from the analysis of peripheral proton transfer reactions.

In this work the results of the differential cross section (DCS) measurements for the proton transfer reaction ^{12}C(^{10}B, ^{9}Be$_{g.s.}$)^{13}N$_{g.s.}$ are reported. The goal of these studies was to obtain the ANC ^{13}N$_{g.s.}$ $\rightarrow$ ^{12}C + p. A ^{10}B beam of 41.3 MeV was delivered by the U-200P cyclotron at the Heavy Ion Laboratory (University of Warsaw). A self-supporting ^{12}C target of thickness 0.14 mg/cm^2 was used. The ICARE scattering chamber was equipped with 4 gas-Si movable telescopes and 3 Si monitors. A typical two–dimensional spectrum (ΔE, E) and the energy spectrum of ^{9}Be ions from the ^{12}C+^{10}B interaction are shown in Figs. 1, 2.

The DCS $\dfrac{\sigma^{MDW}}{d\Omega}$ of the peripheral reaction A (x, y) B, where x = y + p and B = A + p, in the MDWBA formalism is represented for the reaction ^{12}C (^{10}B, ^{9}Be) ^{13}N as follows:

$$\frac{d\sigma^{MDW}}{d\Omega} = C^2_{^{13}N\rightarrow^{12}C+p} R(E;\theta;b_{^{13}N\rightarrow^{12}C+p}) \tag{1}$$

$$R(E;\theta;b_{^{13}N\rightarrow^{12}C+p}) = \frac{C^2_{^{10}B\rightarrow^{9}Be+p}\ \sigma^{DW}\ (E;\theta;b_{^{13}N\rightarrow^{12}C+p})}{b^2_{^{10}B\rightarrow^{9}Be+p}\qquad b^2_{^{13}N\rightarrow^{12}C+p}} \tag{2}$$

For a peripheral reaction, the values of R(b) must remain constant if one changes the shape of the potential of the proton bound state, i.e. the value of b (b - single-particle asymptotic normalization coefficient) by varying the geometric parameters of the potential. Fig. 3 shows that the function R(b) depends very slightly on b, so the reaction ^{12}C(^{10}B, ^{9}Be$_{g.s.}$)^{13}N$_{g.s.}$ is practically peripheral; hence the MDWBA formalism [2] can be applied to analyze the data.

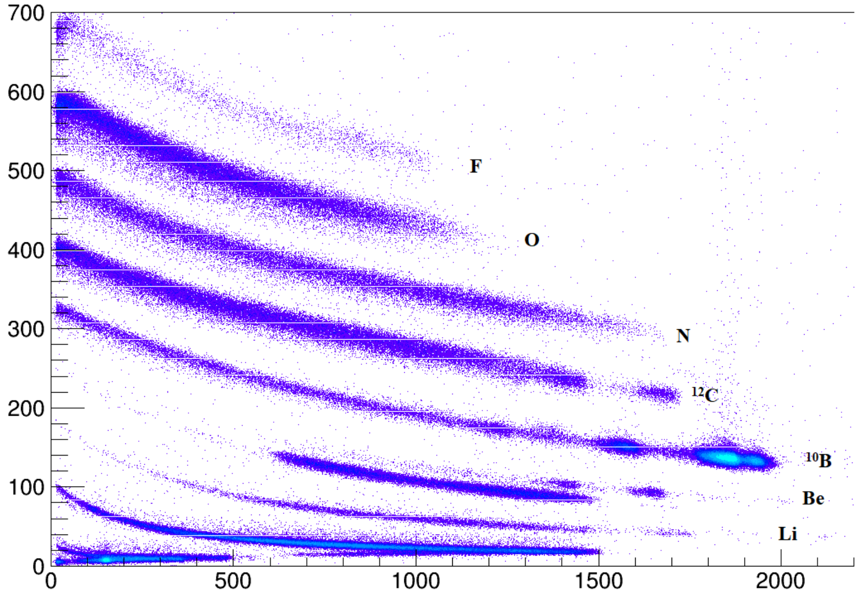

Figure 1: The raw two–dimensional (ΔE, E) spectrum from the ^{12}C +^{10}B interaction (θ_{lab}=15°).

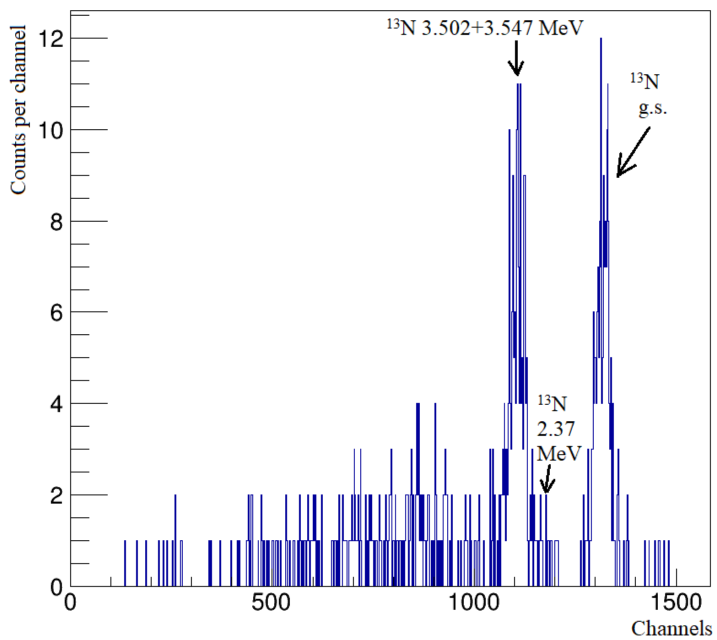

Figure 2: Fragment of the energy spectrum of ^{9}Be ions from the ^{12}C+^{10}B interaction, measured at an angle of 25° in the lab system.

Fig. 4 presents the experimental and calculated DCS (solid curve) of the reaction, where the single particle cross section σ^{DW} was calculated by the code LOLA [4].

According to equations (1) and (2) the DCS of the reaction is calibrated by the product of the ANCs squares $(C_{^{10}B\rightarrow{}^{9}Be+p})^2 \times (C_{^{13}N\rightarrow{}^{12}C+p})^2$, which is found to be 10.9 fm^{-2}. So the ANC $(C_{^{13}N\rightarrow{}^{12}C+p})^2 \approx 2.503$ fm^{-1} was preliminary evaluated from the MDWBA analysis (curve in Fig. 4) as the ANC $(C_{^{10}B\rightarrow{}^{9}Be+p})^2 = 4.35$ fm^{-1} is the corrected in [5] value taken from [6, 7]. The parameters of the optical potential (OP) for the entrance

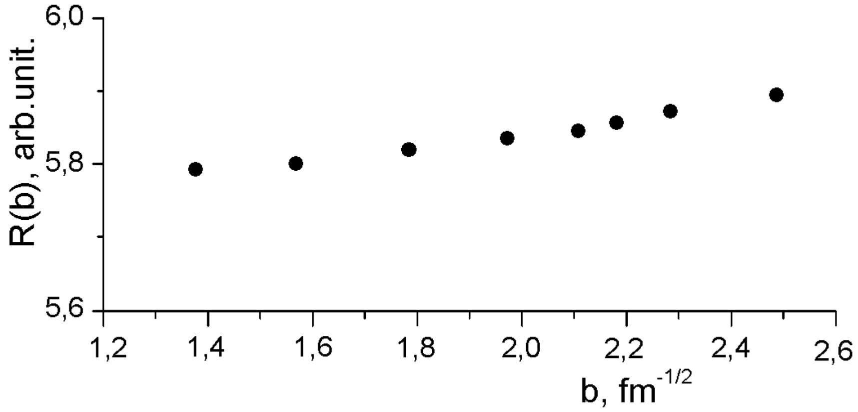

Figure 3: R(b) function ($\theta_{c.m.} = 16°$).

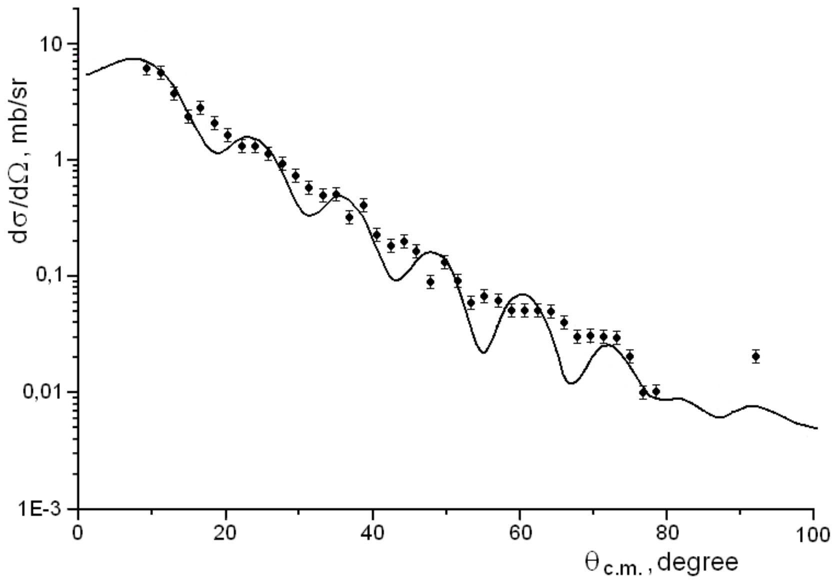

Figure 4: Experimental and calculated DCS of the reaction ^{12}C(^{10}B, ^{9}Be$_{g.s.}$) ^{13}N$_{g.s.}$.

channel were obtained in the same experiment [8] and for the exit channel OP were taken from Ref. [9] (for ^{13}N + ^{10}B scattering at the nearest energy).

The channel coupling was found to be not more then experimental errors by evaluation with the FRESCO code. A more precise value of the ANC will be found by analysis of the data in the framework of the developed asymptotic reaction theory [5] along with a careful selection of the OP parameters.

Bibliography

[1] E.G. Adelberger *et al.*, Rev.Mod.Phys **83** (2011) 195–245.
[2] R.E. Tribble *et al.*, Rep.Prog.Phys. **77** (2014) 1–49.
[3] O.R. Tojiboev *et al.*, Phys. Rev. **C 94** (2016) 054616.
[4] R.M. DeVries, Phys. Lett. **B36** (1971) 18.
[5] R. Yarmukhamedov, K.I. Tursunmakhatov, N. Burtebayev., Int. J. Mod. Phys. **49** (2019) 1960016.
[6] S.V. Artemov *et al.*, Phys. At. Nucl. **59** (1996) 428–438.
[7] A. M. Mukhamedzhanov *et al.*, Phys. Rev. **C 56** (1997) 1302–1312.
[8] N. Burtebayev *et al.*, Int. J. Mod. Phys. **28** (2019) 1950028.
[9] C.M. Perey and F.G. Rerey, Atom. Data and Nucl. Data Tables **17** (1976) 1.

C.11 Estimation of the thickness homogeneity of a target prepared by evaporation based on Lambert's emission law

A. Stolarz
Heavy Ion Laboratory, University of Warsaw, Warszawa, Poland

In most cases when experiments in nuclear physics are performed with isotopically enriched material the target has to be prepared with minimal loss of the usually very expensive separated isotopes. The required target parameters (especially thickness) often dictate the preparation method. In the case of targets with thicknesses achievable only by vapour deposition material consumption can be minimised either by applying a small distance between the substrate and vapour source or using a crucible with a narrow exit. In both cases the evaporation set-up geometry entails a significant variation in the thickness of the deposited material even over relatively small areas.

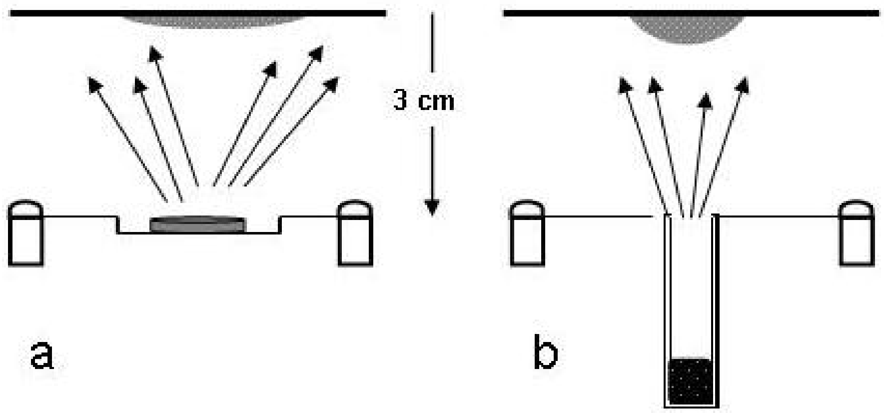

Figure 1: Schematics of the material distribution deposited from flat (a) and tube-shaped (b) crucibles.

In the case of an open vapour source the deposited material exhibits much higher thickness homogeneity but this option results in a much higher material consumption than use of a tube-shaped or pin-hole crucible. The thickness fluctuation/material distribution can be estimated employing Lambert's emission law known from optics. The law defines the light intensity at a point Φ_x on the illuminated surface as proportional to the cosine of the angle between the normal to the source surface and the incident light ray. For a point light source the light intensity at the point x is described by:

$$\Phi_x = \Phi_0 \cdot cos\theta \tag{1}$$

where Φ_0 is the intensity of the light flux emerging from the source and cosθ is the cosine of the angle between the normal to the source surface and the incident light ray. During the evaporation process the distribution of the material which grows on the substrate depends on the distribution of the vapour stream emerging from the vapour source. Similarly to the light intensity, the amount of deposited material depends on the vapour stream intensity and for deposition on a flat substrate the deposit thickness variation between the centre and the border of the deposit may be estimated applying the cosine law:

$$I(\alpha) = I_0 \cdot \cos^n \cdot \alpha \tag{2}$$

where $I(\alpha)$ and I_0 are the vapour stream intensities at angles α and 0, respectively and $n \geq 1$ depending on the vapour source type, which can not be treated as a point source and has to be defined experimentally.

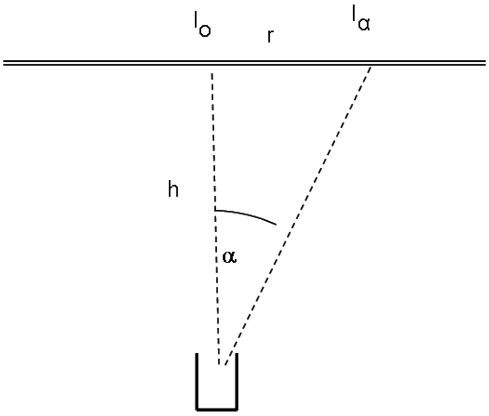

Figure 2: Evaporation geometry.

Taking into account the geometry parameters the thickness of the deposit d at point $I(\alpha)$ may be estimated from:

$$d(r) = d_0[1 + (r/h)^2]^{-n/2} \tag{3}$$

where: $d(r)$ is the deposit thickness at distance r from the normal to the vapour source, d_0 the thickness of the deposit at the point placed directly above the vapour source (centre of the deposit), h – distance between the vapour source and the substrate (on which the vapour condenses).

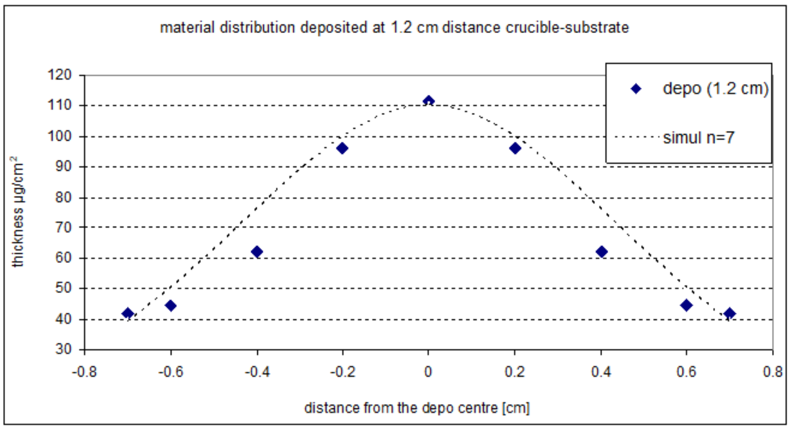

Figure 3: Thickness distribution of a Te layer deposited from a tube-type crucible with a distance of 1.2 cm between the crucible and substrate.

C.12 Lifetime studies in neutron deficient ^{176}Pt using the recoil distance Doppler-shift technique

C. Fransen[1], C. Müller-Gatermann[1], A. Dewald[1], T. Abraham[2], M. Beckers[1], A. Blazhev[1], A. Goldkuhle[1], K. Hadyńska-Klęk[2], J. Jolie[1], G. Jaworski[2], M. Kowalczyk[2], P. Napiorkowski[2], M. Palacz[2], B. Radomyski[2], K. Rusek[2], J. Srebrny[2], A. Tucholski[2], K. Wrzosek-Lipska[2], F. von Spee[1], K.O. Zell[1]

1) Institute for Nuclear Physics, University of Cologne, Germany

2) Heavy Ion Laboratory, University of Warsaw, Warszawa, Poland

A measurement with the Cologne plunger device [1] coupled to the EAGLE γ-ray spectrometer was performed at HIL in June 2019 for the first time. The aim was the measurement of yrast level lifetimes in neutron deficient ^{176}Pt using the recoil distance Doppler-shift method (RDDS). In this region experimental findings both on level schemes and absolute $E2$ transition strengths yielded effects like shape coexistence in the Hg and Pb isotopic chains. These result from low-lying intruding structures, e.g., from excitation of otons above the Z=82 main shell. In neutron deficient Hg isotopes close to neutron midshell, a weakly deformed ground state configuration and a prolate intruder structure were clearly identified. For the neighbouring midshell Pt isotopes (^{178,180}Pt) it has already been shown that the prolate deformation becomes the ground state configuration, where the corresponding deformation is similar to that of the intruder configuration in Hg [2, 3]. The experimental observables are in agreement with predictions from the interacting boson model (IBM) or mean-field (MF) calculations [4]. For the lighter Pt isotopes these model predictions differ from each other, exactly at ^{176}Pt a dramatic change towards a herical ground state configuration is foreseen by the IBM, whereas MF theory prognosticates almost no change towards even more neutron deficient nuclei. Existing data prior to is work do not allow conclusions to be drawn, motivating the measurement of the yrast transition strengths in ^{176}Pt.

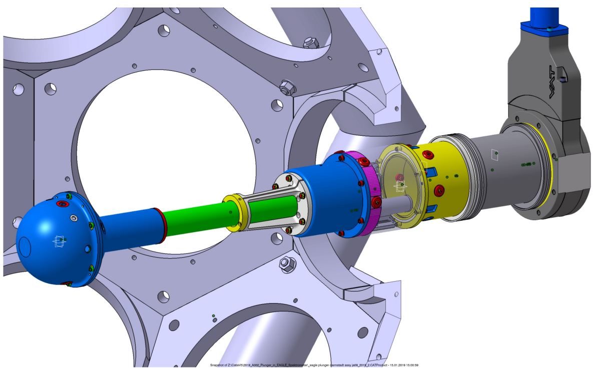

Figure 1: Drawing of the Cologne plunger mounted at the EAGLE γ-ray spectrometer at HIL. The yellow part is a new adaptor part that was made to connect the plunger to a SO-K 100 bellows (dark grey) that is mounted on the final valve of the EAGLE beamline and is used to align the plunger. Only the frame of EAGLE is shown, i.e., the HPGe detectors and the respective anti-Compton shields are not shown.

The Cologne plunger was mounted for the first time on the EAGLE spectrometer for this measurement (see Fig. 1). We used the ^{150}Sm(^{32}S,6n)^{176}Pt reaction with a ^{32}S beam energy of 198 MeV to populate yrast states in ^{176}Pt. The plunger target consisted of a 1.0 mg/cm^2 ^{150}Sm layer evaporated onto a 1.2 mg/cm^2 Ta stretchable support foil facing the beam. A 6.8 mg/cm^2 gold foil was used to stop the recoiling nuclei.

EAGLE was equipped with 13 anti-Compton shielded high-purity Germanium detectors arranged in 3 rings with respect to the beam axis where 5 detectors were mounted at an angle of 37 degrees, 3 at 63 degrees, and 5 at 143 degrees. The data were sorted into $\gamma\gamma$ coincidence matrices aiming for the determination of level lifetimes from direct gates on flight components of feeding transitions to exclude any contribution from delayed sidefeeding. The experiment suffered seriously from too low beam current on the plunger target and several interruptions of the beam due to technical issues. Thus we were only able to perform measurements at 2 target–degrader distances of 100 μm and 200 μm and an dditional shorter run at 5 μm instead of the foreseen 12 distances. Fig. 2 depicts a γ-ray spectrum where shifted and unshifted components of the γ-ray lines of ^{176}Pt can be clearly identified. The data are analysed at the moment but only allow the determination of lifetimes of the 4_1^+ and 6_1^+ states in ^{176}Pt with rather low precision.

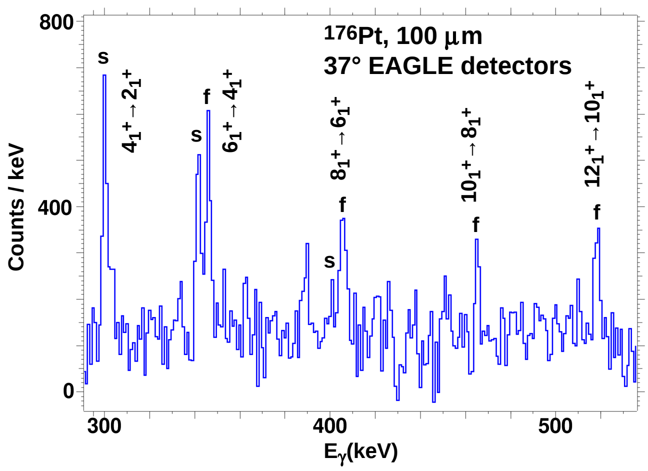

Figure 2: Spectrum from the experiment on ^{176}Pt for the EAGLE detectors at a forward angle of 37 degrees with respect to the beam line gated on the $2_1^+ \to 0_1^+$ transition. “f” denotes the flight components and “s” the stopped components of the respective γ-ray transitions.

Nevertheless, from the technical point of view the experiment was successful as it was proven that the Cologne plunger coupled to EAGLE represents a valuable setup for future experimental campaigns with the RDDS technique. Also, it was confirmed that the cross section of the ^{150}Sm(^{32}S,6n)^{176}Pt reaction of about 10 mb that was estimated before the experiment is correct, allowing the determination of yrast level lifetimes with high precision for unique interpretation of the structure of ^{176}Pt. Thus, the periment on ^{176}Pt will be redone to achieve the aims of this work.

Bibliography

[1] A. Dewald, O. Möller, P. Petkov, Prog. Part. Nucl. Phys. **67** (2012) 786.

[2] C. Müller-Gatermann *et al.*, Phys. Rev.**C 97** (2018) 024336.

[3] C. Fransen *et al.*, EPJ Web of Conferences **223** (2019) 01016.

[4] J.E. Garcia-Ramos *et al.*, Phys. Rev. **C 89** (2014) 034313.

C.13 Silicon epitaxial 20 μm thick double sided strip test detector with read-out of induced signals on the back detector strips

A. J. Kordyasz[1], *L. Kordyasz*[2]

1) Heavy Ion Laboratory, University of Warsaw, Warszawa, Poland
2) SonicTech, Lomianki, Poland

L.S. Barabash and E. Belcarz [1] produced a one dimensional silicon strip detector 21 x 5 mm^2, obtaining position information by registration of induced signals propagating along the detector RC line on the back detector strips. The signals registered in the strips were induced through the isolation layer (mylar foil). The idea of this detector will be used for the present construction of a 20 μm thick double sided silicon strip detector produced by the low-temperature technique (see Fig. 1 and Fig. 2).

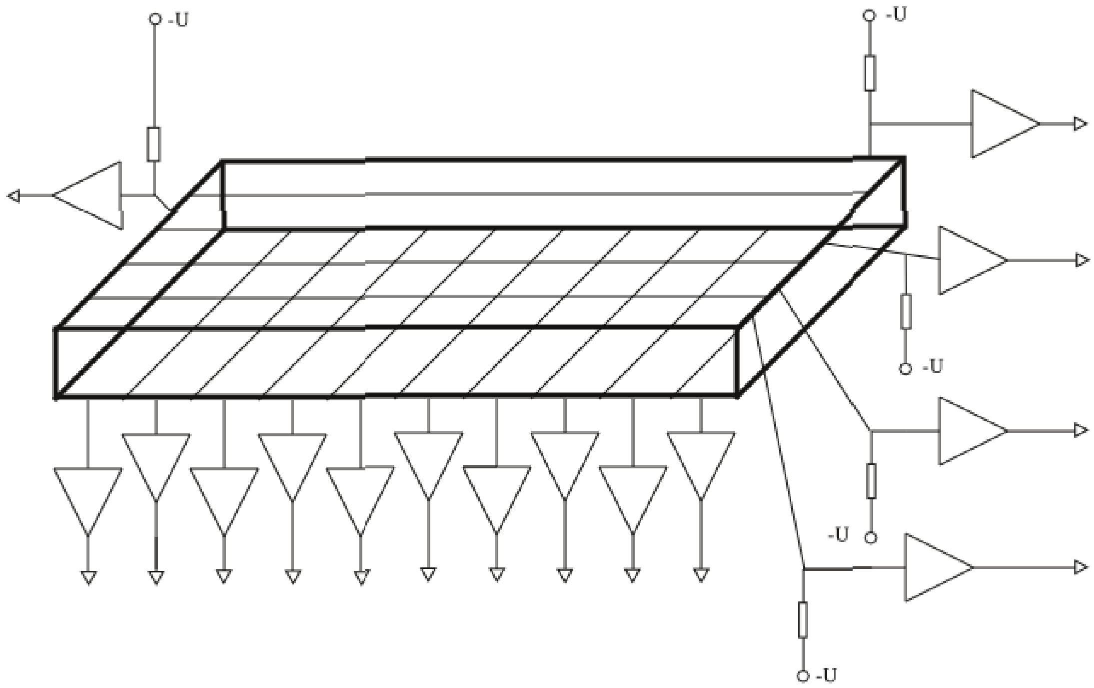

Figure 1: Schematic of the construction of a 20 μm thick double sided silicon strip epitaxial detector. On the back side of the silicon epitaxial $n^+ - n$ structure the detector resistive layer will be formed by the anodic dissolution of n^+ silicon substrate which will be grounded at the edges through evaporated Al contacts. On the back side of the wafer, a SiO_2 isolation layer will be evaporated followed by evaporation of Al strips connected with charge preamplifiers for registration of induced signals propagating along the detector RC line. On the upper wafer side, the detector strips (orthogonal to the bottom strips) will be created using the low-temperature technique for thin transmission detectors [2] and thin strip detectors [3]. The upper strips will be connected to the charge preamplifiers with negative bias potentials.

Silicon test detectors will be produced using 21 x 21 mm^2 $n^+ - n$ silicon epitaxial structures from which the low-resistivity substrate n^+ will be removed by anodic dissolution.

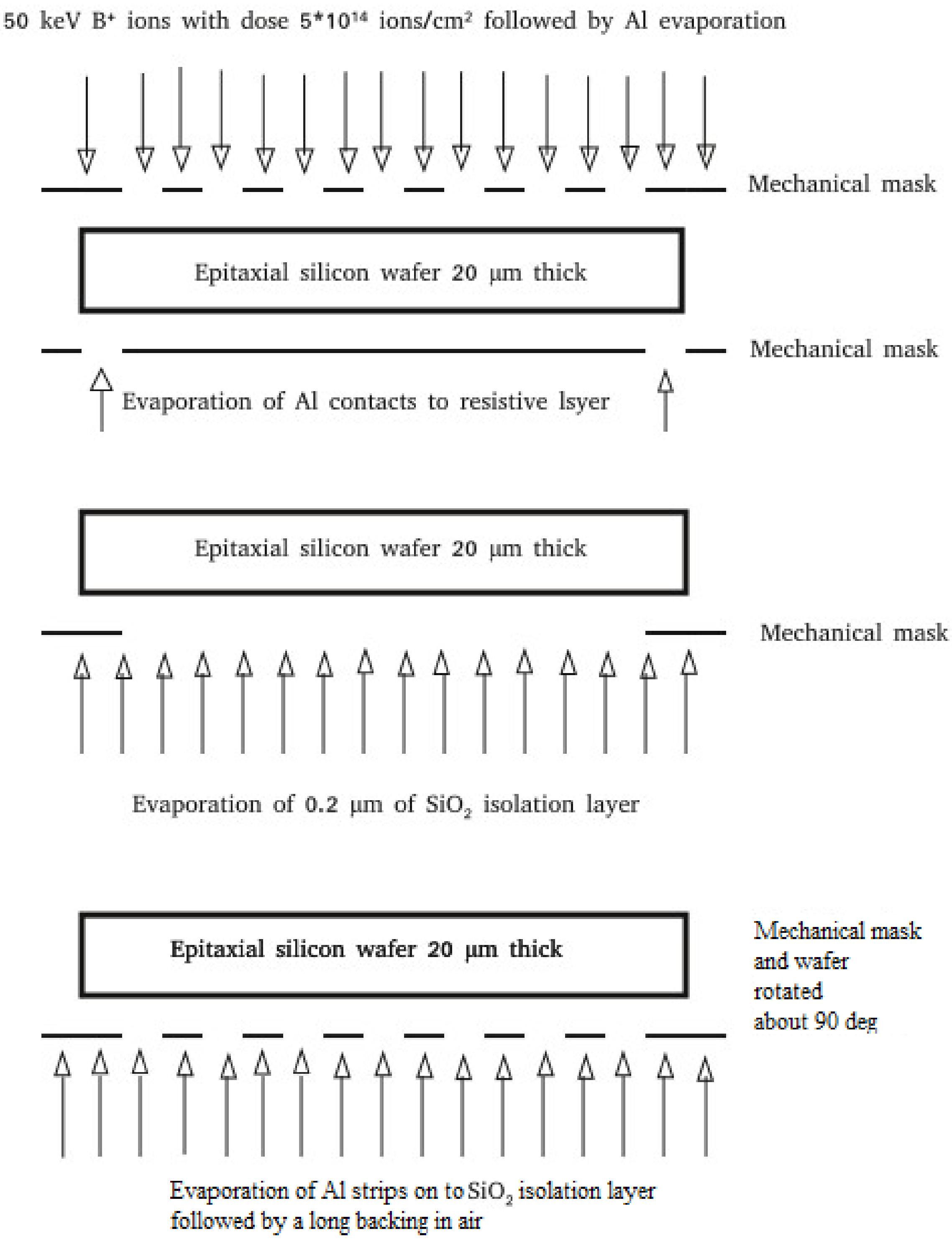

Figure 2: Technique of production of a 20 μm thick double sided epitaxial silicon detector using the low-temperature technique.

The edges of the detector back side resistive layer will be grounded using evaporation of Al contacts. We will use 0.1 mm thick Al masks prepared by cutting Al foil with a laser beam.

The active area of the double strip detector will be 17 x 17 mm^2. On each detector side there will be 7 strips 2 mm wide with a strip pitch 0.5 mm. Ion implantation of B^+ ions with an energy of 50 keV and dose 5x10^{14} ions/cm^2 will be performed using the mass separator (at the Igisol system) of the Heavy Ion Laboratory of Warsaw University supplied with a plasma ion source operating with diboron gas, a beam scanner with the possibility of motion in the X, Y plane and a focused beam to obtain very uniform ion implantation on the sample.

Bibliography

[1] L.S. Barabash *et al.*, NIM **A288** (1990) 375–378.
[2] A.J. Kordyasz *et al.*, Eur. Phys. J. **A51** (2015) 15.
[3] A.J. Kordyasz *et al.*, Acta Phys. Pol. **B47** (2016) 207.

C.14 Ultrasonic solder contacts for 20 μm thick epitaxial silicon detectors

A. J. Kordyasz, A. Bednarek

Heavy Ion Laboratory, University of Warsaw, Warszawa, Poland

Detector contacts for conventional silicon detectors are made by ultrasonic bonding. However, this technique is impossible for thin epitaxial silicon detectors since the mechanical pressure of the bonding tool can crush the thin, delicate silicon surface. To avoid this we propose ultrasonic solder contacts for thin silicon detectors. The scheme of ultrasonic solder contacts for thin silicon detectors is presented in Fig. 1.

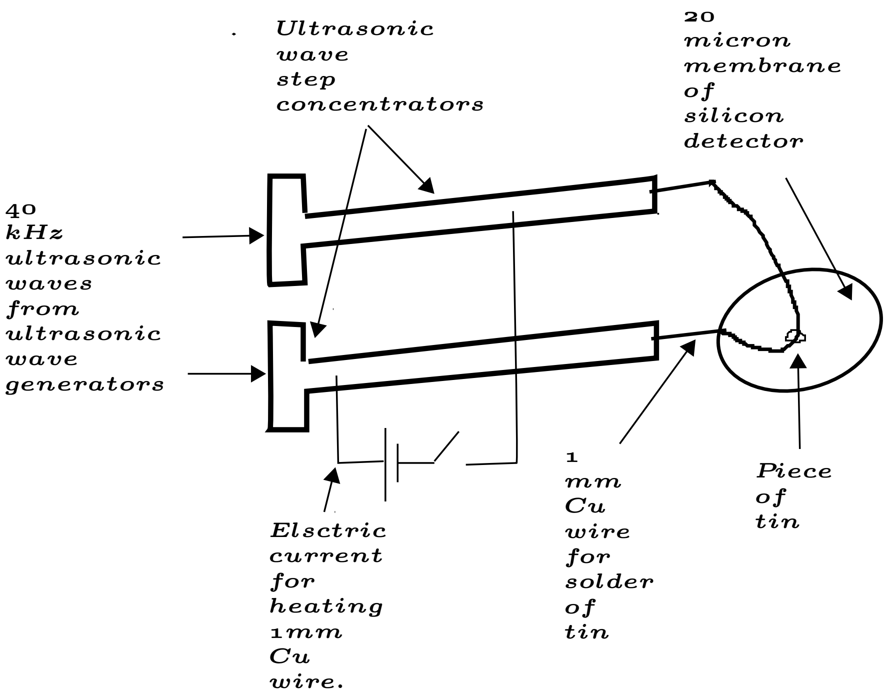

Figure 1: Scheme for the application of ultrasonic solder contacts to thin epitaxial silicon detectors.

The upper electrode of the thin detector of thickness 20 μm is made from a 2000 angstroms thick Al layer covered by Al_2O_3 oxide oxidised in air. This oxide should be removed for a proper solder process. To remove this oxide, ultrasonic vibration is necessary to solder the Al detector layer to a thin Cu wire contact of thickness about 0.05 mm. The small piece of tin on the silicon surface is melted by a 1 mm Cu wire heated by an electric current. Immediately after the ultrasonic vibration has been switched on to remove the Al oxide a good solder contact to the thin detector surface covered by the Al layer is made via the 0.05 mm Cu wire. The pressure of the vibrated and heated 1 mm Cu wire on the detector surface is about 2 grams. First tests of ultrasonic solder contacts for 20 μm thick epitaxial silicon detectors made good electric contacts and did not destroy the thin silicon detector membrane and are very promising. An example of the application of ultrasonic solder contacts to 300 μm silicon detectors is presented in Fig. 2. Four detectors mounted in an Al frame covered by Cu are shown in Fig. 2. These detectors were successfully tested with fission fragments from a ^{252}Cf source.

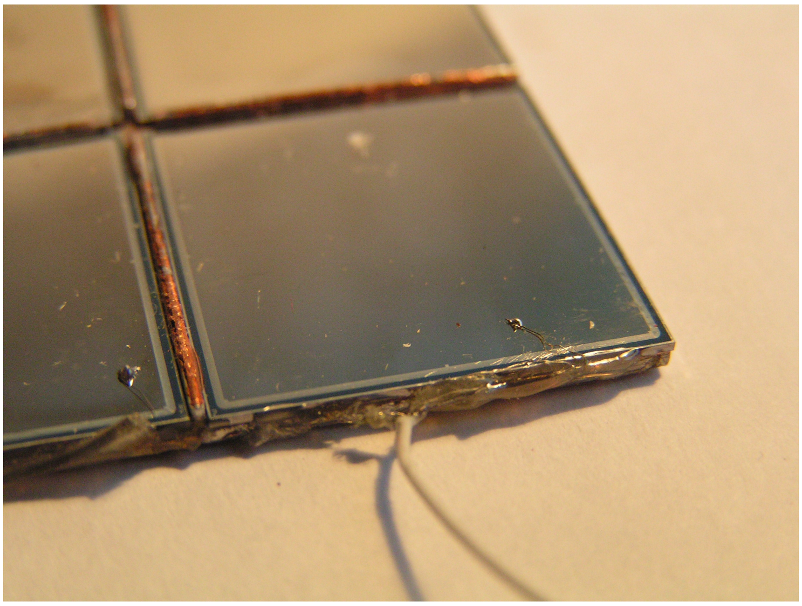

Figure 2: An example of ultrasonic solder contacts in a pair of silicon detectors.

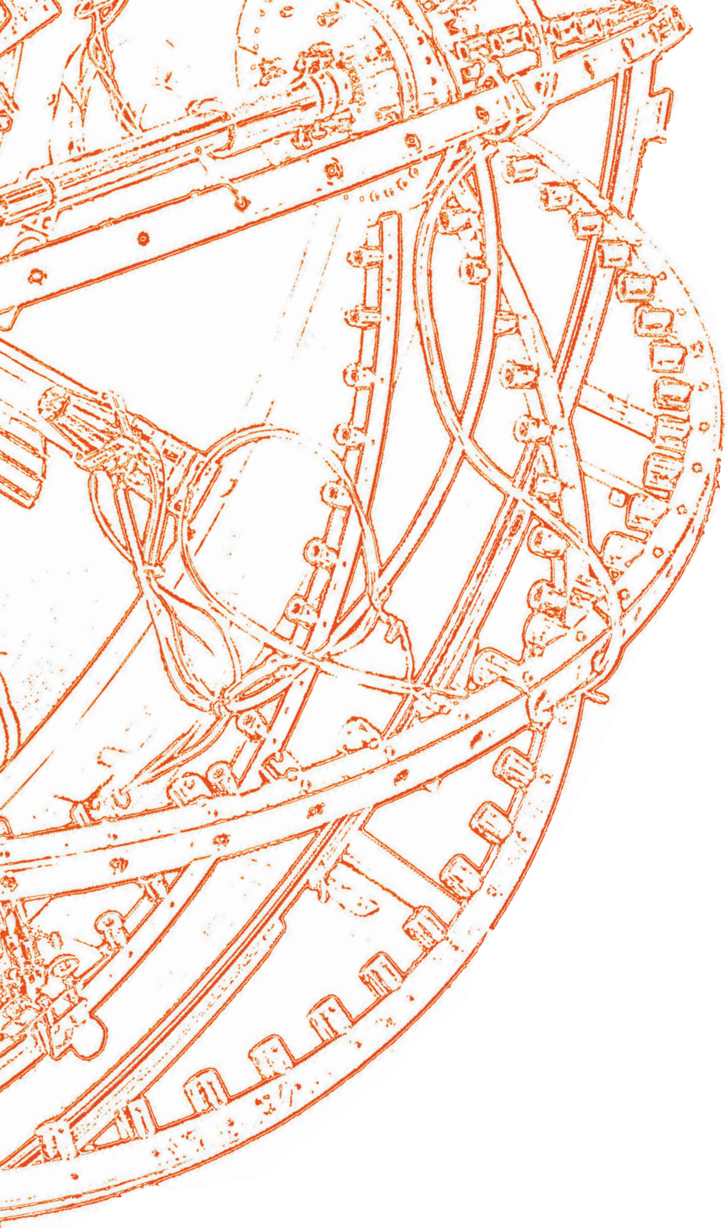

Part D
Experiments using external facilities

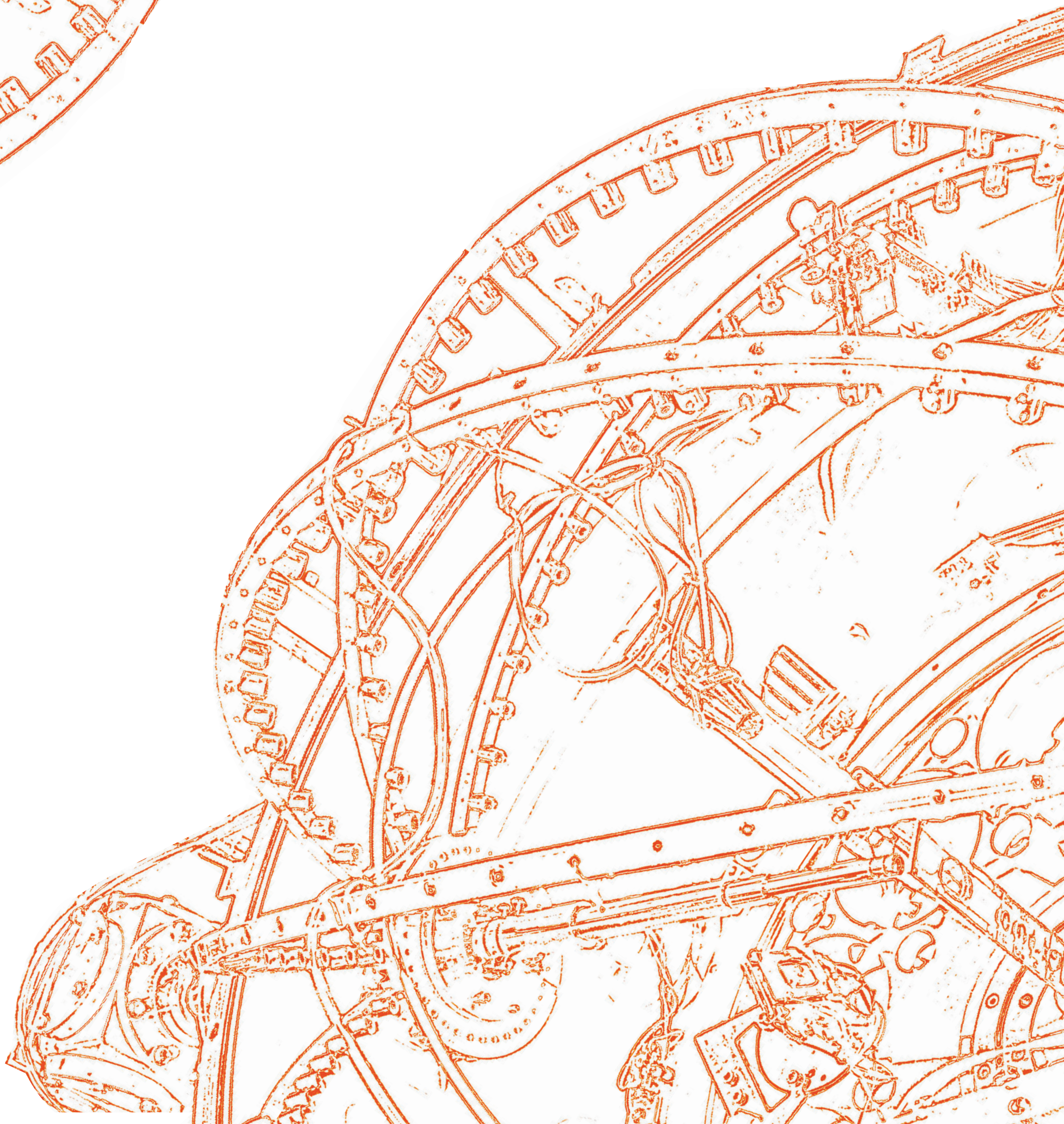

D.1 Barrier distributions of the ^{24}Mg + ^{90,92}Zr systems. Influence of energy dissipation

A. Trzcińska[1], E. Piasecki[1], G. Cardella[2], D. Dell'Aquila[3], S. De Luca[2,4], E. De Filippo[2], B. Gnoffo[2,5], M. Kowalczyk[1], G. Lanzalone[6,7], I. Lombardo[8], C. Maiolino[6], N. S. Martorana[6,5], A. Pagano[2], E. V. Pagano[6], S. Pirrone[2], G. Politi[2,5], L. Quattrocchi[2,5], F. Rizzo[6,5], P. Russotto[6], A. Trifiro[2,4], M. Trimarchi[2,4]

1) Heavy Ion Laboratory, University of Warsaw, Warszawa, Poland
2) INFN – Sezione di Catania, Catania, Italy
3) NFN – Sezone di Napoli and Dip. di Fisica Universita di Napoli Federico II Napoli, Italy
4) Dip. di Sci. Matematiche e Informatiche, Sci. Fisiche e Dci. della Terra Universitá di Messina, Italy
5) Dip. di fisica e astronomia Universitá di Catania, Catania, Italy
6) INFN-LNS, Catania, Italy
7) Universita Kore, Enna, Italy
8) INFN – Sezione di Napoli and Dip. di Fisica Universita di Napoli Federico II Napoli, Italy

Studies of barrier height distributions (BD) is a long-term project of the Barrier collaboration. The results of experiments in which the BD was determined for ^{20}Ne + ^{90,92}Zr and ^{20}Ne + ^{58,60,61}Ni indicate that dissipation (in this case due to non-collective excitations) can influence the barrier distribution shape [1–3]. To progress our understanding of this phenomenon, we changed the projectile to ^{24}Mg, which in some respects is similar to ^{20}Ne: it is also strongly clustered (consisting of not 5, but 6 α particles) and is also strongly deformed. Thus, the experiment aimed to accomplish a more stringent test of theoretical predictions by measurements of the quasielastic barrier distributions for the ^{24}Mg + ^{90,92}Zr systems. The experiment and preliminary results have already been reported [4, 5].

Due to the experimental possibilities of the CHIMERA detection system [6], we were able to measure simultaneously barrier distributions for a wider angular range and at a greater number of angles than in our previous experiments and found that, especially for smaller angles, their angular dependence is significant (Figs. 1, 2), being seen especially well for the ^{90}Zr target. This means that the scaling, given by the transformation from projectile energy to the effective energy E_{eff} is not sufficient for the description of the barrier distribution. The reason why this scaling is not good enough is that to compute E_{eff} one uses the classical approximation of the Coulomb trajectory, disregarding any quantal coupling effects due to the nuclear potential. As a result, we get only the shift of the BD along the energy axis. In reality, it is obvious that different angles mean different impact parameters and that at some distance the nuclear interaction comes into play.

The most important conclusion from the results is qualitative support of our hypothesis of the influence of dissipation on the BD shape: the structure turned out to be visible in the ^{90}Zr and washed out in the ^{92}Zr target cases. Calculations using the CC+RMT model [3] qualitatively agree with this observation: the partial energy dissipation, caused by the coupling of the relative motion of the projectile and target nuclei to many s.p. excitations is more than enough to explain the experimentally observed structure smoothing. However, the calculated barrier distributions are visibly too narrow in comparison with experiment, although the agreement is much better than without taking into account the partial energy dissipation.

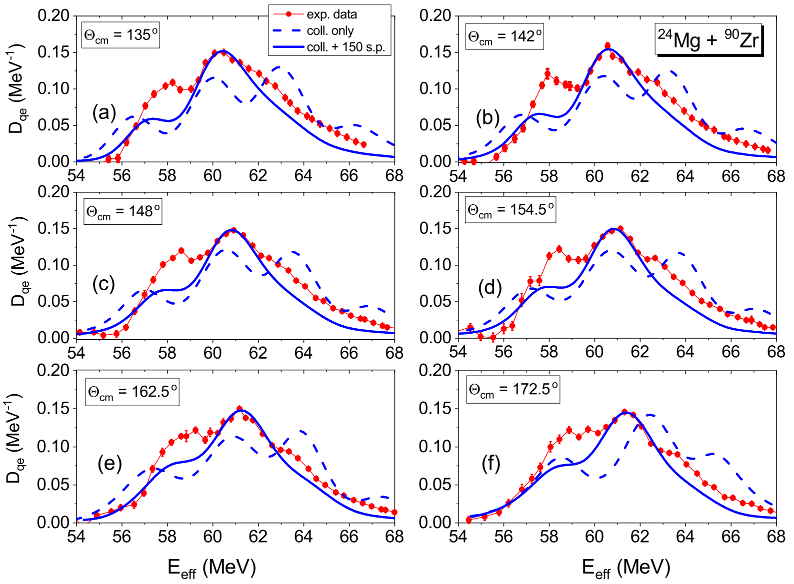

Figure 1: Comparison of experimental barrier distributions for ^{24}Mg + ^{90}Zr (red points connected for better visibility by red lines) with calculated results without dissipation (dashed blue lines) and with dissipation switched on by including couplings to 150 s.p. levels (solid blue lines). The experimental energy resolution was taken into account.

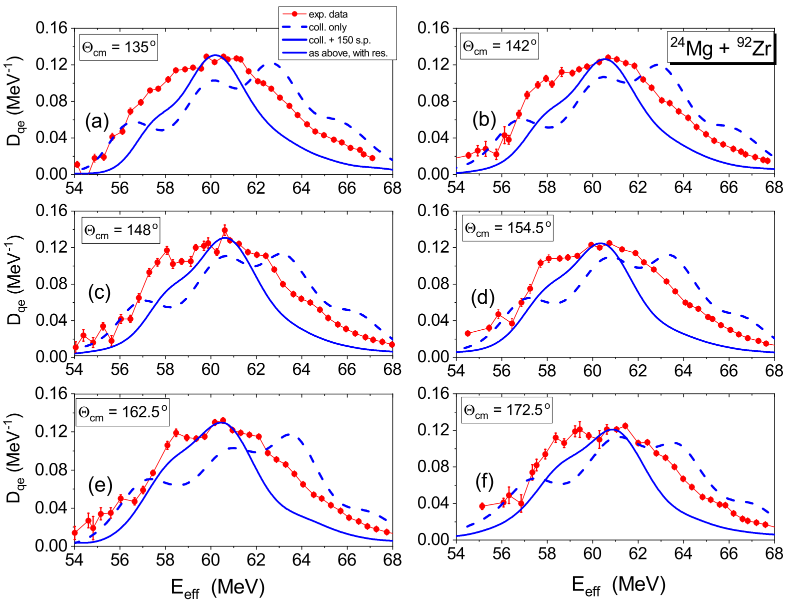

Figure 2: The same as in Fig. 1 for the ^{92}Zr target.

Bibliography

[1] E. Piasecki *et al.*, Phys. Rev. **C 80** (2009) 054613.
[2] A. Trzcińska *et al.*, Phys. Rev. **C92** (2015) 034619.
[3] E. Piasecki *et al.*, Phys. Rev. **C 100** (2019) 014616.
[4] A. Trzcińska *et al.*, HIL Annual Report 2016, p. 62.
[5] A. Trzcińska *et al.*, Acta Phys. Pol. **B 49** (2018) 387.
[6] A. Pagano, Nucl. Phys. **A 734** (2004) 504.

D.2 Study of the ^{10}Li low energy spectrum via the ^{2}H(^{9}Li,p) reaction

A. Bezbakh[1,2], S.G. Belogurov[1,3], V. Chudoba[1,2], A.S. Fomichev[1,4], E.M. Gazeeva[1], M.S. Golovkov[1,4], A.V. Gorshkov[1], G. Kamiński[1,5], S.A. Krupko[1], B. Mauyey[1,6], I.A. Muzalevsky[1,2], E.Yu. Nikolsky[1,7], Yu.L. Parfenova[1], W. Piątek[1,5], A.M. Quynh[1,8], A. Serikov[1], S.I. Sidorchuk[1], P.G. Sharov[1,2], R.S. Slepnev[1], S.V. Stepantsov[1], A. Świercz[1,9], P. Szymkiewicz[1,9], G.M. Ter-Akopian[1,4], R. Wolski[1,10], B. Zalewski[1,5]

1) Flerov Laboratory of Nuclear Reactions, International Intergovernmental Organization Joint Institute for Nuclear Research, Dubna, Russia
2) Institute of Physics, Silesian University, Opava, Czech Republic
3) National Research Nuclear University "MEPhI", Moscow, Russia
4) Dubna State University, Dubna, Russia
5) Heavy Ion Laboratory, University of Warsaw, Warszawa, Poland
6) Institute of Nuclear Physics of the National Nuclear Center, Almaty, Kazakhstan
7) National Research Center "Kurchatov Institute", Moscow, Russia
8) Nuclear Research Institute, Dalat, Vietnam
9) AGH University of Science and Technology, Faculty of Physics and Applied Computer Science, Krakow, Poland
10) Institute of Nuclear Physics PAN, Kraków, Poland

The ^{2}H(^{9}Li,p)^{10}Li one-neutron transfer reaction has been investigated at an incident energy of 29 AMeV at the ACCULINNA-2 facility of the Flerov Laboratory of Nuclear Reactions at the Joint Institute for Nuclear Research (FLNR, JINR) in order to measure the ^{10}Li low energy spectrum. A ^{9}Li secondary beam was produced by fragmentation of a ^{11}B primary beam of 33.4 AMeV impinging on a 1 mm thick beryllium target. A cryogenic deuterium gas cell was used as a secondary target. Secondary beam tracking was provided by two multi-wire proportional chambers (MWPC). Ion identification was performed using the standard dE-TOF technique [1].

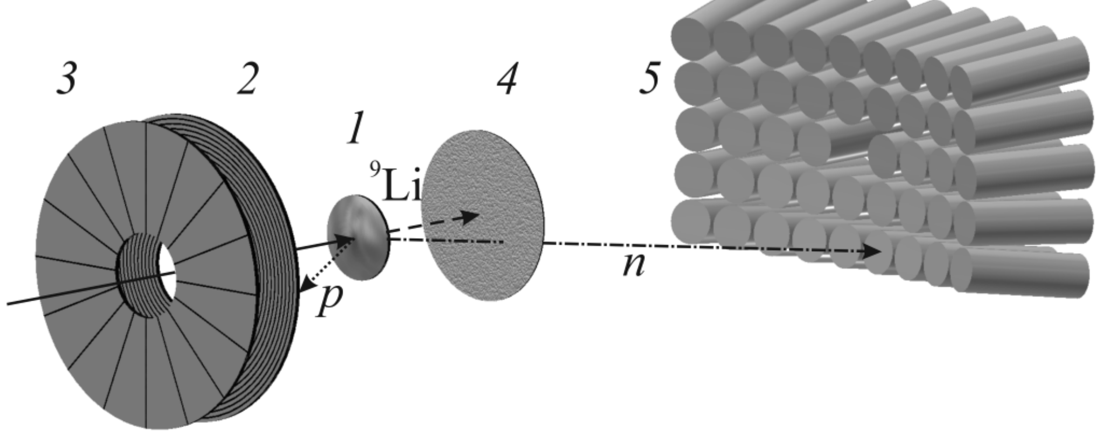

Figure 1: Schematic view of the experimental setup: deuterium target (1), double-sided Si strip detector (2), veto detector (3), plastic scintillator (4), array of neutron detectors (5).

Fig. 1 shows a schematic drawing of the experimental setup used. A 1 mm thick position sensitive annular double-sided Si strip detector (DSSD), located upstream from the target, was used to detect protons emitted in the ^{2}H(^{9}Li,p) reaction in the backward direction. A silicon detector of the same construction was placed upstream of the DSSD detector and used as a veto detector. Detection of ^{9}Li ions from the decay of ^{10}Li resonant states was provided by a thin plastic scintillator installed downstream from the target. Neutrons were detected by means of an array of 44 modules. Each module consists of a cylindrical stilbene monocrystal optically coupled with a photomultiplier which is housed in a stainless steel cylindrical case.

The measurement of the proton energy and angle relative to the incoming ^{9}Li projectile direction provided by the annular Si detector is sufficient to reconstruct the missing mass spectrum of the ^{10}Li system appearing in the ^{2}H(^{9}Li,p) reaction. The obtained missing mass spectrum is presented in Fig. 2. This spectrum is similar to that presented in [2] measured at 10 AMeV beam energy with the same reaction. Two main structures dominate the spectrum, a relatively narrow peak at ~0.5 MeV above the neutron decay threshold and a broad structure centred at 4 – 5 MeV. The latter looks more pronounced than in [2] due to the higher energy of the ^{9}Li beam used in our measurements. We attribute the peak in the missing-mass spectrum at 0.5 MeV to the population of a p-wave resonance of ^{10}Li. The width of this peak is defined by the instrumental resolution which depends mainly on the target thickness. The main goal of the measurements was to get as high as possible statistics to analyze triple proton – ^{9}Li – neutron coincidence events. Subsequent analysis of the neutron data will improve the resolution of the excitation spectrum measurement up to 200 – 250 keV (FWHM) as a Monte Carlo simulation of the experiment shows. In addition, we hope to identify the ^{10}Li decay mode and to analyze angular correlations. Analysis of the triple coincidences is in progress now.

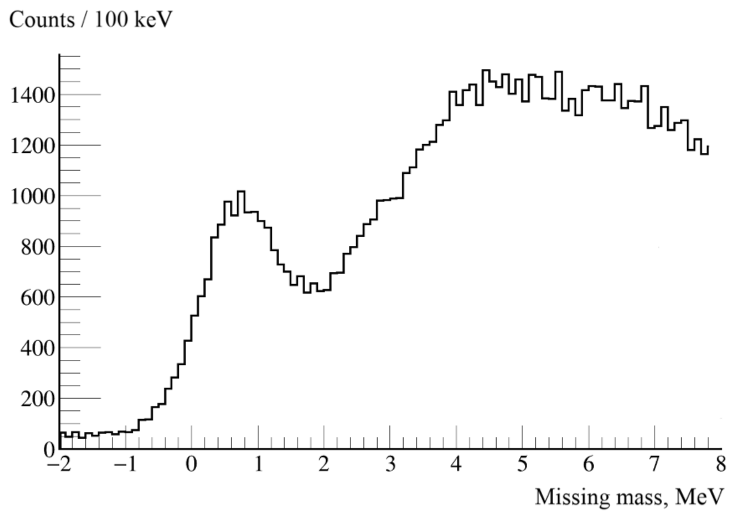

Figure 2: ^{10}Li missing mass spectrum measured in the ^{2}H(^{9}Li,p) reaction at 29 AMeV beam energy. The zero of the energy scale corresponds to the ^{10}Li → ^{9}Li + n decay threshold.

Bibliography

[1] A.S. Fomichev *et al.*, Eur. Phys. J. **A54** (2018) 97.
[2] M. Cavallaro *et al.*, Phys. Rev. Lett. **118** (2017) 012701.

D.3 AGATA-NEDA-DIAMANT data analysis

G. Jaworski[1], M. Palacz[1], D. Wójcik[1,2] and the NEDA and N=Z Collaborations

1) Heavy Ion Laboratory, University of Warsaw, Warszawa, Poland
2) Faculty of Physics, University of Warsaw, Warszawa, Poland

The participation of the Warsaw group in the construction of the new NEutron Detection Array (NEDA) was covered in contributions to earlier editions of the HIL annual report [1–3]. The NEDA project has been described in more detail in several regular papers, see [4, 5] and references therein. The construction stage of the device was followed by an experimental campaign at GANIL in which 54 NEDA detectors were coupled to the 1Π AGATA array [6], together with the DIAMANT charged particle detector [7] and 42 NWall detectors [8, 9]. Five experiments were run in the period April-July 2018, see also Ref. [5]. First results of one of these experiments have already been published [12]. Data analysis of another experiment, E703, is in progress in Warsaw, Stockholm and Uppsala. This measurement aimed at studies of excited states in ^{102,103}Sn to deduce two-body neutron interactions, single-particle energies and $N = Z = 50$ core excitations. Selected aspects of the analysis which is pursued in Warsaw are briefly described below.

During the measurement, the NEDA signals were stored as waveforms with 232 samples each and a sampling frequency of 200 MHz, covering a time range of 1160 ns. An off-line analysis of the signals was performed with the aim of: i) possibly recovering detectors which performed poorly on-line , ii) possibly recovering events for which detectors produced signals which were not accepted by the on-line constant fraction algorithm, iii) improving the time resolution, iv) improving efficiency and quality of neutron-gamma discrimination based on the shape of the signal.

For the timing, a digital constant fraction algorithm was employed, see Fig. 1. There were six parameters to optimise: delay, fraction, zero-crossing line, CFD threshold, the number of samples averaged to smooth the signal, and the threshold on the differential of the waveform. The latter prevents triggering on noise. In the optimisation procedure the parameters were varied and data were processed for each set of parameter values. The digital constant fraction algorithm was employed to calculate the time of flight (ToF) with respect to the RF signal. Finally, the parameter values which give the minimum FWHM of the prompt gamma peak in the ToF spectrum were selected. Fig. 1 illustrates how the minimum was found on the delay–fraction plane.

A similar procedure was applied to the algorithm used to discriminate detected neutrons and γ-rays based on the shape of the signal (NGD) using the charge comparison method [10, 11]. In this case there were five parameters: 3 limits of the time intervals used to integrate the slow and fast parts of the signal, and 2 limits used to exclude part of the signal in which a structure appeared due to a defect of the cables (of unknown origin).

As a results of this analysis, the fraction of events lost due to wrong timing was reduced from 20 to 1%. The FWHM of the NEDA time signals was reduced by up to 10%, depending on the detector. The quality of the neutron-gamma discrimination, expressed in terms of the figure-of-merit [13], was improved by 32% on average.

Other topics which are dealt with in the analysis include: determination of the multiplicity of the detected neutrons, optimisation of the gates used to discriminate protons and α particles detected in the DIAMANT detectors, conditions and timing of event building, precise timing conditions for all the detectors with respect to the RF, etc.

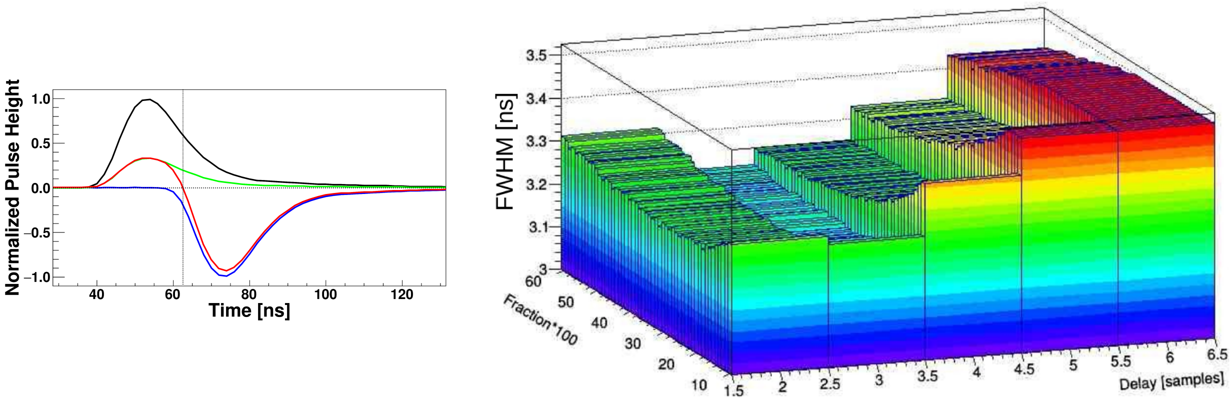

Figure 1: Illustration of the timing optimisation procedure. The following signals are shown in the left pannel: input (black), delayed and inverted (blue), scaled down (green), bi-polar (red). The zero-crossing point of the bipolar signal determines the constant fraction time (CFD), which depends on the fraction parameter (the scaling factor) and the delay. In the right pannel, the FWHM of the prompt γ peak in one NEDA detector is shown as a function of the CFD fraction and delay. In this example the delay of 3 samples (15 ns), and the fraction of 38% give the minimum FWHM of 3.185 ns.

Acknowledgement: the Polish contribution to NEDA and related investigations of rare proton-rich isotopes are supported by the Polish National Science Centre (grants nos. 2017/25/B/ST2/01569, 2016/22/M/ST2/00269, and 2014/14/M/ST2/00738), COPIN-IN2P3, COPIGAL, and POLITA projects.

Bibliography

[1] M. Palacz *et al.*, HIL Annual Report 2016, page 79.
[2] M. Palacz *et al.*, HIL Annual Report 2017, page 70.
[3] M. Palacz *et al.*, HIL Annual Report 2018, page 77.
[4] J.J. Valiente-Dobon *et al.*, Nucl. Inst. and Meth. **A673** (2012) 64.
[5] G. Jaworski *et al.*, Acta Phys. Pol. **B50** (2019) 585.
[6] E. Clément *et al.*, Nucl. Inst. and Meth. **A855** (2017) 1.
[7] J.N. Scheurer *et al.*, Nucl. Inst. and Meth. **A385** (1997) 501.
[8] Ö. Skeppstedt *et al.*, Nucl. Inst. and Meth. **A421** (1999) 531.
[9] J. Ljungvall, M. Palacz, J. Nyberg, Nucl. Inst. and Meth. **A528** (2004) 741.
[10] F.D. Brooks, Nucl. Inst. and Meth. 4 (1959) 151.
[11] P.A. Söderström *et al.*, Nucl. Inst. and Meth. **A594** (2008) 79.
[12] B. Cederwall *et al.*, Phys. Rev. Lett. **124** (2020) 062501
[13] R.A. Winyard *et al.*, Nucl. Inst. and Meth. **95** (1971) 141

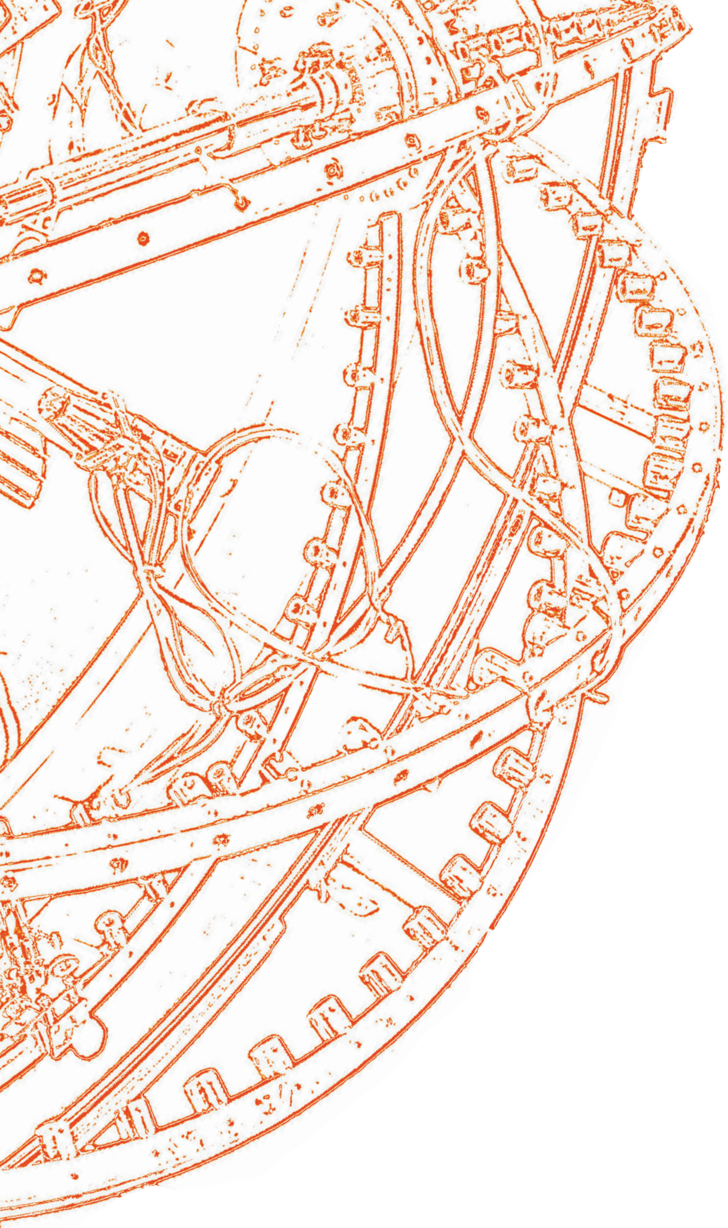

Part E
Appendices

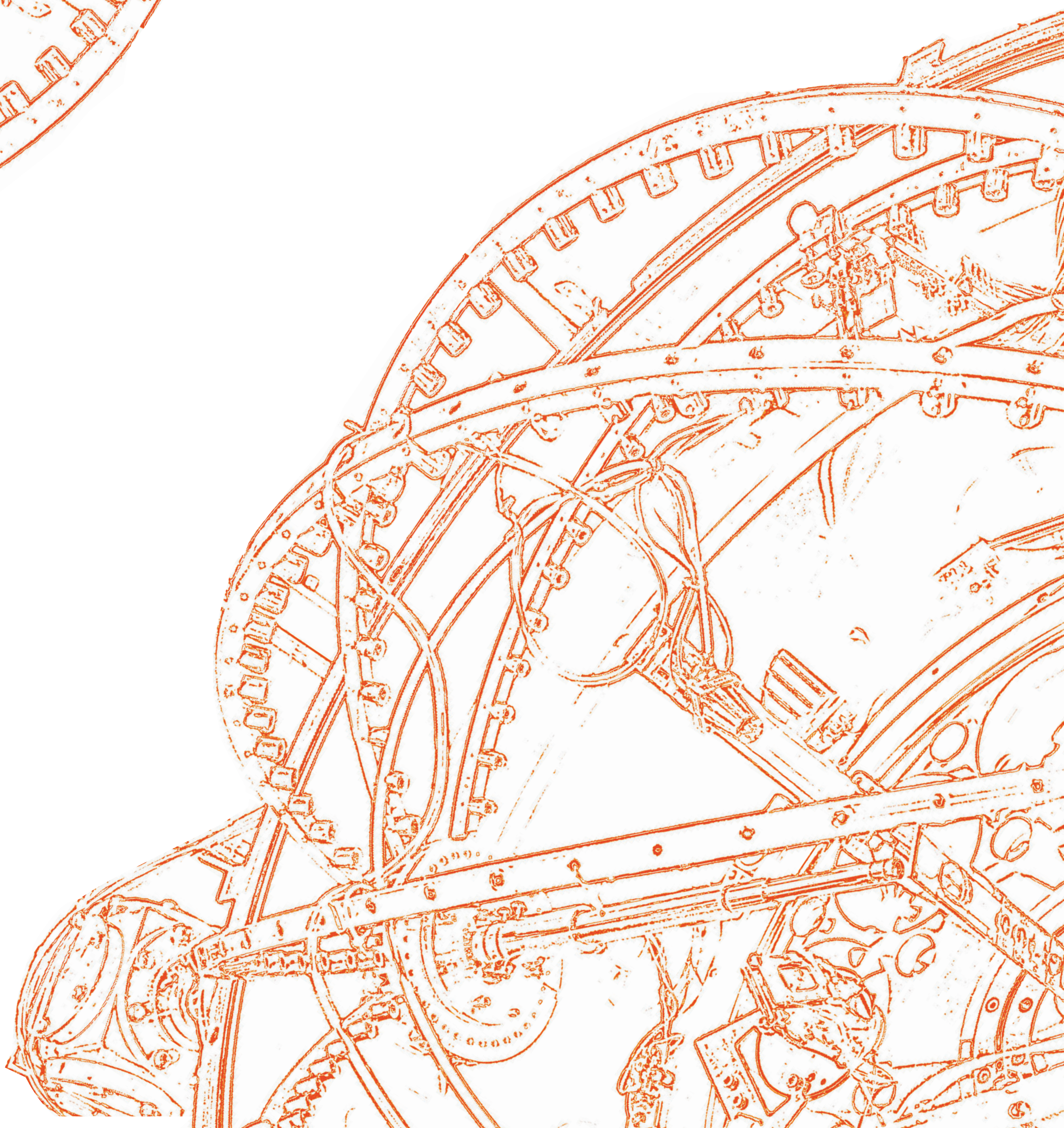

E.1 List of experiments performed at HIL in 2019

A list of the experiments performed in 2019 is presented in the following pages. The following acronyms of institution names are used in the list:

- HIL — Heavy Ion Laboratory, University of Warsaw, Warszawa, Poland;
- AKNU Almaty — Al-Farabi Kazakh National University, Almaty, Kazakhstan;
- CEA Saclay — IRFU/SPhN, CEA Saclay, Gif-sur-Yvette, France;
- EU Izmir — Physics Department, Ege University, Izmir, Turkey;
- FPACS UŁ — Faculty of Physics and Applied Computer Science, University of Lodz, Łódź, Poland;
- FP UW — Faculty of Physics, University of Warsaw, Warszawa, Poland;
- GANIL — GANIL, Caen, France;
- INCT Warszawa — Institute of Nuclear Chemistry and Technology, Warszawa, Poland;
- INFN SP — INFN Sezione di Padova, Padova, Italy;
- INFN LNL — INFN, Laboratori Nazionali di Legnaro, Legnaro, Italy;
- INP Kraków — The H. Niewodniczański Institute of Nuclear Physics PAN, Kraków, Poland;
- INP UC Cologne — Institute for Nuclear Physics, University of Cologne, Germany;
- INPME Almaty — Institute of Nuclear Physics, Ministry of Energy of the Republic of Kazakhstan, Almaty, Kazakhstan;
- IP US Szczecin — Institute of Physics, University of Szczecin, Szczecin, Poland;
- IP JKU Kielce — Institute of Physics, Jan Kochanowski University, Kielce, Poland;
- ISSNP Berlin — Institute for Solid-State Nuclear Physics, Berlin, Germany;
- iThemba — iThemba Lab. for Accelerator Based Sciences, Faure, South Africa;
- NCNR Świerk — National Centre for Nuclear Research, Otwock, Poland;
- NRCKI Moscow — National Research Center "Kurchatov Institute", Moscow, Russia;
- PU Padova — Padova University, Padova, Italy;
- PUT Poznań — Poznań University of Technology, Poznań, Poland;
- SIP JU Kraków — M. Smoluchowski Institute of Physics, Jagiellonian Univ., Kraków, Poland;
- UAM Madrid — Universidad Autonoma de Madrid, Madrid, Spain;
- UAS Tashkent — Uzbekistan Academy of Sciences, Institute of Nuclear Physics, Tashkent, Uzbekistan;
- UF INFN Florence — University of Florence, INFN Sezione di Firenze, Italy;
- UJ Jyväskylä — Department of Physics, University of Jyväskylä, Finland;
- UMCS Lublin — Inst. of Physics, Maria Curie-Sklodowska Univ., Lublin, Poland;
- UO Oslo — Department of Physics, University of Oslo, Oslo, Norway;
- UZG Zielona Góra — University of Zielona Góra, Zielona Góra, Poland;
- US Surrey — University of Surrey, Guildford, Surrey, United Kingdom;

For each experiment the following information is provided: ion, energy, setup/beam line information, date, proposal number, subject, spokespersons and institutions.

$^{12}C^{+2}$ — 46 MeV — Radiobiology 7.01 – 11.01
HIL078 — Particle track structure for Carbon ions (PTSCI)
(M. Pietrzak, A. Bantsar)
NCNR Świerk, FP UW

$^{14}N^{+3}$ — 90 MeV — ICARE 21.01 – 25.01
HIL070 — Testing of radiation hardness for heavy ions (N-14) of 5 μm thin strip silicon detector operating with build-in field
(A. Kordyasz)
HIL

$^{14}N^{+3}$ — 90 MeV — EAGLE 28.01 – 31.01
HIL072 — Searching for the E0 transitions in the ^{160}Yb nucleus
(J. Perkowski)
FPACS UŁ, HIL

$^{12}C^{+2}$ — 36 MeV — Radiobiology 4.03 – 7.03
HIL083 — Study of the biological response of glioblastoma cells irradiated with C-12 ion beam -preliminary research
(M. Paluch-Ferszt)
HIL

$^{12}C^{+2}$ — 36 MeV — Radiobiology 25.03 – 27.03
HIL083 — Study of the biological response of glioblastoma cells irradiated with C-12 ion beam -preliminary research, continuation
(M. Paluch-Ferszt)
HIL

$^{10}B^{+2}$ — 41 MeV — ICARE 6.05 – 17.05
HIL080 — Study of the elastic scattering and one-nucleon transfer in the $^{11}B(^{10}B,\ ^{11}B)^{10}B$ and $^{11}B(^{10}B,\ ^{9}Be)^{12}C$ reactions at energies near the Coulomb barrier
(N. Burtebayev, W. Trzaska)
INPME Almaty, UAS Tashkent, NRCKI Moscow, AKNU Almaty, UJ Jyväskylä, HIL

$^{10}B^{+2}$ — 55 MeV — EAGLE 27.05 – 30.05
HIL073 — Spin deorientation measurements in the Coulomb excitation of ^{148}Nd with plunger device - test experiment.
(A.Tucholski)
HIL

$^{32}S^{+7}$ — 192 MeV — EAGLE 10.06 – 18.06
HIL084 — Lifetime studies in neutron-deficient ^{176}Pt using the RDDS technique

(Ch. Fransen, C. Müller-Gatermann)
INP UC Cologne, INFN LNL, PU Padova, EU Izmir, HIL

1.07 – 5.07

HIL000 — Beam development
(P. Gmaj)
HIL

$^{12}C^{+3}$ — 48 MeV — Radiobiology 8.07 – 10.07
HIL083 — Study of the biological response of glioblastoma cells irradiated with C-12 ion beam - preliminary research
(U. Kaźmierczak)
HIL, FP UW, IP JKU Kielce

$^{20}Ne^{+3}$ — 60 MeV — EAGLE 21.10 – 21.10
HIL086 — Radiation hardness studies of PiN-diode detectors
(P.J. Napiorkowski, K.Wrzosek-Lipska)
HIL

$^{20}Ne^{+3}$ — 60 MeV — EAGLE, Radiobiology 22.10 – 24.10
HIL001 — Students' workshop
HIL

4.11 – 8.11

HIL000 — Beam development
(P. Gmaj)
HIL

$^{40}Ar^{+7}$ — 144 MeV — EAGLE 12.11 – 22.11
HIL085 — Coulomb excitation of the strongly deformed band in ^{40}Ar
(K. Hadyńska-Klęk, M. Rocchini, P. J. Napiorkowski)
US Surrey, UF INFN Florence, FP UW, INP Kraków, UO Oslo, INFN LNL, CEA Saclay, UAM Madrid, GANIL, iThemba, HIL

$^{40}Ar^{+8}$ — 200 MeV — Radiobiology 2.12 – 6.12
HIL082 — Irradiation of ceramic materials relevant for high temperature nuclear reactors by heavy ions
(K. Czerski)
IP US Szczecin, MUS Szczecin, NCNR Świerk, ISSNP Berlin, HIL

9.12 – 13.12

HIL000 — Beam development
(P. Gmaj)
HIL

E.2 Degrees and theses completed in 2019 or in progress

E.2.1 DSc (habilitation) degrees of HIL staff members

Krzysztof Kilian, Faculty of Chemistry, University of Warsaw
Statyczne i przepływowe metody wydzielania i zatężenia jonów metali na stałych sorbentach – zastosowania analityczne i radiochemiczne
Static and flow methods of isolation and preconcentration of metal ions on solid sorbents - analytical and radiochemical applications
September 2019.

E.2.2 DSc (habilitation) degrees based on experiments performed at HIL

Ernest Grodner, National Centre for Nuclear Research (NCBJ)
Weryfikacja hipotezy naruszenia jądrowej symetrii chiralnej
Verification of the hypothesis of chiral symmetry breaking in atomic nuclei
December 2019.

E.2.3 PhD theses of students affiliated to HIL, of HIL staff members, and supervised by HIL staff

Mateusz Sitarz, Faculty of Physics, University of Warsaw and Faculty of Science and Technology, University of Nantes
Badanie produkcji nowych izotopów medycznych z wykorzystaniem cyklotronu
Research on the production of new medical radioisotopes with a cyclotron
Supervisors: prof. dr hab. T. Matulewicz, dr A. Trzcińska, prof. F. Haddad. (programme cotutelle) Thesis completed in September 2019, with honorus.

Michalina Komorowska, Faculty of Physics, University of Warsaw
Korelacje oktupolowe w jądrach atomowych z obszaru $N \sim 88$
Pear-shaped Nuclei in the $N \sim 88$ *mass region*
Supervisors: dr hab. L. Próchniak, dr P. Napiorkowski, dr W. Korten, dr M. Zielińska. (programme cotutelle) Expected completion time: 2020.

Tomasz Marchlewski, Faculty of Physics, University of Warsaw
Pomiar czasów życia jądrowych stanów wzbudzonych w izotopie ^{124}Cs ***- badanie mechanizmu spontanicznego łamania symetrii chiralnej***
Measurement of nuclear excited state lifetimes in ^{124}Cs *- study of the mechanism of spontaneous chiral symmetry breaking*
Supervisors: prof. dr hab. K. Rusek, dr E. Grodner. Expected completion time: 2020.

Mateusz Pęgier, Faculty of Chemistry, University of Warsaw
Wykorzystanie techniki ekstrakcji do fazy stałej do wydzielania i zatężania jonów skandu
Application of solid phase extraction for separation and preconcetration of scandium ions
Supervisor: prof. dr hab. K. Pyrzyńska. Expected completion time: 2020.

Olga Saeed Mohamed Nassar, Faculty of Physics, Warsaw University of Technology
Optyka jonowa w centrum cyklotronu U-200P
Ion trajectories in the central region of the U-200P cyclotron
Supervisors: dr hab. M. Palacz, dr I. Ivanenko. Expected completion time: 2021.

Łukasz Standyło, National Centre for Nuclear Research, Świerk
Badanie mechanizmu wychwytu i termalizacji strumieni jonów i atomów wprowadzonych do plazmy wytwarzanej metodą elektronowego rezonansu cyklotronowego
Investigation of the capture and thermalization mechanism of ion and atom beams injected into plasma produced by the electron cyclotron resonance
Supervisor: prof. dr hab. K. Rusek, dr K. Sudlitz. Expected completion time: 2021.

Bogumił Zalewski, Faculty of Physics, University of Warsaw
Badanie oddziaływania ^{6}He+d
Study of the $^{6}He+d$ interacion
Supervisor: prof. dr hab. K. Rusek. Expected completion time: 2021.

Dominika Wójcik, Faculty of Physics, University of Warsaw
Supervisors: dr hab. M. Palacz. Expected completion time: 2023.

E.2.4 Other PhD theses based on experiments performed at HIL

Tomasz Lehmann, Faculty of Physics, Warsaw University of Technology
Electromagnetic structure studies of excited states in ^{107}Ag
Badanie struktury elektromagnetycznej stanów wzbudzonych w jądrze ^{107}Ag
Supervisors: dr K. Wrzosek-Lipska, prof. dr hab. P. Magierski. Thesis completed in September 2019.

Monika Adamowicz, Faculty of Chemistry, University of Warsaw
Complexes of scandium for molecular imaging purposes
Supervisors: prof. dr hab. K. Pyrzyńska, dr A. Sentkowska. Thesis completed in September 2019.

Sunil Dutt, Aligarh Muslim University, Aligarh, (U.P.) India
Supervisor: prof. A. Rizvii. Expected completion time: 2020.

Feruzjon Ergashev, Institute of Nuclear Physics, Academy of Sciences of the Republic of Uzbekistan, Tashkent, Uzbekistan
Study of nucleon transfer reactions in the $^{10}B+^{16}O$ system at energies near the Coulomb barrier for nuclear astrophysics
Supervisors: prof. S. Artemov. Expected completion time: 2021.

Bakytbek Mauey, L.N. Gumilyov Eurasian National University, Astana, Kazakhstan
Investigation of the elastic scattering of ^{15}N ions on 1p-shell nuclei at energies near the Coulomb barrier
Supervisors: prof. A. Morzabayev. Expected completion time: 2020.

Maulen Nassurlla, Al-Farabi Kazakh National University, Almaty, Kazakhstan
Effects of the cluster structure of stable boron and lithium isotopes in forming the outputs of nuclear reactions in the interaction with deuterium and helium isotopes
Supervisors: prof. N. Burtebayev. Expected completion time: 2020.

Maria Pęgier, Faculty of Chemistry, University of Warsaw
Macrocyclic compounds labelled with metallic isotopes for applications in positron emission tomography
Supervisors: prof. dr hab. Krystyna Pyrzyńska, dr Krzysztof Kilian. Expected completion time: 2020.

Daniel Andrzej Piętak, Faculty of Electronics and Information Technology, Warsaw University of Technology
Metoda oceny jakości wyników z eksperymentów wzbudzeń kulombowskich z wykorzystaniem algorytmu genetycznego
Evaluation method based on a genetic algorithm for the results of Coulomb excitation experiments
Supervisors: dr hab. inż. P. Bilski. Expected completion time: 2021.

Auganbek Sabidolda, Al-Farabi Kazakh National University, Almaty, Kazakhstan
Study of nucleon transfer reactions in the $^{10}B+^{12}C$ system at energies near the Coulomb barrier for nuclear astrophysics
Supervisors: prof. N. Burtebayev. Expected completion time: 2022.

E.2.5 MSc and BSc theses supervised by HIL staff members

Aleksandra Lenartowicz, Faculty of Physics, University of Warsaw
Synteza radiofarmaceutyku 18FHBG na syntezerze Synthra RN
Synthesis of radiopharmaceutical 18FHBG using synthesizer Synthra RN
Supervisor: dr Krzysztof Kilian. Bachelor's thesis completed in July 2019.

Aleksandra Hromiuk, Faculty of Physics, University of Warsaw
Badanie reakcji kompleksowania skandu z DOTA z wykorzystaniem spektrometrii mas
Study of the scandium complexation reaction with DOTA using mass spectrometry
Supervisor: dr Krzysztof Kilian. Bachelor's thesis completed in July 2019.

Michał Smolarek, Jakub Krauz, Jakub Łaguna, Krzysztof Witczyński, Faculty of Mathematics, Informatics and Mechanics, University of Warsaw
System sterowwania warszawskim cyklotronem
Control system for the Warsaw Cyclotron
Supervisors: mgr Grzegorz Grudziński, mgr inż. Jan Miszczak. Expected completion time: 2020.

E.3 Publications

E.3.1 Publications in Web of Knowledge and/or Scopus data bases

B. Brzozowska, M. Gałecki, A. Tartas, J. Ginter, U. Kaźmierczak, L. Lundholm. *Freeware tool for analysing numbers and sizes of cell colonies.* Radiat. Environ. Biophys. **58**,109 (2019).

N. Burtebayev, S. Hamada, A. A. Ibraheem, K. Rusek, M. Wolińska-Cichocka, J. Burtebayeva, N. Amangeldi, M. Nassurlla, M. Nassurlla, A. Sabidolda. *Effect of the transfer reactions for $^{16}O+^{10}B$ elastic scaterring.* Acta Phys. Pol. B **50**, 1423 (2019).

N. Burtebayev, Z. K. Kerimkulov, M. Nassurlla, J. T. Burtebayeva, M. Nassurlla, S. B. Sakuta, T. Suzuki, K. Rusek, A. Trzcińska, M. Wolińska-Cichocka. *Study of the $^{7}Li(d, t)^{6}Li$ reaction at the energy of 14.5 MeV.* Acta Phys. Pol. B **50**, 703 (2019).

N. Burtebayev, M. Nassurlla, A. Sabidolda, S. B. Sakuta, A. A. Karakhodjaev, F. X. Ergashev, K. Rusek, E. Piasecki, A. Trzcińska, M. Wolińska-Cichocka, M. Kowalczyk, B. Mauyey, D. Janseitov, B. Zalewski, S. Hamada, K. W. Kemper, A. A. Ibraheem. *Measurement and analysis of $^{10}B+^{12}C$ elastic scattering at energy of 41.3 MeV.* Int. J. Mod. Phys. E **28**, 1950028 (2019).

N. Burtebayev, S. B. Sakuta, M. Nassurlla, N. Saduyev, M. Nassurlla, T. K. Sadykov, A. Trzcińska, M. Wolińska-Cichocka, R. Khojayev. *Mechanism of the $^{11}B(\alpha, t)^{12}C$ reaction at an energy of 40 MeV, role of exchange processes and collective excitations.* Eur. Phys. J. A **55**, 38 (2019).

P. A. Butler, L. P. Gaffney, P. Spagnoletti, J. Konki, M. Scheck, J.F. Smith, K. Abrahams, M. Bowry, J. Cederkall, T. Chupp, G. de Angelis, H. De Witte, P. E. Garrett, A. Goldkuhle, C. Henrich, A. Illana, K. Johnston, D. T. Joss, J. M. Keatings, N. A. Kelly, M. Komorowska, T. Kröll, M. Lozano, B. S. N. Singh, D. O'Donnell, J. Ojala, R. D. Page, L. G. Pedersen, C. Raison, P. Reiter, J. A. Rodriguez, D. Rosiak, S. Rothe, T. M. Shneidman, B. Siebeck, M. Seidlitz, J. Sinclair, M. Stryjczyk, P. Van Duppen, S. Vinals, V. Virtanen, N. Warr, K. Wrzosek-Lipska, M. Zielińska. *The observation of vibrating pear-shapes in radon nuclei.* Nat. Commun. **10**, 2473 (2019).

P. A. Butler, L. P. Gaffney, P. Spagnoletti, J. Konki, M. Scheck, J.F. Smith, K. Abrahams, M. Bowry, J. Cederkall, T. Chupp, G. de Angelis, H. De Witte, P. E. Garrett, A. Goldkuhle, C. Henrich, A. Illana, K. Johnston, D. T. Joss, J. M. Keatings, N. A. Kelly, M. Komorowska, T. Kröll, M. Lozano, B. S. N. Singh, D. O'Donnell, J. Ojala, R. D. Page, L. G. Pedersen, C. Raison, P. Reiter, J. A. Rodriguez, D. Rosiak, S. Rothe, T. M. Shneidman, B. Siebeck, M. Seidlitz, J. Sinclair, M. Stryjczyk, P. Van Duppen, S. Vinals, V. Virtanen, N. Warr, K. Wrzosek-Lipska, M. Zielińska. *Coulomb excitation of pear-shaped nuclei.* EPJ Web Conf. **223**, 01007 (2019).

T. Cap, K. Siwek-Wilczyńska, J. Wilczyński, L. Auditore, G. Cardella, E. De Filippo, E. Geraci, A. Grzeszczuk, E. La Guidara, G. Gnoffo, T. Kozik, G. Lanzalone, I. Lombardo, M. Martorama, R. Najman, N. G. Nicolis, A. Pagano, E. V. Pagano, M. Papa, E. Piasecki,

S. Pirrone, R. Planeta, G. Politi, F. Rizzoi, P. Russotto, I. Skwira-Chalot, A. Trifiro, M. Trimarchi, G. Verde, W. Zipper. *Competition Between Dynamical and Sequential Reaction Channels in* $^{197}Au+^{197}Au$ *Collisions at a Bombarding Energy of 23A MeV.* Acta Phys. Pol. B **50**, 501 (2019).

V. Chudoba, L. Grigorenko, A. Fomichev, A. Bezbakh, I. Egorova, S. Ershov, A. Gorshkov, V. Gorshkov, G. Kamiński, S. Krupko,I. Mukha, E. Nikolskii, Y. Parfenova, S. Sidorchuk, P. Sharov, R. Slepnev, Ł. Standyło, S. Stepantsov, G. Ter-Akopian, R. Wolski, M. Zhukov. *Detailed Study of External Correlations in the Low-Energy Spectrum of Beryllium-6.* Bull. Russ. Acad. Sci.: Phys. **83**, 392 (2019).

M. Ciemała, S. Ziliani, F. Crespi, S. Leoni, B. Fornal, A. Maj, P. Bednarczyk, G. Benzoni, A. Bracco, C. Boiano, S. Bottoni, S. Brambilla, M. Bast, M. Beckers, T. Braunroth, F. Camera, N. Cieplicka-Oryńczak, E. Clement, O. Dorvaux, S. Erturk, G. De France, A. Goldkuhle, J. Grębosz, M. N. Harakeh, L. W. Iskra, B. Jacquot, A. Karpov, M. Kicińska-Habior, Y. Kim, M. Kmiecik, A. Lemasson, H. Li, I. Matea, K. Mazurek, C. Michelagnoli, B. Millon, C. Mueller-Gatermann, P. Napiorkowski, V. Nanal, M. Matejska-Minda, M. Rejmund, B. Sowicki, Ch. Schmitt, M. Stanoiu, I. Stefan, B. Wasilewska, M. Zielińska, M.Ziębliński. *Determination of Lifetimes of Excited States in Neutron-rich* ^{20}O *Isotope from Experiment with the AGATA+PARIS+VAMOS Setup.* Acta Phys. Pol. B **50**, 615 (2019).

J. Czub, D. Banaś, J. Braziewicz, I. Buraczewska, M. Jaskóła, U. Kaźmierczak, A. Korman, A. Lankoff, H. Lisowska, Z. Szefliński, M. Wojewódzka, A. Wójcik. *Biological effects of mixed-ion beams. Part 2: The relative biological effectiveness of CHO-K1 cells irradiated by mixed- and single-ion beams.* Appl. Radiat. Isot. **150**, 192 (2019).

E. De Filippo, P. Russotto, E. V. Pagano, L. Acosta, L. Auditore, T. Cap, G. Cardella, B. Gnoffo, G. Lanzalone, I. Lombardo, C. Maiolino, N. S. Martorana, A. Pagano, M. Papa, E. Piasecki, S. Pirrone, G. Politi, L. Quattrocchi, F. Rizzo, K. Siwek-Wilczyńska, A. Trifiro, M. Trimarchi. *Dependence from the Isospin of the entrance channel in Projectile-like (PLF) break-up at Fermi energies.* Nuovo Cimento C **42**, 97 (2019).

P. Dróżdż, A. Sentkowska, K. Pyrzyńska. *Potentilla erecta (L.) rhizomes as a source of phenolic acids.* Nat. Prod. Res. **33**, 2128 (2019)

S. Dutt, M. Saxena, P. J. Napiorkowski, R. Kumar, T. Abraham, J. M. Allmond, A. Gawlik, K. Hadyńska-Klęk, M. Hlebowicz, J. Iwanicki, M. Kisieliński, M. Komorowska, M. Kowalczyk, T. Marchlewski, M. Matejska-Minda, F. Oleszczuk, M. Palacz, W. Piątek, L. Próchniak, I. A. Rizvi, J. Samorajczyk, J. Srebrny, A. Tucholski, W. Wróblewski, K. Wrzosek-Lipska. *Multi-step Coulomb excitation of Ba-132 at HIL, Warsaw.* Indian J. Pure Appl. Phys. **57**, 599–601 (2019).

L. Dziawer, A. Majkowska-Pilip, D. Gaweł, M. Godlewska, M. Pruszynski, J. Jastrzębski, B. Was, and A. Bilewicz. *Trastuzumab-Modified Gold Nanoparticles Labeled with* ^{211}At *as a Prospective Tool for Local Treatment of HER2-Positive.* Breast Cancer. Nanomaterials **9**, 632 (2019)

A. Fomichev, A. Bezbakh, S. Belogurov, R.Wolski, E. Gazeeva, A. Gorshkov, L. Grigorenko, B. Zalewski, G. Kamiński, S. Krupko, I. Muzalevskii, E. Nikolskii, Y. Parfenova, S. Sidorchuk, R. Slepnev, G. Ter-Akopian, V. Chudoba, and P. Sharov.

The First Experiments with the New ACCULINNA-2 Fragment Separator. Bull. Russ. Acad. Sci.: Phys. **83**, 385 (2019).

E. Gniazdowska, P. Koźminski, P. Halik, M. Bajda, K. Czarnecka, E. Mikiciuk-Olasik, K. Masłowska, Z. Rogulski, L. Cheda, K. Kilian, P. Szymański. *Synthesis, physicochemical and biological evaluation of tacrine derivative labeled with technetium-99m and gallium-68 as a prospective diagnostic tool for early diagnosis of Alzheimer's disease.* Bioorg. Chem. **91**, UNSP 103136 (2019).

G. Jaworski, A. Goasduff, F. J. E. Canet, V. Modamio, T. Huyuk, A. Triossi, M. Jastrzab, P. A. Soderstrom, S. M. Carturan, A. Di Nitto, G. de Angelis, G. De France, N. Erduran, A. Gadea, M. Moszyński, J. Nyberg, M. Palacz, J. Valiente, R. Wadsworth, R. Aliaga, C. Aufranc, M. Bezard, G. Beaulieu, P. Bednarczyk, E. Bisiato, A. Boujrad, I. Burrows, E. Clement, P. Cocconi, G. Colucci, D. Conventi, M. Cordwell, S. Coudert, J. M. Deltoro, L. Ducroux, T. Dupasquier, S. Erturk, X. Fabian, V. Gonzalez, A. Gottardo, A. Grant, K. Hadyńska-Klęk, A. Illana, M. L. Jurado-Gomez, M. Kogimtzis, I. Lazarus, L. Legeard, J. Ljungvall, A. Maj, G. Pasqualato, R. M. Perez-Vidal, A. Raggio, D. Ralet, N. Redon, F. Saillant, E. Sanchis, B. Saygi, M. Scarcioffolo, M. Siciliano, O. Stezowski, D. Testov, M. Tripon, I. Zanon. *The new neutron multiplicity filter NEDA and its first physics campaign with AGATA.* Acta Phys. Pol. B **50**, 585 (2019).

A. Jhingan, H. J. Wollersheim, R. Kumar, M. Saxena, R. Ahuja, M. Kumar, S. Dutt, N. Saneesh, T. Varughese, S. K. Mondal, and P. Sugathan. *An annular parallel plate avalanche counter for heavy-ion gamma-ray coincidence measurements.* Nucl. Instrum. Methods Phys. Res. A **922**, 209 (2019).

N. Keeley, K. W. Kemper, I. Martel, K. Rusek, A. M. Sanchez-Benitez. *Comparison of the energy dependence of near-barrier* ^{6}He *and* $^{8}He+^{208}Pb$ *optical potentials.* Phys. Rev. C **99**, 024603 (2019).

N. Keeley, A. Pakou, V. Soukeras, F. Cappuzzello, L. Acosta, C. Agodi, A. Boiano, S. Calabrese, D. Carbone, M. Cavallaro, N. Deshmukh, A. Foti, A. Flacisalihoglu, M. La Commara, I. Martel, M. Mazzocco, A. Muoio, C. Parascandolo, D. Pierroutsakou, K. Rusek, A. M. Sanchez-Benitez, G. Santagati, O. Sgouros, G. Souliotis, A. Spatafora, E. Strano, D. Torresi,A. Trzcińska. *Coherent coupled-reaction-channels analysis of existing and new* $p+^{9}Be$ *data between 1.7 and 15 MeV/nucleon.* Phys. Rev. C **99**, 014615 (2019).

D. Kostyleva, I. Mukha, L. Acosta, E. Casarejos, V. Chudoba, A. A. Ciemny, W. Dominik, J. A. Duenas, V. Dunin, J. M. Espino, A. Estrade, F. Farinon, A. Fomichev, H. Geissel, A. Gorshkov, L. V. Grigorenko, Z. Janas, G. Kamiński, O. Kiselev, R. Knobel, S. Krupko, M. Kuich, Y. A. Litvinov, G. Marquinez-Duran, I. Martel, C. Mazzocchi, C. Nociforo, A. K. Orduz, M. Pfutzner, S. Pietri, M. Pomorski, A. Prochazka, S. Rymzhanova, A. M. Sanchez-Benitez, C. Scheidenberger, H. Simon, B. Sitar, R. Slepnev, M. Stanoiu, P. Strmen, I. Szarka, M. Takechi, Y. K. Tanaka, H.Weick,M. Winkler, J. S. Winfield, X. Xu, M.V. Zhukov. *Towards the limits of existence of nuclear structure: observation and first spectroscopy of the isotope* ^{31}K *by measuring its three-proton decay.* Phys. Rev. Lett. **123**, 092502 (2019).

B. F. Lv, C. M. Petrache, Q. B. Chen, J. Meng, A. Astier, E. Dupon, P. Greenlees, H. Badran, T. Calverley, D. M. Cox, T. Grahn, J. Hilton, R. Julin, S. Juutinen, J. Konki, J. Pakarinen, P. Papadakis, J. Partanen, P. Rahkila, P. Ruotsalainen, M. Sandzelius, J. Saren, C. Scholey, J. Sorri, S. Stolze, J. Uusitalo, B. Cederwall, A. Ertoprak, H. Liu, S. Guo, M. L. Liu, J. G. Wang, X. H. Zhou, I. Kuti, J. Timar, A. Tucholski, J. Srebrny,

C. Andreoiu. *Chirality of ^{135}Nd reexamined: Evidence for multiple chiral doublet bands.* Phys. Rev. C **100**, 024314 (2019).

M. Matejska-Minda, P. Bednarczyk, B. Fornal, F. R. Xu, W. Y. Liang, G. de Angelis, S. Aydin, S. Brambilla, M. Ciemała, E. Farnea, T. Huyuk, G. Jaworski, M. Kmiecik, M. Krzysiek, S. Leoni, A. Maj, R. Menegazzo, W. Męczynski, C. Michelagnoli, M. Palacz, F. Recchia, E. Sahin, J. Styczeń, B. Szpak, C. A. Ur, R. Wadsworth, M. Ziębliński. *Lifetime measurements of short-lived excited states, and shape changes in ^{69}As and ^{66}Ge nuclei.* Phys. Rev. C **100**, 054330 (2019).

M. Matejska-Minda, R. Kumar, P. J. Napiorkowski, M. Saxena, S. Dutt, A. Agarwal, I. Ahmed, S. Bhattacharya, A. Jhingan, J. Kaur, M. Kicinska-Habior, M. Kumar, S. Kumar, D. Kumar, V. Nanal, R. Palit, N. K. Rai, M. Shuaib, A. Sood, A. Stolarz, T. Trivedi, A. K. Tyagi, R. K. Bhowmik, H. J.Wollersheim. *Investigation of an intruder band in ^{45}Sc via Coulomb excitation.* Acta Phys. Pol. B **50**, 411 (2019).

M. Mazzocco, N. Keeley, A. Boiano, C. Boiano, M. La Commara, C. Manea, C. Parascandolo, D. Pierroutsakou, C. Signorini, E. Strano, D. Torresi, H. Yamaguchi, D. Kahl, L. Acosta, P. Di Meo, J. P. Fernandez-Garcia, T. Glodariu, J. Grębosz, A. Guglielmetti, Y. Hirayama, N. Imai, H. Ishiyama, N. Iwasa, S. C. Jeong, H. M. Jia, Y. H. Kim, S. Kimura, S. Kubono, G. La Rana, C. J. Lin, P. Lotti, G. Marquinez-Duran, I. Martel, H. Miyatake, M. Mukai, T. Nakao, M. Nicoletto, A. Pakou, K. Rusek, Y. Sakaguchi, A. M. Sanchez-Benitez, T. Sava, O. Sgouros, V. Soukeras, F. Soramel, E. Stiliaris, L. Stroe, T. Teranishi, N. Toniolo, Y.Wakabayashi, Y. X. Watanabe, L. Yang, Y. Y. Yang, H. Q. Zhang. *Elastic scattering for the ^{8}B and ^{7}Be+^{208}Pb systems at near-Coulomb barrier energies.* Phys. Rev. C **100**, 024602 (2019).

A. Pakou, F. Cappuzzello, L.Acosta, C.Agodi, S. Calabrese, D. Carbone, M. Cavallaro, N. Keeley, I. Martel, K. Rusek, A. M. Sanchez-Benitez, O. Sgouros, V. Soukeras, G. Souliotis, A. Spatafora, D. Torresi. *A microscopic approach for p+^{9}Be at energies between 1.7 to 15 MeV/nucleon.* Acta Phys. Pol. B **50**, 1547 (2019).

D. Perez-Loureiro, J. Benlliure, J. Diaz-Cortes, J. L. Rodriguez-Sanchez, H. Alvarez-Pol, B. Blank, E. Casarejos, D. Dragosavac, V. Foehr, M. Gascon, W. Gawlikowicz, A. Heinz, I. K. Helariutta, A. Kelic-Heil, S. Lukic, F. Montes, L. Pieńkowski, K. H. Schmidt, M. Staniou, K. Subotic, K. Suemmerer, J. Taieb, A. Trzcińska. *Neutron-rich fragments produced by in-flight fission of ^{238}U.* Phys. Rev. C **99**, 054606 (2019).

C. M. Petrache, S. Frauendorf, B. F. Lv, A. Astier, E. Dupont, S. Guo, M. L. Liu, X. H. Zhou, K. L. Wang, P. T. Greenlees, H. Badran, D. M. Cox, T. Grahn, R. Julin, S. Juutinen, J. Konki, J. Pakarinen, P. Papadakis, J. Partanen, P. Rahkila, M. Sandzelius, J. Saren, C. Scholey, J. Sorri, S. Stolze, J. Uusitalo, B. Cederwall, O. Aktas, A. Ertoprak, H. Liu, I. Kuti, J. Timar, A. Tucholski, J. Srebrny, C. Andreoiu. *Collective rotation of an oblate nucleus at very high spin.* Phys. Rev. C **99**, 041301 (2019).

C. M. Petrache, B. F. Lv, A. Astier, E. Dupont, K. K. Zheng, P. T. Greenlees, H. Badran, T. Calverley, D. M. Cox, T. Grahn, J. Hilton, R. Julin, S. Juutinen, J. Konki, J. Pakarinen, P. Papadakis, J. Partanen, P. Rahkila, P. Ruotsalainen, M. Sandzelius, J. Saren, C. Scholey, J. Sorri, S. Stolze, J. Uusitalo, B. Cederwal, O. Aktas, A. Ertoprak, H. Liu, S. Guo, M. L. Liu, J. G. Wang, X. H. Zhou, I. Kuti, J. Timar, A. Tucholski, J. Srebrny, C. Andreoiu. *Highly deformed bands in Nd nuclei: New results and consistent interpretation within the cranked Nilsson-Strutinsky formalism.* Phys. Rev. C **100**, 054319 (2019).

C. M. Petrache, P. M. Walker, S. Guo, Q. B. Chen, S. Frauendorf, Y. X. Liu, R. A. Wyss, D. Mengoni, Y. H. Qiang, A. Astier, E. Dupont, R. Li, B. F. Lv, K. K. Zheng, D. Bazzacco, A. Boso, A. Goasduff, F. Recchia, D. Testov, F. Galtarossa, G. Jaworski, D. R. Napoli, S. Riccetto, M. Siciliano, J. J. Valiente-Dobon, M. L. Liu, X. H. Zhou, J. G. Wang, C. Andreoiu, F. H. Garcia, K. Ortner, K. Whitmore, T. Back, B. Cederwall, E. A. Lawrie, I. Kuti, D. Sohler, J. Timar, T. Marchlewski, J. Srebrny, A. Tucholski. *Diversity of shapes and rotations in the gamma-soft ^{130}Ba nucleus: First observation of a t-band in the A=130 mass region.* Phys. Lett. B **795**, 241 (2019).

V. H. Phong, G. Lorusso, T. Davinson, A. Estrade, O. Hall, J. Liu, K. Matsui, F. Montes, S. Nishimura, A. Boso, P. H. Regan, R. Shearman, Z. Y. Xu, J. Agramunt, J. M. Allmond, D. S. Ahn, A. Algora, H. Baba, N. T. Brewer, C. G. Bruno, R. Caballero-Folch, F. Calvino, M. Wolińska-Cichocka, G. Cortes, I. Dillmann, C. Domingo-Pardo, A. Gargano, S. Go, C. J. Griffin, R. K. Grzywacz, L. Harkness-Brennan, T. Isobe, A. Jungclaus, D. Kahl, L. H. Khiem, G. Kiss, A. Korgul, S. Kubono, K. Miernik, A. Morales, I, N. Nepal, M. Piersa, Z. Podolyak, B. C. Rasco, K. P. Rykaczewski, H. Sakurai, Y. Shimizu, D. W. Stacener, T. Sumikama, H. Suzuki, H. Takeda, J. L. Tain, A. Tarifeno-Saldivia, A. Tolosa-Delgado, V. Vaquero, P. J. Woods, R. Yokoyama, C. Yuan. *Observation of a μs isomer in $^{134}_{49}\mathrm{In}_{85}$: Proton-neutron coupling "southeast" of $^{132}_{50}\mathrm{Sn}_{82}$.* Phys. Rev. C **100**, 011302 (2019).

S. Piantelli, G. Pastore, R. Alba, S. Barlini, M. Bini, E. Bonnet, B. Borderie, R. Bougault, M. Bruno, A. Buccola, A. Camaiani, G. Casini, A. Chbihi, C. Ciampi, M. Cicerchia, M. Cinausero, D. Dell'Aquila, J. A. Duenas, D. Fabris, L. Francalanza, J. D. Frankland, C. Frosin, F. Gramegna, D. Gruyer, M. Henri, A. Kordyasz, T. Kozik, N. LeNeindre, I. Lombardo, O. Lopez, C. Maiolino, G. Mantovani, T. Marchi, L. Morelli, A. Olmi, P. Ottanelli, M. Parlog, G. Pasquali, G. Poggi, D. Santonocito, A. A. Stefanini, S. Valdre, G. Verde, E. Vient, M. Vigilante. *Isospin transport phenomena in semiperipheral heavy ion collisions at Fermi energies.* Nuovo Cimento C **42**, 104 (2019).

E. Piasecki, M. Kowalczyk, S. Yusa, A. Trzcińska, K. Hagino. *Dissipation and tunneling in heavy-ion reactions near the Coulomb barrier.* Phys. Rev. C **100**, 014616 (2019).

S. Pirrone, G. Politi, B. Gnoffo, M. La Commara, E. De Filippo, P. Russotto, M. Trimarchi, M. Vigilante, M. Colonna, S. A. Kalandarov, F. Amorini, L. Auditore, C. Beck, G. Cardella, A. D'Onofrio, E. Geraci, D. Lacroix, E. La Guidara, G. Lanzalone, A. Pagano, E. V. Pagano, M. Papa, E. Piasecki, L. Quattrocchi, F. Rizzo, E. Rosato, G. Spadaccini, A. Trifiro. *Isospin influence on fragments production in ^{78}Kr+^{40}Ca and ^{86}Kr+^{48}Ca collisions at 10 MeV/nucleon.* Eur. Phys. J. A **55**, 22 (2019).

K. Pyrzyńska, K. Kilian, M. Pęgier. *Separation and purification of scandium: From industry to medicine.* Sep. Purif. Rev. **48**, 65 (2019).

K. Pyrzyńska, A. Sentkowska. *Liquid chromatographic analysis of selenium species in plant materials.* TrAC, Trends Anal. Chem. **111**, 128 (2019).

M. Pęgier, K. Kilian, K. Pyrzyńska. *Kinetics of scandium ion sorption onto oxidized carbon nanotubes.* Monatsh. Chem. **150**, 1569 (2019).

Y. H. Qiang, C. M. Petrache, S. Guo, P. M. Walker, D. Mengoni, Q. B. Chen, B. F. Lv, A. Astier, E. Dupont, M. L. Liu, X. H. Zhou, J. G. Wang, D. Bazzacco, A. Boso, A. Goasduff, F. Recchia, D. Testov, F. Galtarossa, G. Jaworski, D. R. Napoli, S. Riccetto, M. Siciliano, J. J. Valiente-Dobon, C. Andreoiu, F. H. Garcia, K. Ortner, K. Whitmore, B. Cederwall, E. A. Lawrie, F. Kuti, D. Solder, T. Marchlewski, J. Srebrny, A. Tucholski,

A. C. Dai, F. R. Xu. *Identification of high-K rotation in* ^{130}*Ba: Testing the consistency of electromagnetic observables.* Phys. Rev. C **99**, 014307 (2019).

A. T. Rudchik, A. A. Rudchik, O. E. Kutsyk, K. W. Kemper, K. Rusek, E. Piasecki, A. Trzcińska, S. Kliczewski, E. I. Koshchy, V. M. Pirnak, O. A. Ponkratenko, I. Strojek, V. A. Plujko, S. B. Sakuta, R. Siudak, A. P. Ilyin, Y. M. Stepanenko, Y. O. Shyrma, V. V. Uleshchenko. $^{12}C(^{15}N,\ ^{14}C)^{13}N$ *reaction at 81 MeV. Competition between one and two particle transfers.* Nucl. Phys. A **992**, UNSP 121638 (2019).

A. T. Rudchik, A. A. Rudchik, O. E. Kutsyk, K. W. Kemper, S. Kliczewski, K. Rusek, E. Piasecki, A. Trzcińska, E. I. Koshchy, V. M. Pirnak, O. A. Ponkratenko, I. Strojek, V. A. Plujko, A. Stolarz, S. B. Sakuta, R. Siudak, O. V. Herashchenko, A. P. Ilyin, Y. M. Stepanenko, Y. O. Shyrma, V. V. Uleshchenko. *Elastic and inelastic scattering of* ^{15}N *ions by* ^{12}C *at 81 MeV and the effect of transfer channels.* Acta Phys. Pol. B **50**, 753 (2019).

A. T. Rudchik, A. A. Rudchik, O. E. Kutsyk, K. Rusek, K. W. Kemper, E. Piasecki, A. Stolarz, A. Trzcińska, V. M. Pirnak, O. A. Ponkratenko, I. Strojek, E. I. Koshchiy, R. Siudak, S. B. Sakuta, V. A. Plujko, A. P. Ilyin, Y. M. Stepanenko, V. V. Uleshchenko, Y. O. Shyrma. $^{12}C(^{15}N,\ ^{14}C)^{13}N$ *reaction mechanisms at energy 81 MeV and* $^{14}C + {}^{13}N$ *nuclei interaction.* Nucl. Phys. At. Energy (Iader. Fiz. Enerh.) **20**, 221 (2019).

A. T. Rudchik, A. A. Rudchik, O. O. Chepurnov, K. Rusek, K.W. Kemper, E. Piasecki, A. Stolarz, A. Trzcińska, V. M. Pirnak, O. A. Ponkratenko, I. Strojek, E. I. Koshchy, R. Siudak, S. B. Sakuta, A. P. Ilyin, Y. M. Stepanenko, V. V. Uleshchenko, Y. O. Shyrma. *Elastic and inelastic scattering of* ^{15}N *ions by* ^{6}Li *nuclei at energy 81 MeV* Nucl. Phys. At. Energy (Iader. Fiz. Enerh.) **20**, 366 (2019).

M. Sadowska, H. Gogolewska, N. Pawelec, A. Sentkowska, B. Krasnodebska-Ostrega. *Comparison of the contents of selected elements and pesticides in honey bees with regard to their habitat.* Environ. Sci. Pollut. Res. **26**, 371 (2019).

M. Saxena, P.Napiorkowski, L. Próchniak, R.Kumar, A. Stolarz, K.Wrzosek-Lipska, T. Abraham, S. Dutt, M. Kicinska-Habior, M. Kisielinski, M. Komorowska, M. Kowalczyk, M. Matejska-Minda, M. Palacz, W. Piątek, J. Srebrny, A. Tucholski, H. J. Wollersheim. *Deformation in* ^{120}*Te described experimentally by quadrupole invariants.* Acta Phys. Pol. B **50**, 417 (2019).

M. Sitarz, J. Jastrzębski, F. Haddad, T. Matulewicz, K. Szkliniarz, W. Zipper. *Can we extract production cross-sections from thick target yield measurements? A case study using scandium radioisotopes.* MDPI Instruments **3(2)**, 29 (2019).

M. Sitarz, E. Nigron, A. Guertin, F. Haddad, T. Matulewicz. *New cross-sections for* $^{nat}Mo(\alpha,x)$ *reactions and medical* ^{97}Ru *production estimations with radionuclide yield calculator.* MDPI Instruments **3(1)**, 7 (2019).

A. Sentkowska, K. Pyrzyńska. *Investigation of antioxidant activity of selenium compounds and their mixtures with tea polyphenols.* Mol. Biol. Rep. **46**, 3019 (2019).

P.A. Soderstrom, G. Jaworski, J. J. V. Dobon, J. Nyberg, J. Agramunt, G. de Angelis, S. Carturan, J. Egea, M. N. Erduran, S. Erturk, G. de France, A. Gadea, A. Goasduff, V. Gonzalez, K. Hadyńska-Klęk, T. Huyuk, V. Modamio, M. Moszyński, A. Di Nitto, M. Palacz, N. Pietralla, E. Sanchis, D. Testov, A. Triossi, R. Wadsworth. *Neutron detection and gamma-ray suppression using artificial neural networks with the liquid scintillators BC-501A and BC-537.* Nucl. Instrum. Methods Phys. Res. A **916**, 238 (2019).

A. M. Stefanini, G. Montagnoli, M. Del Fabbro, G. Colucci, P. Colovic, L. Corradi, E. Fioretto, F. Galtarossa, A. Goasduff, J. Grębosz, M. Heine, G. Jaworski, M. Mazzocco, T. Mijatovic, S. Szilner, M. Bajzek, D. Brugnara, M. Siciliano, I. Zanon. *Fusion hindrance and Pauli blocking in* $^{58}Ni+^{64}Ni$. Phys. Rev. C **100**, 044619 (2019).

A. Tucholski, C. Droste, J. Srebrny, C. M. Petrache, J. Skalski, P. Jachimowicz, M. Fila, T. Abraham, M. Kisielinski, A. Kordyasz, M. Kowalczyk, J. Kownacki, T. Marchlewski, P. J. Napiorkowski, L. Próchniak, J. Samorajczyk-Pyśk, A. Stolarz, A. Astier, B. F. Lv, E. Dupont, S. Lalkovski, P. Walker, E. Grodner, Z. Patyk. *Lifetime of the recently identified* 10^{+} *isomeric state at 3279 keV in the* ^{136}Nd *nucleus.* Phys. Rev. C **100**, 014330 (2019).

P. Ujic, J. C. Cam, B. M. Retailleau, E. Traykov, L. Standyło,J. Choiński, P. Delahaye. *EBIS debuncher experimental performance.* Nucl. Instrum. Methods Phys. Res. A **918**, 30 (2019).

S. Valdre, G. Casini, N. Le Neindre, M. Bini, A. Boiano, B. Borderie, P. Edelbruck, G. Poggi, F. Salomon, G. Tortone, R. Alba, S. Barlini, E. Bonnet, B. Bougard, R. Bougault, G. Bruhn, M. Bruno, A. Buccola, A. Camaiani, A. Chbihi, C. Ciampi, M. Cicerchia, M. Cinausero, D. Dell'Aquila, P. Desrues, J. A. Duenas, D. Fabris, M. Falorsi, J. D. Frankland, C. Frosin, E. Galichet, R. Giordano, F. Gramegna, L. Grassi, D. Gruver, M. Guerzoni, M. Henri, M. Kajetanowicz, K. Korcyl, A. Kordyasz, T. Kozik, P. Lecomte, I. Lombardo, O. Lopez, C. Maiolino, G. Mantovani, T. Marchi, A. Margotti, Y. Merrer, L. Morelli, A. Olmi, A. Ordine, P. Ottanelli, C. Pain, M. Pałka, M. Parlog, G. Pasquali, G. Pastore, S. Piantelli, H. de Preaumont, R. Revenko, A. Richard, M. F. Rivet, J. Ropert, E. Rosato, F. Saillant, D. Santonocito, E. Scarlini, S. Serra, C. Soulet, G. Spadaccini, A. A. Stefanini, G. Tobia, S. Upadhyaya, A. Vanzanella, G. Verde, E. Vient, M. Vigilante, E. Wanlin, G. Wittwer, A. Zucchini. *The FAZIA setup: A review on the electronics and the mechanical mounting.* Nucl. Instrum. Methods Phys. Res. A **930**, 27 (2019).

S. Valdre, G. Poggi, A. Buccola, G. Pasquali, G. Casini, N. Le Neindre, R. Alba, S. Barlini, M. Bini, A. Boiano, E. Bonnet, B. Borderie, R. Bougault, G. Brulin, M. Bruno, A. Camaiani, A. Chbihi, C. Ciampi, M. Cicerchia, M. Cinausero, D. Dell'Aquila, J. A. Duenas, D. Fabris, J. D. Frankland, C. Frosin, E. Galichet, F. Gramegna, D. Gruyer, M. Henri, A. Kordyasz, T. Kozik, I. Lombardo, O. Lopez, C. Maiolino, G. Mantovani, T. Marchi, L. Morelli, A. Olmi, A. Ordine, P. Ottanelli, M. Parlog, G. Pastore, S. Piantelli, D. Santonocito, C. Soulet, A. A. Stefanini, G. Tortone, S. Upadhyaya, G. Verde, E. Vient, M. Vigilante. *Time of flight identification with FAZIA.* Nuovo Cimento C **42**, 75 (2019).

J. J. Valiente-Dobon, G. Jaworski, A. Goasduff, J. Egea, V. Modamio, T. Huyuk, A. Triossi, M. Jastrząb, P. A. Soderstrom, A. Di Nitto, G. de Angelis, G. de France, N. Erduran, A. Gadea, M. Moszyński, J. Nyberg, M. Palacz, R. Wadsworth, R. Aliaga, C. Aufranc, M. Bezard, G. Baulieu, E. Bissiato, A. Boujrad, I. Burrows, S. Carturan, P. Cocconi, G. Colucci, D. Conventi, M. Cordwell, S. Coudert, J. M. Deltoro, L. Ducroux, T. Dupasquier, S. Erturkr, X. Fabian, V. Gonzalez, A. Grant, K. Hadyńska-Klęk, A. Illan, M. L. Jurado-Gomez, M.Kogimtzis, I. Lazarus, L. Legeard, J. Ljungvall, G. Pasqualato, R. M. Perez-Vidal, A. Raggio, D. Ralet, N. Redon, F. Saillant, B. Saygi, E. Sanchis, M. Scarcioffolo, M. Siciliano, D. Testov, O. Stezowski, M. Tripon, I. Zanon. *NEDA-NEutron Detector Array.* Nucl. Instrum. Methods Phys. Res. A **927**, 81 (2019).

R.Walczak, W. Gaweda, J. Dudek, J. Choiński, A. Bilewicz. *Influence of metal ions on the* ^{44}Sc*-labeling of DOTATATE.* J. Radioanal. Nucl. Chem. **322**, 249 (2019).

W. D. Weintraub, N. Keeley, K. W. Kemper, K. Kravvaris, F. Marechal, D. Robson, B. T. Roeder, K. Rusek, A. Volya. *Analyzing powers and the role of multistep processes in the* $^{12}C(^{7}Li, t)^{16}O$ *reaction.* Phys. Rev. C **100**, 024604 (2019).

W. Wojdowska, D. Pawlak, I. Cieszykowska, M. Zoltowska, T. Janiak, T. Barcikowski, A. Stolarz, J. Choiński, J. Parus, P. Garnuszek, R. Mikołajczak. *Improved procedures of Sc(OH)(3) precipitation and UTEVA extraction for* ^{44}Sc *separation.* Nucl. Med. Rev. **22**, PMID 31482557(2019).

K. Wrzosek-Lipska, K. Rezynkina, N. Bree, M. Zielińska, L. P. Gaffney, A. Petts, A. Andreyev, B. Bastin, M. Bender, A. Blazhev, B. Bruyneel, P. A. Butler, M. P. Carpenter, J. Cederkall, E. Clement, T. E. Cocolios, A. N. Deacon, J. Diriken, A. Ekstrom, C. Fitzpatrick, L. M. Fraile, C. Fransen, S. J. Freeman, J. E. Garcia-Ramos, K. Geibel, R. Gernhauser, T. Grahn, M. Guttormsen, B. Hadinia, K. Hadyńska-Klęk, M. Hass, P. H. Heenen, R. D. Herzberg, H. Hess, K. Heyde, M. Huyse, O. Ivanov, D. G. Jenkins, R. Julin, N. Kesteloot, T. Kröll, R. Kruecken, A. C. Larsen, R. Lutter, P. Marley, P. J. Napiorkowski, R. Orlandi, R. D. Page, J. Pakarinen, N. Patronis, P. J. Peura, E. Piselli, L. Próchniak, P. Rahkila, E. Rapisarda, P. Reiter, A. P. Robinson, M. Scheck, S. Siem, K. S. Chakkal, J. F. Smith, J. Srebrny, I. Stefanescu, G. M. Tveten, P. Van Duppen, J. Van de Walle, D. Voulot, N. Warr, A. Wiens, J. L. Wood. *Electromagnetic properties of low-lying states in neutron-deficient Hg isotopes: Coulomb excitation of* ^{182}Hg*,* ^{184}Hg*,* ^{186}Hg *and* ^{188}Hg*.* Eur. Phys. J. A **55**, 130 (2019).

R. Yokoyama, R. Grzywacz, B. C. Rasco, N. Brewer, K. P. Rykaczewski, I. Dillmann, J. L. Tain, S. Nishimura, D. S. Ahn, A. Algora, J. M. Allmond, J. Agramunt, H. Baba, S. Bae, C. G. Bruno, R. Caballero-Folch, F. Calvino, P. J. Coleman-Smith, G. Cortes, T. Davinson, C. Domingo-Pardo, A. Estrade, N. Fukuda, S. Go, C. J. Griffin, J. Ha, O. Hall, L. J. Harkness-Brennan, J. Heideman, T. Isobe, D. Kahl, M. Karny, T. Kawano, L. H. Khiem, T. T. King, G. G. Kiss, A. Korgul, S. Kubono, M. Labiche, I. Lazarus, J. Liang, J. Liu, G. Lorusso, M. Madurga, K. Matsui, K. Miernik, F. Montes, A. I. Morales, P. Morrall, N. Nepal, R. D. Page, V. H. Phong, M. Piersa, M. Prydderch, V. F. E. Pucknell, M. M. Rajabali, B. Rubio, Y. Saito, H. Sakurai, Y. Shimizu, J. Simpson, M. Singh, D.W. Stracener, T. Sumikama, R. Surman, H. Suzuki, H. Takeda, A. Tarifeno-Saldiyia, S. L. Thomas, A. Tolosa-Delgado, M.Wolińska-Cichocka, P. J. Woods, X. X. Xu. *Strong one-neutron emission from two-neutron unbound states in beta decays of the r-process nuclei* ^{86}Ga*,* ^{87}Ga*.* Phys. Rev. C **100**, 031302 (2019).

R. Yokoyama, M. Singh, R. Grzywacz, A. Keeler, T. T. King, J. Agramunt, N. T. Brewer, S. Go, J. Heideman, J. Liu, S. Nishimura, P. Parkhurst, V. H. Phong, M. M. Rajabali, B. C. Rasco, K. P. Rykaczewski, D. W. Stracener, J. L. Tain, A. Tolosa-Delgado, K. Vaigneur, M.Wolińska-Cichocka. *Segmented YSO scintillation detectors as a new beta-implant detection tool for decay spectroscopy in fragmentation facilities.* Nucl. Instrum. Methods Phys. Res. A **937**, 93 (2019)

S. Ziliani, M. Ciemała, F. Crespi, S. Leoni, B. Fornal, A. Maj, P. Bednarczyk, G. Benzoni, A. Bracco, C. Boiano, S. Bottoni, S. Brambilla, M. Bast, M. Beckers, T. Braunroth, F. Camera, N. Cieplicka-Oryńczak, E. Clement, O. Dorvaux, S. Erturk, G. De France, A. Goldkuhle, J. Grebosz, M. N. Harakeh, L. W. Iskra, B. Jacquot, M. Kicińska-Habior, Y. Kim, M. Kmiecik, A. Lemasson, H. Li, I. Matea, K. Mazurek, C. Michelagnoli, B. Million, C. Mueller-Gatermann, P. Napiorkowski, V. Nanal, M. Matejska-Minda, M. Rejmund, C. Schmitt, M. Stanoiu, I. Stefan, B.Wasilewska, M. Ziębliński. *Spectroscopy*

of neutron-rich C, O, N and F isotopes with the AGATA+PARIS+VAMOS setup at GANIL
Acta Phys. Pol. B **50**, 635 (2019).

E.4 Seminars

E.4.1 Seminars co-organised by HIL

Nuclear Physics Seminars

Seminars organised jointly by the divisions of Nuclear Physics and Nuclear Structure Theory of the Faculty of Physics, University of Warsaw and the Heavy Ion Laboratory, University of Warsaw

M. Kowalska — ISOLDE, CERN, Geneve, Switzerland 10 January 2019
Spin-polarized exotic nuclei: from fundamental interactions, via nuclear structure, to biology and medicine

K. Kilian — Heavy Ion Laboratory, University of Warsaw, Warszawa, Poland 24 January 2019
Pozytonowa Tomografia Emisyjna w badaniach przedklinicznych
Positron Emission Tomography in preclinical studies

M. Moszyński — National Centre for Nuclear Research 28 February 2019
Nagroda IEEE NPSS im. Prof. Glenna Knolla, czyli moja przygoda z detektorami scyntylacyjnymi
IEEE NPSS Professor Glenn Knoll Award, my adventure with scintillation detectors

R. Skibiński — Jagiellonian Univ., Kraków, Poland 7 March 2019
Rozpraszanie nukleon-deuteron – przewidywania i niepewności teoretyczne
Nucleon-deuteron scattering – theoretical predictions and uncertainties

M. Kowal — National Centre for Nuclear Research 14 March 2019
Kandydaci na długo-żyjące jądra superciężkie w stanach z wysokim K
Candidates for long-lived super-heavy nuclei in states with high K

P. Moskal — M. Smoluchowski Institute of Physics, Jagiellonian Univ., Kraków, Poland 21 March 2019
Studies of discrete symmetries, quantum entanglement and positronium imaging with J-PET tomography

J. Srebrny — Heavy Ion Laboratory, University of Warsaw, Warszawa, Poland 28 March 2019
EAGLE (ORIRIS II) – czego nauczyliśmy się dzięki naszym eksperymentom
EAGLE (ORIRIS II) – what have we learned through our experiments

W. Urban — Institute of Experimental Physics, University of Warsaw, Warszawa, Poland 4 April 2019
Zagadka niskoenergetycznych stanów 0^+ w jądrach parzysto-parzystych
The riddle of low-energy 0^+ states in even-even nuclei

A. Płochocki — Institute of Experimental Physics, University of Warsaw, Warszawa, Poland 11 April 2019
Własności neutronowo nadmiarowych izotopów z obszaru od niobu do srebra,

o liczbach masowych 107-119; w tym – zagadki rozpadu beta, własności stanów izomerycznych, deformacje stanów jądrowych. Wyniki bada eksperymentalnych wykonanych w Laboratorium Cyklotronowym Uniwersytetu Jyväskylä
Properities of neutron rich isotopes from niobium to silver of mass numbers 107-119; including – the beta decay riddle, isomeric states properities, nuclear state deformations. The results of experimental tests carried out at the JYFL Accelerator laboratory at the University of Jyväskylä

P. Garrett — University of Guelph, Ontario, Canada 25 April 2019
Are there spherical vibrational nuclei?

K. Piasecki — Institute of Experimental Physics, University of Warsaw, Warszawa, Poland 9 May 2019
Czy kaony zmieniają masę w gęstej i gorącej materii jądrowej?
Do kaons change their mass in hot and dense nuclear matter?

M. Kuich — Institute of Experimental Physics, University of Warsaw, Warszawa, Poland 16 May 2019
Dziwność a przejście fazowe silnie oddziałującej materii
Strangeness and phase transitions in strongly interacting matter

G. Jaworski — Heavy Ion Laboratory, University of Warsaw, Warszawa, Poland 30 May 2019
12 lat projektu NEDA – od koncepcji do pierwszej serii eksperymentów ze spektrometrem AGATA
12 years of the NEDA project – from the idea to the first experimental campaign with the AGATA spectrometer

A. Sentkowska — Heavy Ion Laboratory, University of Warsaw, Warszawa, Poland 6 June 2019
Od parzenia herbaty do syntezy radiofarmaceutyku. Potencjalne zastosowania związków polifenolowych jako ligandów do analizy radiochemicznej
From tea brewing to the synthesis of radiopharmeceuticals. Potential applications of polyphenolic compounds as ligands for radiochemical analysis

B. Cheal — Deptartment of Physics, University of Liverpool, Liverpool, UK 13 June 2019
Studying Nuclear Sizes and Shapes with Laser Spectroscopy

P. Bączyk — Institute of Theoretical Physics, University of Warsaw, Warszawa, Poland 3 October 2019
Naruszenie symetrii izospinowej przez oddziaływanie silne w podejściu opartym na teorii funkcjonału gęstości
Strong-interaction isospin-symmetry breaking within the density functional theory

M. Jentschel — Institut Laue Langevin, Grenoble, France 10 October 2019
GRIDSA: Measuring Femtosecond Nuclear Lifetimes with a Germanium

Detector Array

M. Kusiak — Institute of Geophysics, Polish Academy of Sciences, Warszawa, Poland 17 October 2019
Frozen in time – Pb nanospheres in zircon

A. Tucholski — Heavy Ion Laboratory, University of Warsaw, Warszawa, Poland 24 October 2019
Wzbudzenia kwazicząstkowe daleko od ścieżki stabilności
Quasi-particle excitation far from the path of stability

M. Ciemała — The H. Niewodniczański Institute of Nuclear Physics PAN, Kraków, Poland 31 October 2019
Excited state lifetime measurements in neutron rich carbon and oxygen isotopes
Pomiary czasów życia wzbudzonych stanów jądrowych w neutronowo-nadmiarowych izotopach węgla i tlenu

J. Choiński — Heavy Ion Laboratory, University of Warsaw, Warszawa, Poland 7 November 2019
Ośrodek produkcji i badań radiofarmaceutyków w Środowiskowym Laboratorium Ciężkich Jonów – stan aktualny i perspektywy
The facility for radiopharmeceutical studies and production at the Heavy Ion Laboratory – current status and prospects

M. Stryjczyk — Instituut voor Kern- en Stralingfysica, K.U. Leuven, Leuven, Belgium 14 November 2019
Shape coexistence in atomic nuclei studied through β decay at ISOLDE, CERN

N.Cieplicka-Oryńczak — The H. Niewodniczański Institute of Nuclear Physics PAN, Kraków, Poland 21 November 2019
Struktura jąder z okolic podwójnie magicznego rdzenia ^{208}Pb badana przy pomocy koincydencji gamma-gamma
The structure of nuclei in the vicinity of the doubly magic core of ^{208}Pb studied through gamma-gamma coincidences

E. Grodner — National Centre for Nuclear Research 28 November 2019
Jak zweryfikować istnienie zjawiska chiralności jądrowej?
How to verify the existence of chirality phenomenon

I. Izosimov — Joint Institute for Nuclear Research, Dubna, Russia 5 December 2019
Application of nuclear spectroscopy methods to the study of beta-decay

J. Skalski — National Centre for Nuclear Research 12 December 2019
Rozszczepienie jądrowe – główne problemy, czasy życia jąder nieparzystych i K-izomerów oraz metoda instantonów

Nuclear fission – main issues, odd nuclei and K-isomer lifetimes and the instanton method

K. Hadyńska-Klęk — Heavy Ion Laboratory, University of Warsaw, Warszawa, Poland 19 December 2019
Wzbudzenia kulombowskie w INFN Laboratori Nazionali di Legnaro – przeszłość, teraźniejszość, przyszłość
Coulomb excitation at INFN Laboratori Nazionali di Legnaro – past, present and future

E.4.2 Other seminars organised at HIL

Internal semi-formal HIL seminars

N. Zandi — Heavy Ion Laboratory, University of Warsaw, Warszawa, Poland 23 January 2019
A new design of irradiation box in the Tehran Research Reactor to the increase fast neutron flux for ^{67}Cu production

M. Zielińska — IRFU/SPhN, CEA Saclay, Gif-sur-Yvette, France 26 April 2019
Coulomb-excitation experiments with the Q3D spectrometer at MLL

E.4.3 External seminars given by the HIL staff

K. Rusek 14 January 2019
History of nuclear physics in Poland
Przyszłość fizyki jądrowej niskich energii w Polsce a rozwój krajowej infrastruktury badawczej, Heavy Ion Laboratory, Warszawa, Poland

K. Rusek 14 January 2019
HIL – status and plans for the future
Przyszłość fizyki jądrowej niskich energii w Polsce a rozwój krajowej infrastruktury badawczej, Heavy Ion Laboratory, Warszawa, Poland

K. Wrzosek-Lipska 15 January 2019
Deformations of atomic nuclei studied with Coulomb excitation – perspectives and experimental needs
Przyszłość fizyki jądrowej niskich energii w Polsce a rozwój krajowej infrastruktury badawczej, Heavy Ion Laboratory, Warszawa, Poland

G. Jaworski 15 January 2019
NEDA – status, perspectives for installation in Poland and possible physics case
Przyszłość fizyki jądrowej niskich energii w Polsce a rozwój krajowej infrastruktury badawczej, Heavy Ion Laboratory, Warszawa, Poland

U. Kaźmierczak 15 January 2019
Challenges in radiobiology research with heavy ion beams in Poland
Przyszłość fizyki jądrowej niskich energii w Polsce a rozwój krajowej infrastruktury

badawczej, Heavy Ion Laboratory, Warszawa, Poland

M. Paluch-Ferszt 15 January 2019
How to test electronics used in the Cosmos?
Przyszłość fizyki jądrowej niskich energii w Polsce a rozwój krajowej infrastruktury badawczej, Heavy Ion Laboratory, Warszawa, Poland

M. Filipek 20 February 2019
Wydajność detekcji jonów w nanodozymetrze Jet Counter
Ion detection efficieny in Jet Counter nanodosimeter
Ogólnopolska Konferencja PTFM OW, Warszawa, Poland

K. Kilian 25 February 2019
Statystyczne i przepływowe metody wydzielania i zatężania jonów metali na stałych sorbentach – zastosowania analityczne i radiochemiczne
Statistical and flow methods for the separation and concentration of metal ions on solid sorbents – analytical and radiochemical applications
Faculty of Chemistry, University of Warsaw, Warszawa, Poland

K. Rusek 1 March 2019
Nuclear physics research infrastructures in Poland
NuPECC Meeting, Heavy Ion Laboratory, Warszawa, Poland

K. Kilian 3 March 2019
Medical radioisotopes – clinical applications and preclinical studies
NuPECC Meeting, Heavy Ion Laboratory, Warszawa, Poland

K. Wrzosek-Lipska 6 March 2019
A future Coulomb excitation project at HIL and LNL – the nature of low-energy collectivity in stable Cd isotopes
Joint LIA COLL-AGAIN, COPIGAL, and POLITA Workshop (French-Italian-Polish Collaborations), Heavy Ion Laboratory, Warszawa, Poland

K. Kilian 6 March 2019
From beam to image – PET in preclinical studies
Joint LIA COLL-AGAIN, COPIGAL, and POLITA Workshop (French-Italian-Polish Collaborations), Heavy Ion Laboratory, Warszawa, Poland

J. Choiński 7 March 2019
Ongoing development of the cyclotron and experimental setups at HIL
Joint LIA COLL-AGAIN, COPIGAL, and POLITA Workshop (French-Italian-Polish Collaborations), Heavy Ion Laboratory, Warszawa, Poland

M. Palacz 7 March 2019
NEDA —- construction, setup and experimental campaign at GANIL with AGATA
Joint LIA COLL-AGAIN, COPIGAL, and POLITA Workshop (French-Italian-Polish

Collaborations), Heavy Ion Laboratory, Warszawa, Poland

K. Kilian 8 March 2019
Positron Emission Tomography in preclinical studies
Seminar on High Energy Physics, Faculty of Physics, University of Warsaw, Warszawa, Poland

K. Kilian 22 March 2019
Wytwarzanie radiofarmaceutyków do Pozytonowej Tomografii Emisyjnej (PET)
Radiopharmaceutical production for Positron Emission Tomography (PET)
Selected topics on nuclear energy, Faculty of Physics, University of Warsaw, Warszawa, Poland

K. Wrzosek-Lipska 25–26 March 2019
Nature of low-energy collectivity in stable Cd isotopes studied through Coulomb excitation and electron spectroscopy
Workshop AGATA@LNL for stable beams, INFN Laboratori Nazionali di Legnaro, Italy

K. Hadyńska-Klęk 26 March 2019
Coulomb excitation of the super-deformed structures in the A∼4- mass region
Workshop AGATA@LNL for stable beams, INFN Laboratori Nazionali di Legnaro, Italy

K. Wrzosek-Lipska 16–18 April 2019
Shape coexistence in neutron-deficient Hg studied trough Coulomb excitation at HIE-ISOLDE
Physics between lead and uranium: in preparation of new campaigns at ISOLDE, Leuven, Belgium

M. Wolińska-Cichocka 23–26 April 2019
The modular Total Absorption Spectrometer (MTAS) and anti-neutrino properties in fission products
IAEA Technical Meeting on Nuclear Data for Anti-Neutrino Spectra and Applications

M. Filipek 17 May 2019
Uszkodzenie DNA w komórkach nowotworowych wystawionych na działanie promieniowania jonizującego - symulacje Monte Carlo
DNA damage in cancer cells exposed to ionizng radiation - Monte Carlo simulations
II Ogólnopolska Konferencja Fizyka Medyczna - Farmacja Fizyczna 2019, Warszawa, Poland

M. Sitarz 20–22 May 2019
Research on the production of therapeutic ^{105}Rh with deuteron beams
1st Meeting of the International Biophysics Collaboration, Darmstadt, Germany

M. Filipek 24 May 2019
Uszkodzenie DNA w komórkach nowotworowych wystawionych na działanie promieniowania jonizującego - symulacje Monte Carlo

DNA damage in cancer cells exposed to ionizng radiation - Monte Carlo simulations
Ogólnopolska Konferencja PTFM OW: O dawce, Warszawa, Poland

M. Filipek 24 June 2019
DNA damage in cancer cells exposed to beta radiation measured experimentally and modeled in Monte Carlo simulations
ICCR - MCMA, Montreal, Kanada

E. Piasecki 1–5 July 2019
Dissipation and tunneling
LXIX International Conference "Nucleus-2019", Dubna, Russia

K. Hadyńska-Klęk 30 July 2019
Coulomb excitation of the non-axial super-deformed structure in ^{42}Ca
The 27th International Nuclear Physics Conference, Glasgow, United Kingdom

K. Wrzosek-Lipska 1–7 September 2019
Shape coexistence studied with Coulomb excitation in the N$\sim$104 and N$\sim$60 regions
XXXVI Mazurian Lakes Conference on Physics, Piaski, Poland

G. Jaworski 4 September 2019
The new neutron detector array NEDA – milestones and status
XXXVI Mazurian Lakes Conference on Physics, Piaski, Poland

K. Kilian 5 September 2019
Radiofarmaceutyki znakowane ^{18}F w badaniach przedklinicznych
Radiopharmaceuticals marked with ^{18}F in preclinical trials
62. Zjazd Naukowy PTChem 2019, Warszawa, Poland

K. Kilian 13–18 September 2019
Radiofarmaceutyki dla Pozytonowej Tomografii Emisyjnej w badaniach przedklinicznych znakowane ^{18}F w badaniach przedklinicznych
Radiopharmaceuticals for Positron Emission Tomography in preclinical trials
45. Zjazd Fizyków Polskich, Kraków, Poland

K. Rusek 13–18 September
Infrastruktura badawcza dla fizyki jądrowej w Polsce
Nuclear physics research infrastructures in Poland
45. Zjazd Fizyków Polskich, Kraków, Poland

A. Sentkowska 15–18 September 2019
Comparison of Different Chromatographic Modes in the Speciation Analysis of Selenium
The 25th International Symposium on Separation Science, Łódź, Poland

Z. Szefliński 16 September 2019
Radiobiological research and dosimetry using a flat alpha source

International Conference on Radiation Applications, Belgrad, Serbia

K. Rusek 24–28 September 2019
Nuclear clusters in light exotic nuclei – do we need nuclear theory at all?
XXVI Nuclear Physics Workshop, Kazimierz Dolny, Poland

E. Piasecki 26 September 2019
Dissipation and tunneling
XXVI Nuclear Physics Workshop, Kazimierz Dolny, Poland

L. Próchniak 28 September 2019
Collective octuple degrees of freedom – a next piece of the formal background
XXVI Nuclear Physics Workshop, Kazimierz Dolny, Poland

J. Srebrny 28 September 2019
Quadrupole triaxiality softness. From simple phenomenological models to the fully microscopic General Bohr Hamiltonian
XXVI Nuclear Physics Workshop, Kazimierz Dolny, Poland

P.J. Napiorkowski 29 September 2019
Coulomb excitation: experiment and theory, coexistence
XXVI Nuclear Physics Workshop, Kazimierz Dolny, Poland

A. Sentkowska 7–8 October 2019
Antioxidant interactions between polyphenols and other bioactive components of foodstuffs
The 23rd International Conference on Food Technology and Processing, Dublin, Ireland

M. Palacz 7–8 October 2019
E703 data analysis progress report
N=Z Collaboration Meeting, Florence, Italy

P.J. Napriorkowski 15 October 2019
Coulomb excitation: a well established tool for exciting nuclear physics
International Conference on New Frontiers in Nuclear Physics, Department of Physics, Banaras Hindu University, Varanasi, India

K. Wrzosek-Lipska 20–25 October 2019
Low-energy collectivity in ^{110}Cd studied with Coulomb excitation
ISTROS – Isospin, STructure, Reactions and energy Of Symmetry Conference, Casta Papiernicka, Slovakia

P.J. Napiorkowski 24 October 2019
The Quadrupole Rotational Invariants – Some Tricks and Traps
ISTROS – Isospin, STructure, Reactions and energy Of Symmetry Conference, Casta Papiernicka, Slovakia

E. Piasecki 8 November 2019
Dissipation and tunneling
KLTP-BLTP Joint Workshop on Physics of Strong Interaction, Guangzhou, China

P.J. Napiorkowski 8 November 2019
Software development for nuclear physics
Nuclear Physics Research-Technology Coaction 2, Sevilla, Spain

M. Paluch-Ferszt 8 November 2019
A stand for the irradiation of electronic materials and devices at the Heavy Ion Laboratory
Nuclear Physics Research-Technology Coaction 2, Sevilla, Spain

A. Sentkowska 11–12 November 2019
Selenium in foods-it determination, speciation and interaction with other compounds
International Nutritional Science and Food Chemistry Conference, Venice, Italy

E. Piasecki 13 November 2019
Dissipation and tunneling
China Institute of Atomic Energy, Pekin, China

K. Hadyńska-Klęk 28 November 2019
Validity of Cline's safe energy formula for "light" ions and high excitation energies
PARIS Collaboration Meeting, INFN Laboratori Nazionali di Legnaro, Italy

E.4.4 Poster presentations

P.J. Napiorkowski 1 September 2019
Investigation of the $K = 3/2^+$ rotational band in ^{45}Sc – revised lifetime of the $11/2^-$
XXXVI Mazurian Lakes Conference on Physics, Piaski, Poland

J. Choiński 1–7 September 2019
Investigation of the efficient production of ^{135}La for Auger Therapy using medical cyclotrons installed in Poland
XXXVI Mazurian Lakes Conference on Physics, Piaski, Poland

K. Kilian 5 September 2019
Zautomatyzowane wydzielanie ^{44}Sc z tarcz natCaCO3 i synteza ^{44}Sc-DOTATATE
Separation of ^{44}Sc from Natural Calcium Carbonate Targets for the Synthesis of ^{44}Sc-DOTATATE
62. Zjazd Naukowy PTChem 2019, Warszawa, Poland

P.J. Napiorkowski 13–18 September 2019
Badanie odporności radiacyjnej detektorów typu PiN-dioda na oddziaływanie

z ciężkimi jonami
Study of PiN-diode detector radiation resistance in interactions with heavy ions
45. Zjazd Fizyków Polskich, Kraków, Poland

M. Paluch-Ferszt 17 September 2019
Dose in HDR brachytherapy for gynaecological cancer with the use of thermoluminescence dosimetry
International Conference on Radiation Applications, Belgrad, Serbia

K. Kilian 12–16 October 2019
Application of 18F-FMISO in Determination of Hypoxia Level in Murine CT26 Tumours During Various Stages of Development
The 32nd Annual Congress of the European Association of Nuclear Medicine (EANM), Barcelona, Spain

M. Komorowska 5 December 2019
Study of Octupole Collectivity in ^{146}Nd and ^{148}Sm
ISOLDE Workshop and Users meeting 2019, Cern, Switzerland

E.4.5 Lectures for students and student laboratories

K. Kilian summer semester of the academic year 2018/2019, 15 hours
Radiofarmaceutyki — synteza, wytwarzanie i zastosowania
Radiopharmaceuticals — synthesis, production and applications
Faculty of Chemistry, University of Warsaw, Warszawa, Poland

K. Kilian summer semester of the academic year 2018/2019, 60 hours
Pracownia radiofarmaceutyków
Laboratory of Radiopharmaceuticals
Faculty of Physics, University of Warsaw, Warszawa, Poland

K. Kilian winter semester of the academic year 2019/2020, 40 hours
Analiza Środowiska
Environmental Analysis
Faculty of Chemistry, University of Warsaw, Warszawa, Poland

K. Kilian winter semester of the academic year 2019/2020, 30 hours
Metody izotopowe i chemia radiofarmaceutyków
Radiochemistry and radiopharmacy
Faculty of Physics, University of Warsaw, Warszawa, Poland

K. Kilian 22 February 2019
Otrzymywanie cyklotronowe izotopów
Cyclotron production of isotopes
Studium doktoranckie RadFarm, National Centre for Nuclear Research

Z. Szefliński winter semester of the academic year 2018/2019, 45 hours
Energetyka konwencjonalna, odnawialna i jądrowa

Conventional, Renewable and Nuclear Power
Faculty of Physics, University of Warsaw, Warszawa, Poland

Z. Szefliński summer semester of the academic year 2018/2019, 30 hours
Zespołowe projekty studenckie 2
Student team projects 2
Faculty of Physics, University of Warsaw, Warszawa, Poland

Z. Szefliński summer semester of the academic year 2018/2019, 30 hours
Techniki jądrowe w diagnostyce i terapii medycznej
Nuclear Techniques in Medical Diagnostics and Therapy
Faculty of Physics, University of Warsaw, Warszawa, Poland

Z. Szefliński winter semester of the academic year 2019/2020, 30 hours
Pracownia licencjacka I
Bachelor's Diploma Laboratory I
Faculty of Physics, University of Warsaw, Warszawa, Poland

M. Palacz 20 December 2019
Środowiskowe Laboratorium Ciężkich Jonów
Heavy Ion Laboratory
Faculty of Physics, Warsaw University of Technology, Warszawa, Poland

E.4.6 Science popularization lectures

P.J. Napiorkowski lectures for high shool and middle school pupils

Fizyka dla bramkarzy (60 min)
Physics for goalkeepers

P.J. Napiorkowski lectures for middle school pupils

Czy tablica Mendelejewa jest skończona? (3x60 min)
Is Mendeleev's table complete?

A. Sentkowska lectures for middle school pupils

Przypadki chodzą po ludziach, czyli o przypadkowych odkryciach w chemii (2x60 min)
Accidents will happen – accidental discoveries in chemistry

A. Sentkowska lectures for middle school pupils

Czy na pewno wiesz, jak zaparzać herbatę? O zdolnościach antyutleniających herbat słów kilka (2x60 min)
Do you really know how to make tea? A few words about the antioxidant properties of tea

E.5 Honours and Awards

The Rector of the University of Warsaw awards

In 2019 the following employees of the Heavy Ion Laboratory received the Rector of the University of Warsaw award:
Anna Błaszczyk-Duda, Marek Budziszewski, Bartosz Kalisiewicz, Urszula Kaźmierczak, Wojciech Kozaczka, Zbigniew Kruszyński, Piotr Krysiak, Jan Miszczak, Jolanta Ormaniec, Marcin Palacz, Krzysztof Pietrzak, Krzysztof Rusek, Lech Szeląg.

E.6 Laboratory staff

Director:	Krzysztof Rusek
Deputy directors:	Jarosław Choiński
	Paweł Napiorkowski
Financial executive:	Eliza Balcerowska

Senior scientists:

Krzysztof Kilian, Andrzej Kordyasz[a], Marcin Palacz, Ernest Piasecki[a], Leszek Próchniak, Krzysztof Rusek, Anna Stolarz, Zygmunt Szefliński[a]

Scientific staff and engineers:

Tomasz Abraham, Andrzej Bednarek, Jarosław Choiński, Lucia De Dominicis[b], Przemysław Gmaj, Katarzyna Hadyńska-Klęk[c], Grzegorz Jaworski, Grzegorz Kamiński[d], Urszula Kaźmierczak[e], Marian Kopka, Michał Kowalczyk, Ireneusz Mazur, Jan Miszczak, Paweł Napiorkowski, Wojciech Okliński[a,f], Monika Paluch-Ferszt, Wojciech Piątek[d], Bogdan Radomyski, Olga Saeed Mohamed Nassar, Justyna Samorajczyk-Pyśk, Aleksandra Sentkowska, Julian Srebrny[a], Łukasz Standyło, Krzysztof Sudlitz[a,g], Roman Tańczyk, Agnieszka Trzcińska, Andrzej Tucholski, Marzena Wolińska-Cichocka, Katarzyna Wrzosek-Lipska, Bogumił Zalewski[d], Nadia Zandi[h]

Doctoral candidates:

Mateusz Filipek, Michalina Komorowska, Tomasz Marchlewski, Mateusz Pęgier, Mateusz Sitarz[i]

Technicians:

Mariusz Antczak, Tomasz Bracha, Piotr Jasiński, Bartosz Kalisiewicz, Wiesław Kalisiewicz, Robert Kopik, Wojciech Kozaczka, Zbigniew Kruszyński, Piotr Krysiak, Krzysztof Łabęda, Kamil Makowski, Mariusz Matuszewski Zygmunt Morozowicz[j], Bogusław Paprzycki, Andrzej Pietrzak[a,h], Krzysztof Pietrzak, Krzysztof Sosnowski[k], Łukasz Świątek

Administration and support:

Eliza Balcerowska, Anna Błaszczyk-Duda, Marek Budziszewski, Barbara Kowalska[a], Joanna Kowalska, Jolanta Matuszczak, Anna Odziemczyk, Jolanta Ormaniec, Magdalena Piwowarczyk[a,l], Anna Ratyńska, Ewa Sobańska, Lidia Strzelczyk, Lech Szeląg, Andrzej Wiechowski, Katarzyna Włodarczyk[a], Magdalena Zawal[e],

Voluntary scientists:

Jędrzej Iwanicki, Maciej Kisieliński, Jan Kownacki, Piotr Pluciński, Andrzej Wojtasiewicz, Irena Żejmo

---

[a] part time
[b] since 1 November
[c] since 1 March
[d] on leave
[e] on maternity leave
[f] since 1 July
[g] until 28 February
[h] until 31 July
[i] until 30 September
[j] until 30 January
[k] until 27 March
[l] until 30 June

E.7 Laboratory Council

1. Prof. dr hab. Józef Andrzejewski
   Nuclear Physics Division
   University of Łódź, Łódź

2. Prof. dr hab. Janusz Braziewicz
   Institute of Physics
   Jan Kochanowski University, Kielce

3. Prof. dr hab. Mieczysław Budzyński
   Institute of Physics
   Maria Curie-Skłodowska University, Lublin

4. Prof. dr hab. Ewa Bulska
   Biological and Chemical Research Centre
   University of Warsaw, Warszawa

5. Prof. dr hab. Katarzyna Chałasińska-Macukow
   Faculty of Physics
   University of Warsaw, Warszawa

6. Dr Jarosław Choiński
   Heavy Ion Laboratory
   University of Warsaw, Warszawa

7. Prof. dr hab. inż. Andrzej Chmielewski
   Institute of Nuclear Chemistry
   and Technology, Warszawa

8. Przemysław Gmaj
   (representative of the HIL staff)
   Heavy Ion Laboratory
   University of Warsaw, Warszawa

9. Prof. dr hab. Marta Kicińska-Habior
   (**Chairman of the Council**)
   Faculty of Physics
   University of Warsaw, Warszawa

10. Prof. dr hab. Stanisław Kistryn
    M. Smoluchowski Institute of Physics
    Jagiellonian University, Kraków

11. Prof. dr hab. Franciszek Krok
    Department of Physics
    Warsaw University of Technology, Warszawa

12. Prof. dr hab. Leszek Królicki
    Department of Nuclear Medicine
    Medical University of Warsaw, Warszawa

13. Prof. dr hab. inż. Krzysztof Kurek, prof. NCBJ
    The National Centre for Nuclear Research
    Świerk k/Warszawy

14. Prof. dr hab. Adam Maj
    The Henryk Niewodniczański
    Institute of Nuclear Physics
    Polish Academy of Sciences, Kraków

15. Prof. dr hab. Tomasz Matulewicz
    Faculty of Physics
    University of Warsaw, Warszawa

16. Dr Paweł Napiorkowski
    Heavy Ion Laboratory
    University of Warsaw, Warszawa

17. Prof. dr hab. Wojciech Nawrocik
    Faculty of Physics
    Adam Mickiewicz University, Poznań

18. Prof. dr hab. Paweł Olko
    The Henryk Niewodniczański
    Institute of Nuclear Physics
    Polish Academy of Sciences, Kraków

19. Dr hab. Leszek Próchniak
    Heavy Ion Laboratory
    University of Warsaw, Warszawa

20. Prof. dr hab. Krzysztof Rusek
    (Director of HIL)
    Heavy Ion Laboratory
    University of Warsaw, Warszawa

21. Dr hab. Elżbieta Stephan, prof. UŚ
    Institute of Physics
    University of Silesia, Katowice

E.8 Programme Advisory Committee

PAC members

- Konrad Czerski (Institute of Physics, University of Szczecin, Szczecin, Poland)
- Gilles de France (GANIL, Caen, France)
- Nicholas Keeley (National Centre for Nuclear Research, Otwock, Poland)
- Maria Kmiecik (The H. Niewodniczański Institute of Nuclear Physics PAN, Kraków, Poland)
- Andrzej Magiera (M. Smoluchowski Institute of Physics, Jagiellonian University, Kraków, Poland)
- Chiara Mazzocchi (Faculty of Physics, University of Warsaw, Warszawa, Poland)
- Marco Mazzocco (Padova University, Padova, Italy)
- Leszek Próchniak (Heavy Ion Laboratory, University of Warsaw, Warszawa, Poland)
- Siergiej Sidorczuk (Joint Institute for Nuclear Research, Dubna, Russia)
- Władysław Trzaska (Department of Physics, University of Jyväskylä, Finland)

The international Programme Advisory Committee of the Heavy Ion Laboratory usually meets twice a year, in spring and autumn. The deadline for submitting proposals is three weeks before a PAC meeting. PAC approved experiments are scheduled at the meetings of the Users' Committee, which also serves as a link between cyclotron users and the Laboratory. The Users' Committee is chaired by Jarosław Perkowski (the University of Łódź).

E.9 External users of HIL

In 2019 there were **126** external users and visitors from **35** scientific institutions, including 50 from 15 scientific institutes in Poland, 52 from 12 scientific institutions in the European Union and associated countries and 24 from 9 scientific institutes in other countries.

HIL External users and visitors were from:

Poland

- AGH University of Science and Technology, Kraków, Poland
- Faculty of Physics and Applied Computer Science, University of Lodz, Łódź, Poland
- Faculty of Physics, University of Warsaw, Warszawa, Poland
- Institute of Ceramics and Building Materials, Warszawa, Poland
- Inst. of Physics, Maria Curie-Sklodowska Univ., Lublin, Poland
- Institute of Physics, University of Szczecin, Szczecin, Poland
- Institute of Nuclear Chemistry and Technology, Warszawa, Poland
- Institute of Physics, Jan Kochanowski University, Kielce, Poland
- Maritime University of Stettin, Szczecin, Poland
- M. Smoluchowski Institute of Physics, Jagiellonian Univ., Kraków, Poland
- National Centre for Nuclear Research, Otwock, Poland
- Poznań University of Technology, Poznań, Poland
- The H. Niewodniczański Institute of Nuclear Physics PAN, Kraków, Poland
- University of Białystok, Białystok, Poland
- University of Zielona Góra, Zielona Góra, Poland

European Union and associated countries

- Department of Physics, University of Jyväskylä, Finland
- GANIL, Caen, France
- INFN, Laboratori Nazionali di Legnaro, Legnaro, Italy
- INFN Sezione di Padova, Padova, Italy
- Institute for Nuclear Physics, University of Cologne, Germany
- Institute for Solid-State Nuclear Physics, Berlin, Germany
- IRFU/SPhN, CEA Saclay, Gif-sur-Yvette, France
- Padova University, Padova, Italy
- Universidad Autonoma de Madrid, Madrid, Spain
- University of Florence, INFN Sezione di Firenze, Italy
- University of Huelva, Huelva, Spain
- University of Surrey, Guildford, Surrey, United Kingdom

Other countries

- Al-Farabi Kazakh National University, Almaty, Kazakhstan
- Department of Physics, University of Oslo, Oslo, Norway
- Institute of Nuclear Physics, Ministry of Energy of the Republic of Kazakhstan, Almaty, Kazakhstan
- iThemba Lab. for Accelerator Based Sciences, Faure, South Africa
- Joint Institute for Nuclear Research, Dubna, Russia
- National Research Center "Kurchatov Institute", Moscow, Russia
- Physics Department, Ege University, Izmir, Turkey
- Physics Department, Florida State University, Tallahassee, USA
- Uzbekistan Academy of Sciences, Institute of Nuclear Physics, Tashkent, Uzbekistan

List of Authors